

**EVALUATING THE PERFORMANCE OF W-BEAM
GUARDRAIL ROADSIDE SAFETY BARRIER SYSTEMS**

MEHRTASH SOLTANI

**THESIS SUBMITTED IN FULFILMENT
OF THE REQUIREMENTS
FOR THE DEGREE OF DOCTOR OF PHILOSOPHY**

**FACULTY OF ENGINEERING
UNIVERSITY OF MALAYA
KUALA LUMPUR**

2016

UNIVERSITY OF MALAYA

ORIGINAL LITERARY WORK DECLARATION

Name of Candidate: **Mehrtash Soltani**

Registration/Matric No: **KHA100002**

Name of Degree: **PhD**

Title of Thesis: **Evaluating the performance of w-beam guardrail roadside safety barrier systems**

Field of Study: **Highway and Transportation**

I do solemnly and sincerely declare that:

- (1) I am the sole author/writer of this Work;
- (2) This Work is original;
- (3) Any use of any work in which copyright exists was done by way of fair dealing and for permitted purposes and any excerpt or extract from, or reference to or reproduction of any copyright work has been disclosed expressly and sufficiently and the title of the Work and its authorship have been acknowledged in this Work;
- (4) I do not have any actual knowledge nor do I ought reasonably to know that the making of this work constitutes an infringement of any copyright work;
- (5) I hereby assign all and every rights in the copyright to this Work to the University of Malaya ("UM"), who henceforth shall be owner of the copyright in this Work and that any reproduction or use in any form or by any means whatsoever is prohibited without the written consent of UM having been first had and obtained;
- (6) I am fully aware that if in the course of making this Work I have infringed any copyright whether intentionally or otherwise, I may be subject to legal action or any other action as may be determined by UM.

Candidate's Signature

Date:

Subscribed and solemnly declared before,

Witness's Signature

Date:

Name:

Designation:

ABSTRACT

The last decade has witnessed an increase in the number and speed of vehicles on the roads; these situations greatly affect the occurrence of run-off crashes. Roadside safety barriers serve the purpose of redirecting errant vehicles in addition to providing high levels of safety during and after impacts.

In this study, common guardrail systems, including strong-post systems, guardrails with kerbs, weak-post systems, Midwest systems and Thrie-beam rail systems are evaluated. The goal of this study is to examine the structural adequacy, the vehicle trajectory and the occupant risk factors.

The implementation of a new standard Manual for Assessing Safety Hardware (MASH) for evaluating roadside safety hardware was issued in 2009. The important changes in this new standard are presented. It is found that several types of guardrail systems, including the G4(2W) guardrail system, are unable to satisfy the requirements of the MASH criteria. Therefore, in this study, several options are considered; they include improving the splice connections and adjusting the guardrail height and the post spacing to improve the performance of this system.

In experimental and simulated static tests, the basic mechanical behaviour and the different stages of the deformation mechanism of the beams in a W-beam guardrail system are demonstrated. Based on the results of the static tests, the optimum mesh size for modelling a W-beam is identified for use in a full-scale model of the guardrail. The G4(2W) guardrail system is modelled in LS-DYNA and validated with a previous full-scale crash test conducted at the Texas A&M Transportation Institute.

A parametric study based on the results of the LS-DYNA simulation is conducted to investigate key factors of guardrail systems, including the splice configuration, the post

spacing and the guardrail height, to examine the hypotheses and to achieve the objectives of this study. The purpose of this is to find a model that satisfies the requirements of the MASH's criteria. Finally, a statistical analysis of the different systems highlights the effects of the main parameters, including the guardrail height and the post spacing, on the structural adequacy and the occupant risk factors. The objective is to examine the significance of each factor on the system's behaviour.

University of Malaya

ABSTRAK

Sepanjang dekad yang lepas telah menyaksikan pertambahan bilangan dan kelajuan kenderaan di jalan raya. Situasi ini telah banyak memberi kesan kepada berlakunya kemalangan langgar lari. Penghadang keselamatan di sisi jalan raya bertujuan mengarahkan kembali kenderaan yang tersasar di samping menyediakan tahap keselamatan yang tinggi semasa dan selepas kesan hentaman. Di dalam kajian ini, sistem rel adang biasa, termasuk sistem pasca-kuat, rel adang dengan pengekuat, sistem pasca-lemah, sistem Timur Tengah dan sistem rel rasuk Thrie dinilai. Matlamat kajian ini adalah untuk memeriksa kecukupan struktur, trajektori kenderaan dan faktor-faktor risiko penumpang. Semenjak pelaksanaan piawaian baru Manual bagi Penilaian Keselamatan Perkakasan (MASH) untuk menilai keselamatan perkakasan di sisi jalan raya, yang mana telah dikeluarkan pada 2009, banyak cabaran baru telah diperhatikan. Perubahan penting di dalam piawaian baru ini dibentangkan dan cabaran untuk melaksanakan kriteria-kriteria MASH's dibincangkan. Hasil kajian menunjukkan bahawa terdapat beberapa jenis sistem rel adang, termasuk sistem rel adang G4 (2W) tidak dapat memuaskan keperluan-keperluan yang terkandung di dalam kriteria-kriteria MASH. Sehubungan itu, di dalam kajian ini, beberapa pilihan telah dipertimbangkan, ini termasuklah dengan menyediakan sambungan sambat dan menyelaraskan ketinggian rel adang dan pasca penjarakan untuk memperbaiki prestasi sistem tersebut. Di dalam eksperimen dan ujian-ujian simulasi statik, tingkah laku mekanikal asas dan perbezaan peringkat-peringkat mekanisma ubah bentuk rasuk di dalam sistem rel adang rasuk-W telah ditunjukkan. Berdasarkan kepada keputusan ujian-ujian statik, saiz jaringan optimum untuk permodelan rasuk-W dikenalpasti untuk digunakan di dalam model skala penuh rel adang. Sistem rel adang G4 (2W) dimodelkan dengan menggunakan LS-DYNA dan disahkan melalui ujian hentaman skala penuh yang terdahulu di mana telah dijalankan di Institut Pengangkutan Texas A & M. Kajian parametrik berdasarkan

keputusan simulasi LS-DYNA dijalankan untuk menyiasat faktor-faktor utama sistem rel adang termasuk konfigurasi sambat, penjarakan pasca dan ketinggian rel adang, bagi memeriksa hipotesis dan mencapai objektif kajian ini. Tujuannya ialah untuk mencari model yang dapat memuaskan keperluan kriteria-kriteria MASH's. Akhirnya, analisis statistik ke atas sistem-sistem berbeza menonjolkan kesan-kesan parameter utama, termasuklah ketinggian rel adang dan penjarakan pasca, ke atas kecukupan struktural dan faktor-faktor risiko penumpang. Tujuannya ialah untuk memeriksa signifikan setiap faktor ke atas tingkah laku sistem.

University of Malaya

TABLE OF CONTENTS

ABSTRACT	iii
ABSTRAK	v
TABLE OF CONTENTS	vii
LIST OF FIGURES	xii
LIST OF TABLES	xviii
ACKNOWLEDGEMENTS	xx
1 CHAPTER 1: INTRODUCTION	1
1.1 Introduction.....	1
1.2 Statement of the problem	3
1.3 Research objectives.....	5
1.4 Research hypotheses	5
1.5 Scope of the study	6
1.6 Significance of the study.....	7
1.7 Thesis organisation	7
2 CHAPTER 2: LITERATURE REVIEW	9
2.1 Introduction.....	9
2.2 Assessment of guardrail system performance.....	9
2.2.1 Test levels.....	13
2.3 Review of existing guardrail designs	15
2.3.1 Guardrail system classification	16
2.3.1.1 G4(1S) and G4(2W) strong-post W-beam guardrails	17
2.3.1.2 Midwest guardrail system (MGS).....	19
2.3.1.3 Guardrails with kerbs	20
2.3.1.4 Weak-post W-beam guardrail (G2).....	21
2.3.1.5 Thrie-beam guardrail (G9).....	22

2.4	Analysis of previous guardrail system designs	29
2.4.1	Analysis of the vehicle trajectories of guardrail systems.....	29
2.4.2	Analysis of the occupant risk factors of guardrail systems.....	32
2.4.3	Analysis of the structural adequacy of guardrail systems.....	39
2.5	Comparison of the MASH and NCHRP Report 350	42
2.5.1	Differences in impact severity between NCHRP Report 350 and the MASH 44	
2.5.2	Guardrails that fail to meet the MASH's criteria.....	45
2.6	Failure mechanisms of wood post systems	49
2.6.1	Splice connection failures	51
2.7	Numerical analyses of guardrail systems.....	53
2.8	Static tests	58
2.8.1	General applications.....	59
2.9	Research gaps.....	61
2.10	Chapter summary	62
3	CHAPTER 3: RESEARCH METHODOLOGY	64
3.1	Introduction.....	64
3.1.1	LS-DYNA modelling.....	65
3.2	Strong-post W-beam guardrail model.....	66
3.3	Development of a model of a G4(2W) wood post guardrail system.....	67
3.3.1	Post assembly	70
3.3.1.1	Post-blockout connections	70
3.3.1.2	Assembling the bolt connections	71
3.3.1.3	Fracture region of the wood posts.....	72
3.3.1.4	Guardrail bolt and nut	72

3.3.2	Blockout	73
3.3.2.1	Guardrail bolt and blockout interference	74
3.3.2.2	Contact interference between the bolt and post	75
3.3.3	Soil model	76
3.3.4	W-beam model	81
3.3.4.1	Computer simulations	81
3.3.4.2	Verifying the model of a W-beam segment	85
3.3.4.3	Experimental studies of W-beam guardrail systems	85
3.3.4.4	Test configuration and instrumentation	88
3.3.4.5	Loading and support conditions	88
3.3.4.6	Modelling a W-beam rail using a static test	88
3.3.4.7	Redirection forces	89
3.3.5	Pickup truck model	91
3.4	Test designations and actual impact conditions	91
3.4.1	Test description	92
3.4.2	Impact of the pickup truck with the guardrail system: Baseline model	93
3.4.3	Qualitative validation	94
3.4.4	Quantitative validation	95
3.5	Parametric studies	96
3.5.1	First step: strengthening the connection areas	97
3.5.2	Investigating the effect of guardrail height on safety performance	100
3.5.3	Investigating the effect of the post spacing on safety performance	101
3.6	Statistical analysis	103
3.7	Chapter summary	106
4	CHAPTER 4: RESULTS AND DISCUSSION	108
4.1	Introduction	108
4.2	Validation of the W-beam section	110

4.2.1	Comparison of the numerical model with experimental studies.....	110
4.2.2	Evaluating the load-displacement curves.....	112
4.2.3	Calculating the forces during applying the load	116
4.3	Simulations of a pickup truck impacting the guardrail system	118
4.3.1	Validation of the finite element crash simulation	119
4.3.1.1	Qualitative validation.....	119
4.3.1.2	Quantitative analysis	121
4.4	Parametric study.....	123
4.4.1	Evaluating structural adequacy	124
4.4.1.1	Evaluating the strength of the connection area (spliced W-beams).....	124
4.4.1.2	Evaluating the guardrail deflection	128
4.4.2	Vehicle trajectory	133
4.4.2.1	Impact configurations	134
4.4.2.2	Evaluation of the vehicle's exit speed.....	135
4.4.2.3	Evaluation of the vehicle's exit angle	137
4.4.2.4	Comparing the yaw values	139
4.4.2.5	Comparing the roll values	141
4.4.2.6	Comparing the pitch values.....	143
4.4.3	Evaluating the occupant risk factors	144
4.4.3.1	Comparison of the acceleration data	145
4.5	Statistical analysis.....	148
4.6	Chapter summary	155
5	CHAPTER 5: CONCLUSION	157
5.1	Introduction.....	157
5.1.1	Overview of the study	157
5.2	Conclusion for objective 1 (analysis of previous guardrail systems' performance) .	158
5.3	Conclusion for objective 2: Verification of rail system	159
5.4	Conclusion for objective 3: Validation of the G4(2W) guardrail system	160

5.5	Conclusion for objective 4. Conducting the parametric study	160
5.5.1	Results for the structural adequacy	161
5.5.2	Vehicle trajectory	162
5.5.2.1	Evaluation of the vehicle's exit speed.....	162
5.5.2.2	Evaluation of vehicle Exit angle	163
5.5.2.3	Comparing the yaw values	164
5.5.2.4	Comparing the roll values	164
5.5.2.5	Comparing the pitch values.....	165
5.5.3	Evaluating the occupant risk factors	165
5.6	Conclusion for objective 5: Statistical analysis	167
5.7	Contributions.....	167
5.8	Limitations	168
5.9	Recommendation and future work.....	169
	REFERENCES	170
	Appendix A. Comparison metric values	182
	Appendix B. Sequential figures from LS-DYNA	185

LIST OF FIGURES

Figure 2-1. Requirements for assessing the performance of a guardrail system	9
Figure 2-2. The common types of W-beam guardrail systems (Ferdous et al., 2013)....	17
Figure 2-3. A typical view and detail of a G4(2W) strong-post system (Bullard et al., 2010b)	18
Figure 2-4. Use of midspan splices and offset blocks in a MGS (Ochoa, C & Ochoa, T, 2011)	20
Figure 2-5. Vehicle exit angles for different guardrail systems.....	32
Figure 2-6. Longitudinal impact velocities for different guardrail types.....	34
Figure 2-7. Longitudinal ride-down acceleration for different guardrail types	35
Figure 2-8. Lateral impact velocity for different guardrail types.....	35
Figure 2-9. Lateral ride-down accelerations for different guardrail types	36
Figure 2-10. Longitudinal and lateral impact velocities for different guardrail types	37
Figure 2-11. Longitudinal and lateral ride-down acceleration for different guardrail heights	38
Figure 2-12. Maximum dynamic deflection for different guardrail systems	40
Figure 2-13. Maximum permanent deflection of different guardrail systems	41
Figure 2-14. Comparison of the passenger vehicles in NCHRP Report 350 (left) and the MASH (right).....	43
Figure 2-15. Comparison of the pickup trucks defined in NCHRP Report 350 (left) and the MASH (right)	43
Figure 2-16. Summary of the test results for the guardrail systems subjected to the full-scale crash tests (Polivka et al., 2006b)	47
Figure 2-17. Rail rupture in the G4(2W) guardrail system (Bullard et al., 2010a).....	48
Figure 3-1. Steps in the study.....	64
Figure 3-2. Wood post failure: (a) Material no. 59; (b) Material no. 22.....	69

Figure 3-3. Finite element mesh of a wood post: (a) Isometric and (b) Bottom views ..	70
Figure 3-4. The mesh of a blockout and the upper part of a post	71
Figure 3-5. Post-Blockout attachment modification	71
Figure 3-6. Fracture region of a wood post.....	72
Figure 3-7. Profile of guardrail bolt and nut solid element mesh	73
Figure 3-8. Blockout mesh size.....	73
Figure 3-9. Introducing a layer of NULL shell elements.....	74
Figure 3-10. Guardrail bolt and blockout interference in the physical system and the FEM model	75
Figure 3-11. Interactions between guardrail nuts and posts.....	76
Figure 3-12. Post-impact model using the subgrade modulus for soil discretisation.	77
Figure 3-13. Yield surfaces in plasticity models: (a) Drucker-Prager (pressure dependent); (b) Von Mises (pressure independent).	79
Figure 3-14. Finite element model of a steel post in soil.....	80
Figure 3-15. Null shell elements for simulating contact between a wood post and soil.	80
Figure 3-16. Finite element mesh of the W-beam guardrail.	82
Figure 3-17. Cross section of a W-beam guardrail according to the AAHTSO (2000).	83
Figure 3-18. A sketch of a two-dimensional four-node shell element used in this study with three levels of integration across its thickness (Atahan, 2002).....	84
Figure 3-19. Schematic of the test matrix	86
Figure 3-20. Different mesh sizes used to verify the W-beam rail (a) 40 mm, (b) 20 mm, and (c) 10 mm	89
Figure 3-21. Forces due to membrane action (Px1 and Px2).....	90
Figure 3-22. Reduced Chevrolet Silverado finite element model.....	91
Figure 3-23. Vehicle and installation geometry for test RF476460-1-5 (Bullard et al., 2010a).....	92

Figure 3-24. Summary of the results of Length of Need test 3-11 in the MASH for the G4(2W) W-beam guardrail system	93
Figure 3-25. Finite element model of the pickup truck impacting the guardrail system:	94
Figure 3-26. Proposed locations at which to increase the number of bolts in a splice connection to 10	98
Figure 3-27. Proposed locations at which to increase the number of bolts in a splice connection to 12	98
Figure 3-28. Deleting the element to place the bolts elements	99
Figure 3-29. Merging the new copied elements into the rail elements	99
Figure 3-30. Placing the bolts in the proposed locations	100
Figure 3-31. Increasing the height of the guardrail.....	100
Figure 3-32. Cutting the W-beam to change the post spacing	101
Figure 3-33. Shifting a post to reach the desired post spacing.....	102
Figure 3-34. Deleting the interacting elements	102
Figure 3-35. Modifying the soil box's boundary to create the boundary of new soil box	102
Figure 3-36. Steps involved in the RSM.....	104
Figure 4-1. Comparison of the bulking and flattening of the cross section under a static load. (a) Experiment, (b) simulation with a 20 mm mesh, and (c) simulation with a 40 mm mesh.....	112
Figure 4-2. FEM and experimental results showing the force on a 1.5 metres length with a load at 0.16 of its length (2.66 mm thickness)	113
Figure 4-3. FEM and experimental results showing the force on a 1.5 metres beam with a load at 0.33 of its length (2.66 mm thickness)	113
Figure 4-4. FEM and experimental results showing the force on a 1.5 metres beam with a load at midspan (2.66 mm thickness).....	113

Figure 4-5. FEM and experimental results showing the force on a 2 metres beam with a load at 0.16 of its length (2.66 mm thickness)	114
Figure 4-6. FEM and experimental results showing the force on a 2 metres beam with a load at 0.333 of its length (2.66 mm thickness)	114
Figure 4-7. FEM and experimental results showing the force on a 2 metres beam with a load at midspan (2.66 mm thickness).....	114
Figure 4-8. FEM and experimental force comparison showing the force on a 2.5 metres beam with a load at 0.16 of its length (2.66 mm thickness).....	115
Figure 4-9. FEM and experimental results showing the force on a 2.5 metres beam with a load at 0.333 of its length (2.66 mm thickness)	115
Figure 4-10. FEM and experimental results showing the force on a 2.5 metres beam loaded at midspan (2.66 mm thickness).....	115
Figure 4-11. Schematic of the redirective force	116
Figure 4-12. Redirective forces for loads at different points	117
Figure 4-13. Redirective forces for different loads	117
Figure 4-14. Redirective forces for loads at different points	117
Figure 4-15. The pickup truck in a real crash test and in the LS-DYNA model	118
Figure 4-16. Sequences of photographs from the full-scale crash test and the LS-DYNA simulation.....	121
Figure 4-17. Proposed splice connection locations to increase the number of bolts to 10	125
Figure 4-18. Top view of a splice connection in the ruptured rail	126
Figure 4-19. Proposed splice connection locations for 12 bolts	127
Figure 4-20. Model of a 12-bolt splice connection in the guardrail system (top view)	127
Figure 4-21. Deflection of a W-beam guardrail system.....	128

Figure 4-22. Lateral deflection for a post spacing of 1.5 metres and different guardrail heights	130
Figure 4-23. Lateral deflection for a post spacing of 2 metres and different guardrail heights	130
Figure 4-24. Lateral deflection for a post spacing of 2.5 metres post spacing and different guardrail heights	131
Figure 4-25. Guardrail deflection and vehicle redirection for a guardrail height of 32 inches and a post spacing of 2 metres (a, b, c).....	133
Figure 4-26. Definitions of yaw, pitch and roll.....	134
Figure 4-27. Comparison of the vehicle's exit speed for a post spacing of 1.5 metres and different guardrail heights	135
Figure 4-28. Comparison of the vehicle's exit speed for a post spacing of 2 metres and different guardrail heights	136
Figure 4-29. Comparison of vehicle exit speed for 2.5 metres post spacing guardrail with different guardrail heights.....	136
Figure 4-30. Vehicle trajectory for a guardrail system with a post spacing of 1.5 metres and a guardrail height of	137
Figure 4-31. Vehicle trajectory for a guardrail system with a post spacing of 2 metres and a guardrail height of	138
Figure 4-32. Vehicle trajectory for a guardrail system with a post spacing of 2.5 metres and a guardrail height of	139
Figure 4-33. Yaw calculation for the guardrail system with a post spacing of 1.5 metres	140
Figure 4-34. Yaw calculation for the guardrail system with a post spacing of 2 metres	140

Figure 4-35. Yaw calculation for the guardrail system with a post spacing of 2 metres	141
Figure 4-36. Roll calculation for the guardrail system with a post spacing of 1.5 metres	142
Figure 4-37. Roll calculation for a guardrail system with a post spacing of 2 metres..	142
Figure 4-38. Roll calculation for a guardrail system with a post spacing of 2.5	143
Figure 4-39. Pitch calculation for a guardrail system with a post spacing of 1.5 metres	143
Figure 4-40. Pitch calculation for a guardrail system with a post spacing of 2 metres	144
Figure 4-41. Pitch calculation for a guardrail system with a post spacing of 2.5 metres	144
Figure 4-42. Longitudinal acceleration for a post spacing of 1.5 metres.....	145
Figure 4-43. Lateral acceleration for a post spacing of 1.5 metres	145
Figure 4-44. Longitudinal acceleration for a post spacing of 2 metres.....	146
Figure 4-45. Lateral acceleration for a post spacing of 2 metres	146
Figure 4-46. Longitudinal acceleration for a post spacing of 2.5 metres.....	147
Figure 4-47. Lateral acceleration for a post spacing of 2.5 metres	147
Figure 4-48. Actual and predicted values of the	152
Figure 4-49. Effects of the post spacing and the guardrail height on the lateral deflection	153
Figure 4-50. Effects of the post spacing and the guardrail height on the longitudinal acceleration	154
Figure 4-51. Effects of the post spacing and the guardrail height on the lateral acceleration	155

LIST OF TABLES

Table 2-1: Requirements for assessing the occupant risk factors	10
Table 2-2: Length of Need 3-11 test based on NCHRP Report 350 and the MASH.....	14
Table 2-3: Summary of the test results for a guardrail system (Length of Need 3-11 test)	23
Table 2-4: Summary of the occupant risk results for guardrail systems.....	26
Table 2-5: The Length of Need test procedures for the MASH and NCHRP Report 350	44
Table 2-6: Comparison of the impact conditions in NCHRP Report 350 and the MASH ordered by severity.....	45
Table 2-7: Summaries of the MASH full-scale crash tests conducted with a non- proprietary strong-post W-beam guardrail.....	46
Table 2-8: Applications and limitations of safety feature development techniques (NCHRP Report 350, 1993).....	59
Table 3-1: LS-DYNA material models considered for wood posts.....	68
Table 3-2: Summary of the material properties used in the soil model.	77
Table 3-3: LS-DYNA material models considered for the soil	78
Table 3-4: LS-DYNA material inputs for the W-beam section	84
Table 3-5: Specifications of sample W-beam guardrails	87
Table 3-6: Acceptance criteria used in the RSVVP (Mongiardin & Ray, 2009).....	96
Table 4-1: Time History Evaluation Table for the MASH-based Simulation of a G2(2W) guardrail system.....	123
Table 4-2: The length of the Silverado pickup truck's engagement with the strong-post guardrail system (in ms).....	135
Table 4-3: Preferred maximum exit angles specified in the MASH.....	137
Table 4-4: Finite element results.....	148

Table 4-5: ANOVA and the final equation for the lateral deflection	149
Table 4-6: ANOVA and final equation for the longitudinal acceleration (X)	150
Table 4-7: ANOVA and the final equation for the lateral acceleration (Y).....	150

University of Malaya

ACKNOWLEDGEMENTS

I would like to thank my parents, sisters and brother for their endless love and support during my studies.

Special thanks are due to Professor Ir Dr Mohamed Rehan Karim and Dr Nor Hafizah Ramli Sulong, my supervisors, for their advice, guidance and valuable comments. This project would not have been possible without them.

I would like to thank the Dean and Deputy Dean of the Faculty of Engineering and the head and staff of the Department of Civil Engineering for their continuous support and their help throughout my studies.

Finally, I thank all the friends at University of Malaya (UM) who have always provided an enjoyable and friendly working environment.

CHAPTER 1: INTRODUCTION

1.1 Introduction

People benefit from the economic development stimulated by the automotive industry at the expense of road crashes (Wu & Thomson, 2004). Scholars have affirmed the positive connection between crashes and increases in vehicle ownership and vehicle speeds (Partheeban et al., 2008).

Traffic engineers and planners have recognised the importance of traffic safety in responding to the factors that contribute to run-off crashes, such as road geometry, traffic conditions, driver behaviour, environmental conditions, non-traversable obstacles close to roadways, steep side slopes, deep ditches, and dangerous terminals and transitions (Ayati et al., 2012). Ensuring traffic safety despite crashes (Prentkovskis et al., 2009) involves a prevention aspect and minimising the severity of impacts (Wood, 1997). Recent research has shown that crashes with solid objects located beside highways, such as poles and trees, cause many fatal injuries (Wang et al., 2011). Therefore, effective roadside barrier systems that increase traffic safety (Corben et al., 2010), such as road barriers, guardrails and bridge rails, are called for.

Roadside barrier systems are used to redirect errant vehicles back to the roadway after impact to prevent vehicles from impacting with stiffer roadside objects such as poles and trees (Coon & Reid, 2006). These roadside safety barriers act as blockages for steep slopes and roadside objects (roadside barriers) and for the lanes travelling in the opposite direction (median barriers) (Gabauer et al., 2010) and thus, prevent collisions (Abu-Odeh et al., 2011).

Scholars have recognised the inefficiency of guardrail systems in preventing and minimising the severity of crashes, and they are perceived as roadside hazards by road

users (Ben-Bassat & Shinar, 2011). In the United States, approximately 1,200 fatalities involving guardrails have been reported, and 13% of vehicle rollovers and 2% of fatalities were caused by guardrail crashes (Wolford and Sicking, 1996). Light trucks have been observed to have higher probabilities of rolling over (Bligh & Mak, 1999). In addition, according to Reid et al. (1997), standard W-beam guardrails are inefficient at handling vehicles with higher centres of mass and bumpers, which results in vehicle rollovers. Therefore, attention should be given to constructing a road restraint system in which this helps decrease the risk factors for crashes (Kammel, 2007). Generally, a guardrail is the type of safety barrier that is most commonly used along roadsides to reduce the consequences of crashes (Atahan et al., 2008). However, the best designs are not able to eliminate all serious injuries or all fatalities. Guardrails are used when the risk of striking an object on the road is judged to be more severe than striking the guardrail.

Full-scale crash tests, analytical methods, and finite element analysis have been used to evaluate the performance of guardrail systems (Ray, 1997). A full-scale crash test can predict the most severe scenario involving a vehicle, its occupants and a guardrail system that could occur (Bligh & Mak, 1999). Analytical and finite element methods are used to examine several scenarios before full-scale crash tests are conducted.

Analysing a guardrail system involves highly nonlinear material behaviour and large deformations caused by the dynamic impact load. This system is too complex for standard linear-elastic analytical methods and closed-form solutions (Plaxico et al., 1998). To assess the behaviour of a guardrail system and its posts, finite element analysis appears to be the best tool because it offers full control over all the parameters; therefore, it has become an essential tool in guardrail system analysis and the design of roadside safety hardware. The various parameters can be evaluated using an

optimisation process to improve the design of the guardrail system so that it reduces the risk of Pickup trucks rolling over (Tabiei & Wu, 2000b).

In this thesis, LS-DYNA is used to supplement full-scale crash testing in a cost-effective manner. Qualitative and quantitative methods are used to validate the finite element model. For this reason, the results of previously conducted full-scale crash tests of a failed strong-post guardrail system are used. Subsequently, the finite element simulation replicates the full-scale test with high accuracy. This model is able to investigate the crash-sensitive components of the G4(2W) guardrail safety system.

To simulate the failed system, LS-DYNA is used to identify the origin of the failure and to explore possible solutions for the guardrail system. The important factors identified could be used as feedback to design a new and suitable guardrail system. After the necessary improvements are made, a parametric study of the guardrail system is conducted to investigate the effect of new design changes on the performance. Changing the guardrail system's design parameters, including its splice configuration, guardrail height and post spacing, leads into the process of optimising the design of the roadside structure. This is to eliminate vehicle rollover and failure of the guardrail system. The outcomes of the finite element modelling and the parametric study should improve the performance of the modified design until it exceeds that of the basic design.

1.2 Statement of the problem

The W-beam guardrail system has been the most widely used roadside barrier in the United States since the late 1950s and has performed reasonably well under most impact conditions. However, in recent years, vehicle demographics have changed to include a relatively large proportion of light trucks, such as pickups, vans, and sport-utility vehicles. These vehicles have higher centres of mass and higher bumpers than

conventional automobiles. Standard W-beam guardrails are not able to capture many of these vehicles due to their small effective rail depths and relatively low mounting heights. Furthermore, crash data have shown that light truck impacts with guardrails are more likely to result in rollovers and injuries to occupants than crashes involving conventional automobiles (Ross et al., 2002). In recognition of the potential safety problems associated with light truck crashes, safety performance standards were changed recently as a result of the publication of the Manual for Assessing Safety Hardware, MASH (MASH, 2009), which recommended tests with heavier light trucks to better represent the pickup/van/sport-utility vehicle class.

The weight of the four-door test pickup truck increased from 2,000 kg to 2,270 kg for Length of Need test 3-11. This is because some vehicles specified in the previous criteria (NCHRP Report 350), such as 2000P pickup trucks, have not been manufactured since 2000 or 2001. These changes place greater demands for safety performance on many current roadside safety features. As a result, the severity of the crash impacts described in the MASH has increased significantly when compared with NCHRP Report 350. Recent studies (Bligh et al., 2011) have been conducted to evaluate the performance of guardrail systems under conditions described in the MASH; for instance, a 27 5/8-inch tall, modified G4(1S) steel-post W-beam guardrail and a G4(2W) were unable to redirect the vehicle due to rail rupture when struck by a 5000-lb, 3/4-tonne pickup truck (Bullard et al., 2010a). Length of Need test 3-11 is considered to be the most critical compliance test for evaluating the structural response (Marzougui et al., 2010) that will be used later on for the evaluating the guardrail system of this study. Therefore, in this study, several conditions are considered. These include improving the splice connections, the guardrail height and the post spacing to improve the performance of the guardrail system.

1.3 Research objectives

Impact simulations performed using explicitly nonlinear finite element code are becoming effective tools in the design and validation stages of guardrail systems. The accuracy of the predictions made by these models depends on the model's verification and validation. Some studies of different systems' behaviour have been conducted. To make a contribution that fills the gaps, the objectives of this study are as follows:

1. To evaluate the performance of previous guardrail systems with different designs in terms of vehicle trajectories, occupant risks factors and structural adequacy.
2. To determine the load bearing-displacement response along the beam section by performing experimental assessments that verify the model of the W-beam rail section.
3. To validate the finite element model (created in LS-DYNA) of a G4(2W) wood post guardrail system using data from a previously conducted crash test.
4. To conduct parametric studies of important parameters, including the post spacing and the guardrail height, to improve the performance of guardrail systems.
5. To develop a statistical model that identifies the factors that are significant for guardrail performance.

1.4 Research hypotheses

Different configurations are evaluated through a parametric study of a guardrail system's performance using simulations of full-scale crash tests that focus on guardrail design factors and each system's behaviour. This is done to examine the relationships

among all the design factors and all the performance responses, including the structural adequacy, the vehicle trajectory and the occupational risk factors. Therefore, the following hypotheses are tested using the finite element model and the experimental results.

Hypothesis 1: The mesh size of the W-beam is related to an increase in the accuracy of the results.

Hypothesis 2: Increases in the stiffness of the splice connections are related to increases in the number of bolts.

Hypothesis 3: Higher guardrails are related to increases in guardrail deflection.

Hypothesis 4: Higher guardrails and greater post spacings are related to increases in pickup truck stability and improved trajectories.

Hypothesis 5: Lower occupant risk factors are related to increases in the guardrail height and the post spacing.

1.5 Scope of the study

It would be useful to develop a guardrail with sufficient height and adequate structural adequacy without significantly increasing the cost of the system. Furthermore, a design for a guardrail system that satisfies the MASH's criteria without significantly increasing the cross-sectional area or reducing the post spacing would be beneficial. After identifying gaps in the research, a model of a crash test using a G4(2W) strong wood post system is developed in LS-DYNA.

The scope of this study includes improving the wood post guardrail system until it is able to satisfy the Length of Need criteria given in the MASH for Test 3-11. The improvements to this system include the evaluation of a number of parameters,

including the splice connections, the guardrail height and the post spacing, using computer simulations.

1.6 Significance of the study

One of the major challenges in road safety is to design a guardrail system that provides an adequate level of safety. To provide an appropriate level of safety for an errant vehicle that hits the guardrail system, the safety barrier should be designed to absorb as much energy as possible through deformation of the soil and the guardrail system while maintaining the integrity of the system (Ren & Vesenjak, 2005). Roadside geometries often call for guardrails to be placed close to rigid obstacles. In such cases, guardrail failure is not forgiving; therefore, this study attempts to use LS-DYNA to improve guardrail systems so that they safely and successfully redirect vehicles.

Understanding the characteristics of a guardrail system allows better decisions concerning which systems are more effective in different locations to be made. The parametric study conducted in this study clearly reveals the effectiveness of the design factors on the performance of a guardrail system.

1.7 Thesis organisation

Chapter 1 outlined the following particulars: the rationale for undertaking this study, the problem statement, the objectives, the hypotheses, and the scope and the significance of the study.

Chapter 2 presents a considerable amount of information on previous studies of the design and performance of guardrail systems and pays specific attention to full-scale crash tests of guardrail systems. Furthermore, a brief review of the literature on

numerical and experimental methods and the weaknesses of guardrail systems in terms of the criteria in the MASH are presented.

Chapter 3 describes the research method employed for modelling the G4(2W) guardrail system, developing an LS-DYNA model for static tests and full crash tests involving pickup trucks and the G4(2W) guardrail system and experimental static tests. Furthermore, the parameters involved in the parametric study and the statistical model are presented.

Chapter 4 presents data from experimental tests, finite element models of dynamic crash tests and static tests using LS-DYNA software, the parametric study and the statistical analysis using Design of Experiments Software (DoE). These aspects are discussed on the basis of the objectives and hypothesis.

Chapter 5 summarises the findings and the significance of this study in addition to making recommendations for future research that should to be performed.

CHAPTER 2: LITERATURE REVIEW

2.1 Introduction

W-beam guardrail systems have been widely used in the United States since the late 1950s and have been proven to perform reasonably well under most impact conditions (Reid et al., 1997). However, as new standards are implemented, challenges are observed (MASH, 2009). The results of previous full-scale crash tests for guardrail systems, including the structural adequacy, the vehicle trajectory and the occupant risk factors, are collected and tabulated in Tables 2-3 and 2-4. In addition, the important shift to the new standard for the evaluation of guardrail systems is presented and the weaknesses of guardrail systems according to the newly implemented standard in the MASH are discussed. The last section addresses literature that is relevant to numerical simulations and W-beam sections; it is followed by summaries of the current gaps in the research and the chapter.

2.2 Assessment of guardrail system performance

NCHRP Report 350 and the MASH use three common criteria (Figure 2-1) to assess the safety performance of guardrail systems.

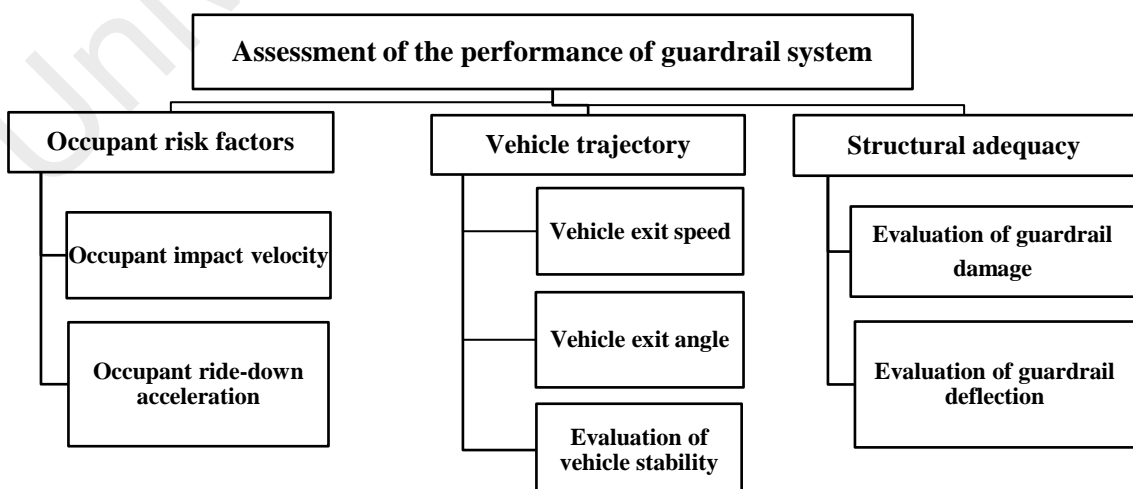


Figure 2-1. Requirements for assessing the performance of a guardrail system

(a) ***Structural adequacy***

Structural adequacy refers to the ability of a barrier to contain and redirect errant vehicles in a controlled manner. In other words, the barrier should not be penetrated during impact and lateral displacement must be controlled.

(b) ***Vehicle trajectory***

The vehicle trajectory refers to ability of a roadside component to keep vehicles upright after an impact. NCHRP Report 350 states that moderate rolling, pitching, and yawing are acceptable. The MASH adds requirements for vehicle stability and limits the maximum roll and pitch angles to 75 degrees. NCHRP Report 350 requires the exit angle to be less than sixty percent of the vehicle angle at the impact point (NCHRP Report 350, 1993; MASH, 2009).

(c) ***Occupant risks factors***

Road safety barriers are designed to absorb the energy generated by an impact and minimise the risk to the vehicle's occupants (Reid et al., 2002; Sicking et al., 1999). The severity of crash is often measured by assessing the most severely injured occupant (Chang & Mannering, 1999). NCHRP Report 350 does not require the occupant risk to be evaluated by means of a flail space model (FSM) for 8000S, 36000V, and 36000T vehicles. Recommended limits on the occupant impact velocity (OIV) and occupant ride-down acceleration (ORA) based on NCHRP Report 350 and the MASH are given for both longitudinal and lateral directions (Table 2-1).

Table 2-1: Requirements for assessing the occupant risk factors

Direction	Occupant Impact Velocity (OIV) Limits (m/s)		Occupant Ride-down Acceleration (ORA) Limits (g)	
	Preferred	Maximum	Preferred	Maximum
Longitudinal and lateral	9	12	15	20

The largest difference in the OIV occurs between the instants of occupant impact and impact with the interior; it is assumed that the occupant remains in contact with the interior and is subjected to the subsequent vehicular acceleration. The highest moving average of the acceleration that occurs after the occupant impacts the interior, 10 m/s^2 , is called the ORA. According to NCHRP Report 350, the preferred limit on the OIV is 9 m/s and the maximum OIV is 12 m/s . In addition, the minimum and maximum ORAs are 15 g and 20 g , respectively.

In this section, common methods of evaluating the occupant risk factors are reviewed. Generally, the amount of danger to occupants during impact is a primary requirement for assessing the performance of roadside safety barrier systems (Polivka et al., 2003). Several methods are used to assess the severity of the risk faced by the occupants of a vehicle. The FSM, which was introduced by Michie in 1981 (and further supported by Gabauer & Gabler, (2008)), calculates the occupant risk by measuring the vehicle's kinematics from the perspective of the velocities of the occupants and their subsequent accelerations. Based on the FSM, the vehicle's occupants are allowed to flail within 0.6 m in the longitudinal direction and 0.3 m in the lateral direction.

The severity of an impact is measured by a crash pulse recorder (CPR), which measures the time history of the acceleration in one direction. Crash pulses were filtered at approximately 100 Hz and changes in the velocity and the mean and peak accelerations are calculated. Changes in velocity (also known as energy equivalent speed (EES) (Zeidler, 1985)) are often used to describe the severity of an impact (Kullgren et al., 1998), which is measured using impact phases (Ydenius, 2009).

To mitigate the severity of single vehicle crashes, passive structures such as guardrails have shown their efficiency to some extent (Taylor, 2005). To ensure that any collision is less severe than one with a hazardous object next to the road, a crash severity measure called the acceleration severity index (ASI) is used to compare the maximum vehicle

acceleration that an occupant is exposed to during the crash. European crash test standard EN-1317 requires the ASI to be below 1.4 (EN 1317-2, 1998; Simpson, 2000). However, there has been little research into the connection between the ASI and actual occupant injuries. Gabauer & Gabler (2008) show that the ASI is as predictive as delta-v in discriminating between serious and non-serious injuries (Ydenius, 2009).

Basically, the acceleration of the vehicle's centre of gravity is recorded and compared using the following techniques:

- The test risk assessment programme (TRAP),
- The numerical analysis of roadside design (NARD) validation parameters,
- Analysis of variance and
- Geer's parameters.

The TRAP measures standard occupant risk factors using vehicle crash data in accordance with the guidelines of the National Cooperative Highway Research Program (NCHRP) and the European Committee for Standardisation (Comite Européen de Normalisation (CEN)) (TRAP, 1998). The NARD validation procedures are consistent with the results of signal analysis and comparison between the acceleration time histories of full-scale tests and finite element method simulations (Basu & Haghighi, 1988). The residual error between two signals is calculated as part of an Analysis of variance (ANOVA) (Ray, 1996). Then, Geer's method is used to compare the magnitude, phase, and correlation of two signals to arrive at a quantitative measure of the similarity between two acceleration time histories (Geers, 1984). The acceleration data used in the TRAP must be filtered at a cut-off frequency of 100 Hz (Plaxico et al., 2000). Both the OIV and the ORA are compared with the NCHRP Report 350's current threshold values to ensure the device's efficiency (Michie, 1981; NCHRP Report 350, 1993).

In this field, Geer's method has yet to be widely studied. Ray et al. (1986), who sought to assess the effectiveness of the lateral OIV, found that the lateral component of the first impact does not always cause serious injuries. Council & Stewart (1993) attempted to link actual injuries obtained in real collisions to those calculated from full-scale crash test data, but due to limited information, their conclusion was not validated. Gabauer & Gabler (2004) asserted that the OIV is useful for assessing injuries to occupants on the basis of 58 frontal crashes and learned that the OIV offers no statistically significant advantage over a traditional and simpler metric of crash severity, delta-V (Gabauer & Gabler, 2008).

Guardrail collisions often result in severe injuries and fatalities (Ray & Weir, 2001). Side-impact crash tests evaluate the possibility of injury to a vehicle's occupants and provide maximum safety during crashes (Ray et al., 1998). The National Highway Traffic Safety Administration (NHTSA) classifies the injuries into three levels: non-severe injuries, severe injuries, and fatal injuries (Kockelman & Kweon, 2002). Most analyses of injury severity have focused on modelling the most severe injuries (Zhu & Srinivasan, 2011). It is assumed that similar injuries result from similarly severe impacts. However, several factors, such as seatbelt use, speed of travel, number of occupants, type of vehicle and crash configuration, affect the severity and outcomes of crashes (Keall & Frith, 2004). Failure to use a seatbelt could result in ejection from the vehicle injuries such as cervical spine injuries (Otte et al., 2005).

2.2.1 Test levels

In general, roadside barrier designers use intuition, real crash tests and engineering-based principles. Analytical methods are less effective for designing systems such as these. In the United States, roadside barriers should meet the requirements of NCHRP Report 350 and the criteria in the recently released MASH.

In 1993, NCHRP Report 350, entitled “Recommended Procedures for the Safety Performance Evaluation of Highway Features”, was published, and most crash tests were conducted according to its criteria. NCHRP Report 350 includes six different test levels for evaluating guardrail system performance. Basically, the lower test levels are used to evaluate safety barriers on low-traffic roadways, and the higher test levels are used to evaluate hardware features on high-traffic roadways. Test level 1 (TL-1) is for features inside work zones and along lower service level roadways. In addition, test level 2 (TL-2) is mostly used to evaluate the hardware used in most local areas and many work zones. Test level 3 (TL-3) is used to assess a wide range of higher service level roadways and high-speed highways. Test levels 4 (TL-4) through 6 (TL-6) are used to determine the applicability of features encountered by heavy vehicles and to understand the behaviour of longitudinal barriers during penetration.

Of the six test levels, TL-3 is used to evaluate the guardrail system in this study because it is designed for a wide range of higher service level roadways and high-speed highways. The recommended test matrix for TL-3 based on NCHRP Report 350 and the MASH is presented in Table 2-2. It should be noted that 820C and 1100C vehicles are passenger sedans and 2000P and 2270P vehicles are pickup trucks and that the weight of each vehicle is recorded in kilograms. During the test, the vehicle is directed towards the guardrail system at the speed and angle specified in NCHRP Report 350 and the MASH.

Table 2-2: Length of Need 3-11 test based on NCHRP Report 350 and the MASH

Test		Impact condition NCHRP Report 350			Impact condition (MASH)		
		Vehicle	Speed (km/h)	Angle (Deg)	Vehicle	Speed (km/h)	Angle (Deg)
Test level	Designation						
3	3-11	2000P	100	25	2270P	100	25

2000P and 2270P vehicles are pickup trucks. The numbers, 2000 and 2270, represent the weights of the vehicles in kilograms.

Given the requirements in NCHRP Report 350 and the MASH for employing the worst test conditions, the critical impact point (CIP) that gives the worst result should be selected (Bligh & Mak, 2002). For guardrail systems subjected to Length of Need test 3-11, the CIP is normally selected based on the maximum potential for wheel snagging at a post section with a rail splice. Nevertheless, for a strong-post guardrail system, the CIP region could be approximately 1 metre with a rail splice every 3.8 m (Rosson et al., 1996).

2.3 Review of existing guardrail designs

The performance of safety barriers has been evaluated by the NCHRP and the American Association of State Highway and Transportation Officials (AASHTO) using NCHRP Report 230 (NCHRP Report 230, 1983), NCHRP Report 350 or the recently released MASH of the AASHTO (MASH, 2009; NCHRP Report 350, 1993). In the last few years, several tests have been performed based on NCHRP Report 230 to assess the performance of safety roadside barriers. These tests reported that most of the designs were acceptable for highway use (Faller et al., 1998).

In July 1993, NCHRP Report 350 added additional aspects, including definitions of test levels for assessing the performance of roadside barriers. The test procedures for Report 230 were changed in NCHRP Report 350 (Mak & Bligh, 2002a). The most significant change was the change from using a 2040 kg sedan to using a 2000P pickup truck as the test vehicle (Mak & Bligh, 2002b).

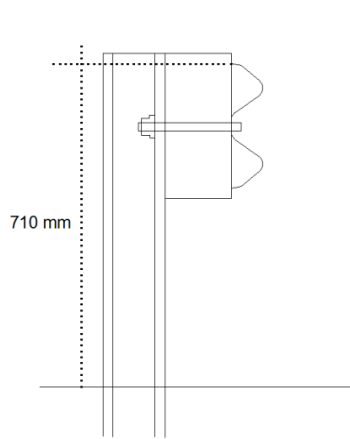
Rather than the successful performance of safety roadside barriers demonstrated with NCHRP Report 230 (Faller et al., 1998), it was shown that most of the guardrail system designs (e.g., the G4(1S), G2 and G9 guardrail systems) are inefficient according to the results of the level 3 Length of Need test described in NCHRP Report 350. After the change of the test vehicle from a 2,040 kg sedan to a 2,000 kg pickup truck in NCHRP

Report 350, several problems were observed; these are because of the centre of gravity of a pickup truck is higher than that of a sedan. In include wheels snagging on guardrail posts and ruptures at the splice connections between the rails. These problems 2009, the AASHTO introduced the MASH, which uses the same procedures as NCHRP Report 350 to assess roadside barrier performance in terms of the speeds, angles of impact and weights of vehicles (MASH, 2009).

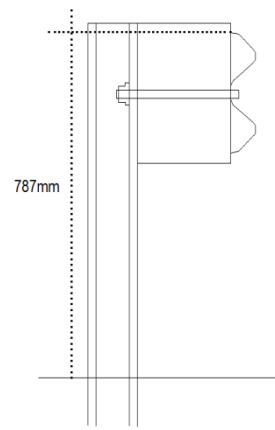
The MASH and NCHRP Report 350 indicate that the evaluating roadside safety barrier performance includes examining their structural adequacy, occupant risk and vehicle trajectory (MASH, 2009; NCHRP Report 350, 1993). A review of common guardrail systems is conducted to evaluate their performance in terms of three main criteria: the occupant risk factor, the vehicle trajectory and the structural adequacy.

2.3.1 Guardrail system classification

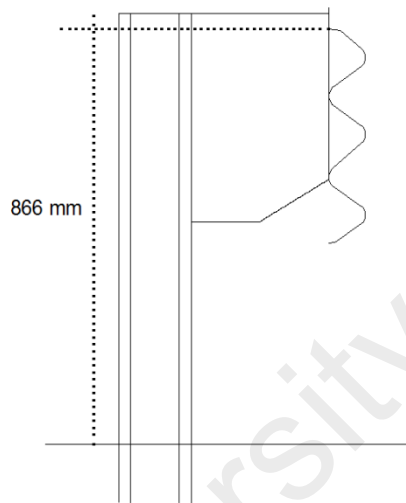
Guardrail systems, which consist of posts and W-beam (or Thrie-beam) rails, use blockouts between the rails and the posts as break joints to provide a higher capacity for energy absorption. Each rail is connected to the blockout with one bolt that passes through a slotted hole (Tabiei & Wu, 2000a). The thickness of a blockout is also called its length or depth. The typical post spacing of a guardrail is the centre-to-centre distance between posts or the distance from the centreline of the bolts attaching the rails to the posts. A system has a splice configuration when a connection between two or more linear materials is located either in midspan or at a post. Figure 2-2 shows the common types of guardrail systems used in highways. Different types of guardrail systems are described in following subsections.



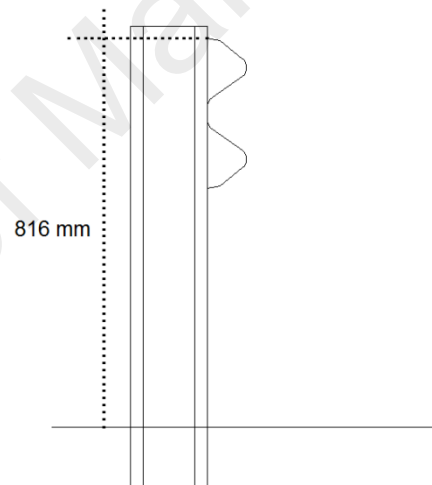
(a) Modified G4(1S) W-beam guardrail



(b) Midwest guardrail system (MGS)



(c) Modified Thrie-beam guardrail



(d) Modified weak-post W-beam guardrail

Figure 2-2. The common types of W-beam guardrail systems (Ferdous et al., 2013)

2.3.1.1 G4(1S) and G4(2W) strong-post W-beam guardrails

A stiffer system should be considered when stiff objects are near roadways to minimise the maximum deflection and reduce the possibility of severe injury (Rosson et al., 1996). Strong-post systems have been used to prevent errant vehicles from crashing into stiff objects and traversing hazardous roadside geometries for a long time (Faller et al., 2007). This system is the most common of the guardrail systems used in the United

States (Coon & Reid, 2005). One location that demands a lower level of barrier deformation is around a culvert. A nested rail with smaller spacing between rigid steel posts is used to increase the stiffness of the strong-post system (Faller et al., 2000). Strong-post guardrails have delivered reasonable performance since 1950 under different crash test conditions (Reid et al., 1997). Recently, the behaviour of this system has become more critical due to the increase in the number of vehicles with higher centres of mass (Reid et al., 1997). Wheel snagging is a major problem with strong-post systems because it results in vehicle instability. This problem could lead to excessive deceleration and cause the vehicle to be redirected in an unstable way (Plaxico et al., 2000). A tyre snagging on a post can cause the wheel assembly to be raised, which causes the vehicle to roll over (Reid, 2000). Two types of strong-post guardrail systems currently used in highways, known as G4(1S) and G4(2W) (Ray & McGinnis, 1997), are illustrated in Figure 2-2(a) and Figure 2-3, respectively. In the G4(1S) type, the rail is supported by steel posts, and the most common type of post used in this type of system is W152×13.4.

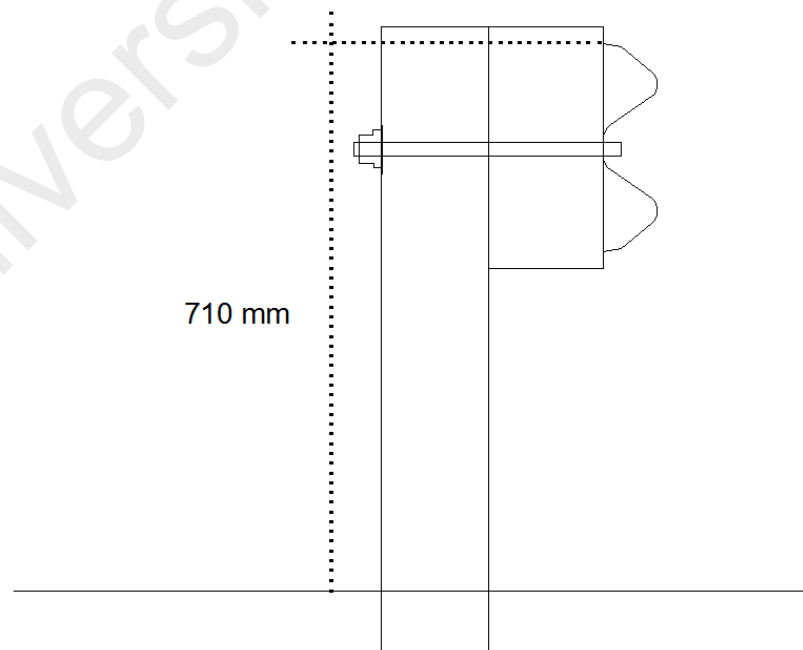


Figure 2-3. A typical view and detail of a G4(2W) strong-post system (Bullard et al., 2010b)

With the G4(2W) system, 150 mm×200 mm wood posts are often used to support the rail. In both the G4(2W) and modified G4(1S) strong-post guardrail systems, the W-beam rail is fastened to the post with a 16 mm bolt that passes through a wood blockout to the back of the guardrail post (Plaxico et al., 2003). A blockout is suggested to ensure that the post and rail are separated to reduce the possibility of wheel snagging after a vehicle hits a post (Kennedy et al., 2006). Subsequent testing showed that a G4(1S) guardrail system supported with W150×13 steel posts is able to contain a 3/4 tonne 2-door pickup truck in accordance with NCHRP Report 350. In addition, G4(2W) strong wood post guardrails with 200 mm wood posts and offset blocks are acceptable, but pickup trucks are unstable after crashing (Bullard et al., 2010b). This system has also been constructed using round wood posts with diameters of 184 mm (7.25 in). Wood posts are popular because they are cheaper than steel and plastic posts (Faller et al., 2009).

2.3.1.2 Midwest guardrail system (MGS)

In 2000, the Midwest Roadside Safety Facility (MWRSF) sought to develop a new guardrail system with better performance for vehicles with higher centres of mass (Polivka et al., 2004). This system is known as the MGS (Figure 2-2(b)). The changes in the MGS are the increased guardrail height of 788 mm (31 in) and the reduction of the posts' embedment depth to 1,016 mm (40 in). For this type of barrier, the depth of the blockout is increased to 305 mm and the splice connection is moved to midspan (Figure 2-4), which results in the barrier being able to contain and redirect both pickup trucks and small cars, according to the impact conditions described in NCHRP Report 350 (Faller et al., 2009). The 706 mm MGS has not yet been tested against NCHRP Report 350; nevertheless, with regard to improving the performance of the G4(1S) system, it is believed that this system should be able to meet the requirements of the TL-3 Length of Need test in NCHRP Report 350 (Faller et al., 2007).

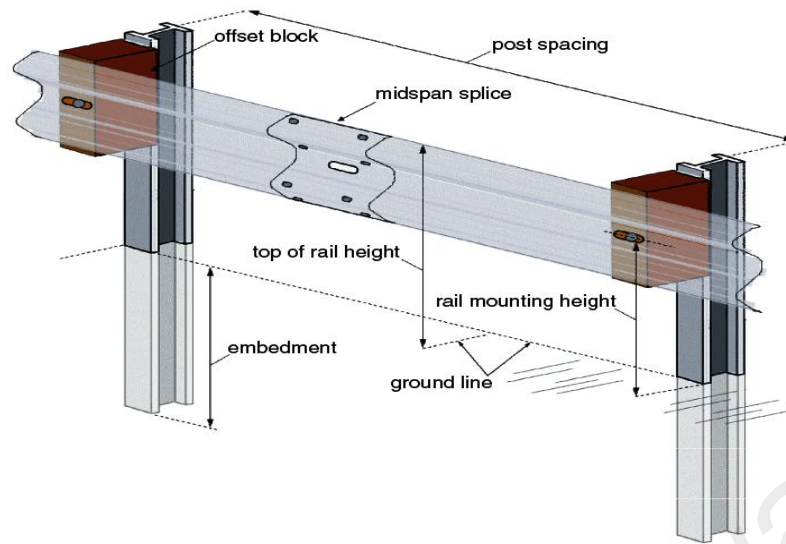


Figure 2-4. Use of midspan splices and offset blocks in a MGS (Ochoa, C & Ochoa, T, 2011)

2.3.1.3 Guardrails with kerbs

Kerbs are special structures used along roadway edges to provide, for example, drainage control, roadway edge delineation and support, right-of-way reduction, and sidewalk separation. Designing W-beam guardrails with kerbs is more complex than designing other guardrail system in terms of the vehicle trajectory criteria. Based on safety standards, it has been reported that guardrails with kerbs higher than 102 mm are not capable of redirecting vehicles safely (Faller et al., 2004). Bligh & Mak (1999) found that kerbs and other non-rigid or short fixed objects caused more rollover crashes than rigid fixed object crashes (Jiang et al., 2011). Some full-scale crash tests have been conducted to assess the performance of guardrails with kerbs higher than 102 mm. The results indicate that although these components were capable of containing and redirecting pickup trucks, in some cases, a W-beam ruptures at a splice connection (the connection between two rails) and vehicles climb or vault over the barrier (Polivka et al., 2000). To obtain a desirable result, several alternatives, including guardrail nesting (to increase the system's stiffness) and using 10 gauge W-beams, have been considered

to improve the system's performance. In addition, placing the kerbs farther from the guardrail may reduce damage to sections of the W-beams (Faller et al., 2004).

2.3.1.4 Weak-post W-beam guardrail (G2)

In the 1960s, it was found that strong-post systems could cause greater deceleration as the result of severe wheel snagging and vehicle pocketing (Burnett et al., 1967). In 1965, the first weak-post guardrail, a set of W-beams connected to S75×8.5 steel posts, was used in New York (Faller et al., 2009). This system (Figure 2-2(d)) is more flexible than other types of guardrail system, such as strong-post guardrail systems (Van Zweden & Bryden, 1977). A modified weak-post guardrail system with improved connections was subjected to full-scale crash tests. This system was deemed similar to cable guardrails in relation to posts that were broken or bent away from the rail during impact. Therefore, rail separation is an important part of this system's design because the rail should be in contact with the vehicle during impact. After separation, the performance of a weak-post system resembles that of a cable anchored at the ends (Ray et al., 2001a).

A G2 guardrail system is a common type of weak-post W-beam guardrail system that includes S3×5.7 posts spaced at 3.81 metres. Although it is effective (Hendricks & Wekezer, 1996), a weak-post W-beam guardrail system is unable to redirect a 2000P pickup truck at test level 3, which results in vehicles overriding the guardrail (Ray & McGinnis, 1997; Ray et al., 2001a). Nevertheless, the occupant risk factors and the vehicle trajectory are considered acceptable based on standard requirements. The most challenging part of designing a weak-post system is its structural adequacy because this system causes the rail to be ruptured or overridden (Ray et al., 2001a).

2.3.1.5 Thrie-beam guardrail (G9)

Two types of Thrie-beam guardrail system are commonly used along highways: standard strong wood with steel posts (G9) and modified Thrie-beam (Figure 2-2(c)). The modified Thrie-beam guardrail system consists of 2.1 m long W6×9 steel posts, W14×22 blockouts, and 3.8 m long sections of standard Thrie-beam guardrail (Ferdous et al., 2011). To improve the performance of standard Thrie-beam guardrails, a modified Thrie-beam system was designed to minimise the possibility of larger vehicles rolling over (Ivey et al., 1986). A full-scale crash test was performed on a Thrie-beam system with steel offset blocks. According to the requirements of NCHRP Report 350, this system failed due to severe wheel snagging (Mak et al., 1990; Mak et al., 1996). This system was modified by replacing the 6 ft-9-1/4-inch long × 6 inch × 8 inch wood posts with wood offset blocks. After this modification, the system was successfully crash tested (Abu-Odeh et al., 2011; Buth et al., 2000b). In addition, a Thrie-beam guardrail on strong wood posts successfully contained and redirected a 2000P pickup truck, according to Length of Need test 3-11 in NCHRP Report 350.

A summary of the crash test results is presented in Tables 2-3 and 2-4. A review of the performance of different guardrail systems is presented in the next sections.

Table 2-3: Summary of the test results for a guardrail system (Length of Need 3-11 test)

Design number	References	Guardrail Type	Post design				Vehicle Speed (Km/hr)		Angle (deg)		Max Deflection (mm)		System Damage	Vehicle Trajectory		Criteria
			Height (mm)	Type	Post Spacing (mm)	Embedment Depth (mm)	Impact	Exit	Impact	Exit	Dynamic	Permanent		Stability	Damage	
Strong-post guardrail systems																
Design 1	(Mak et al., 1995)	W-Beam G4 (2W)	686	St-Wood 152×203	1900	910	100.8	70.8	24.3	8.1	820	690	Moderate	Satisfactory	Moderate	Test 3-11, NCHRP 350
Design 2	(Mak et al., 1995)	G4(1S) W-Beam	686	Steel W152×216	1900	1115	101.4	58.7	26.1	5.2	910	640	Moderate	Failed	Moderate	Test 3-11, NCHRP 350
Design 3	(Buth et al., 1999)	G4(1S)W-beam	710	St-W150×12.6 steel	1905	1118	99.68	N/A	25.6	N/A	1000	ruptured	Extensive	Failed	Extensive	Test 3-11, NCHRP 350
Design 4	(N.S.M, 2007)	W-beam Guardrail	686	St-Nucor post	1905	1294	100.5	N/A	24.5	4.5	1150	900	N/A	Satisfactory	N/A	Test 3-11, NCHRP 350
Design 5	(Kennedy. et al., 2006)	W-beam Guardrail	710	St-HALCO X-44	1905	940	99	64.8	25	13	700	600	Extensive	Satisfactory	Moderate	Test 3-11, NCHRP 350
Design 6	(Bligh et al., 1997)	W-beam Guardrail	710	W 150×13.5	1905	965	101.8	62.3	24.8	9.6	750	450	Moderate	Satisfactory	Minimal	Test 3-11, NCHRP 350
Design 7	(G.H. Products , 2008)	single Face-W-beam	702	St- W 6×8.5	1905	1016	105.7	72	24.6	20	1320	810	N/A	Satisfactory	N/A	Test 3-11, MASH08
Design 8	(Faller et al., 2007)	G4(1S) W-beam	706	St- W 152×13.4	1905	1098	98.3	N/A	25.6	N/A	778	ruptured	Extensive	Satisfactory	Moderate	Test 3-11, NCHRP 350
Design 9	(Faller et al., 2007)	G4(1S) W-beam	706	St- W 152×13.4	1905	1098	100.4	50.4	25.8	20.5	1196	845	Moderate	Satisfactory	Moderate	Test 3-11, NCHRP 350

Table 2-3 continued

Design 10	(Trinity, 2007)	W-beam	702	W 6×8.5	1910	N/A	107.8	52	23.4	16	1040	690	N/A	Satisfactory	N/A	Test 3-11, NCHRP 350
Design 11	(Bullard et al., 1996)	Roadside G4(1S) W-beam	710	St-W150×12.6 steel	1905	1100	101.5	55	25.5	16	1000	700	Minimal	Satisfactory	N/A	Test 3-11, NCHRP 350
Design 12	(Bligh, & Menges, 1997)	G4(1S) W-beam	710	St-W150×13.5 steel	1905	1100	100.9	46.1	25.2	13.4	1130	720	Minimal	Satisfactory	Minimal	Test 3-11, NCHRP 350
Design 13	(N.S.M, 2007)	Roadside-W-beam	788	St-Nucor post	1905	1190	98	N/A	24.5	5	1050	800	N/A	Satisfactory	N/A	Test 3-11, NCHRP 350
Design 14	(G.H. Products, 2006)	Road side-W-beam	788	St- W 6×8.5	1905	N/A	97.7	65	25.9	12	890	560	N/A	Satisfactory	N/A	Test 3-11, NCHRP 350
Design 15	(M.P. Technologies, 2002)	W-beam	N/A	W 150×13.5	1905	N/A	101.4	49.4	25.4	18.4	840	265	N/A	Satisfactory	N/A	Test 3-11, NCHRP 350
Design 16	(M.I. Molding, 2008)	W-beam	N/A	N/A	1910	1016	100.4	N/A	25	N/A	1300	400	N/A	Satisfactory	N/A	Test 3-11, NCHRP 350
Design 17	(N.S.M. Inc, 2009)	Strong-post system	788	St- Nucor post (W6×9)	1905	1190	101	56	25	9.2	1440	980	Moderate	Satisfactory	n/a	Test 3-11, NCHRP 350
Guardrail with kerb																
Design 18	(Bligh et al., 2004)	W-beam	686	W150×13 (W6×9)	1905	1118	99.7	53.6	25.4	15.4	584	84	Major	Satisfactory	Major	Test 3-11, NCHRP 350
Design 19	(Bligh et al., 2004)	W-beam	686	178 mm dia Round wood post	1905	1118	101.7	59.4	25.8	21.2	688	89	Major	Satisfactory	Major	Test 3-11, NCHRP 350
Design 20	Faller et al, 2004)	W-beam Guardrail	788	St- W 152×13.4 Steel	1905	1172	96.6	48	25.8	6.7	1024	611	Moderate	Satisfactory	Moderate	Test 3-11, NCHRP 350

Table 2-3 continued

Weak-post guardrail systems																
Design 21	(Mak et al., 1996)	G2-W-beam	760	Weak-post S 3×5.7	3800	610	99.8	N/A	24.4	N/A	2400	1800	Extensive	Failed	N/A	Test 3-11, NCHRP 350
Design 22	(Buth et al., 2000a)	G2 Rodside W-beam	820	Weak-post S 75×8.5	3810	780	102.4	59.3	26.5	2	2120	1640	Moderate	Satisfactory	Major	Test 3-11, NCHRP 350
Midwest Guardrail systems																
Design 23	(M.R.S. Facility, 2005)	MGS	788	St -W 152×13.4	476	1019	96.8	59.5	25.6	12.9	447	305	Moderate	Satisfactory	Moderate	Test 3-11, NCHRP 350
Design 24	Hascall et al., 2007)	MGS	788	Round Ponderosa Pine Posts	1905	940	100.2	37.4	25.5	19.9	956	705	Moderate	Satisfactory	Moderate	Test 3-11, NCHRP 350
Design 25	(Ferdous et al., 2013)	MGS	788	Round Douglas Fir Posts	1905	940	100	N/A	25.5	N/A	1529	902	Moderate	Satisfactory	Moderate	Test 3-11, NCHRP 350
Design 26	(Polivka et al., 2006a)	MGS	788	St- W152×13. 4	1905	1016	101.1	63.7	25.5	13.5	1114	803	Moderate	Satisfactory	Moderate	Test 3-11, NCHRP 350
Design 27	(Faller et al., 2007)	MGS	788	St- W 152×13.4	1905	1016	100.7	68.4	25.2	7.0	1447	1089	Moderate	Satisfactory	Moderate	Test 3-11, NCHRP 350
Design 28	(M.R.S. Facility, 2005)	MGS	788	St -W 152×13.4	1905	1019	98.1	55.1	25.6	19.3	1094	652	Moderate	Satisfactory	Minimal	Test 3-11, NCHRP 350
Design 29	(Polivka et al 2004)	MGS	788	St- W 152×13.4	1905	1019	99	N/A	24.7	N/A	N/A	N/A	Extensive	Unsatisfactory	Extensive	Test 3-11, NCHRP 350
Design 30	(Karlsson, 2000)	MGS	788	W152×13. 4	1905	959	100.4	N/A	25.9	N/A	1464	870	Moderate	Satisfactory	Minimal	Test 3-11, NCHRP 350
Thrie-beam rail guardrail systems																
Design 31	(Buth, & Menges , 1999)	Roadside- Thrie-beam	804	St- Wood 150×200	1905	1231	99.6	73.6	23.6	14.7	680	390	Minimal	Satisfactory	Minimal	Test 3-11, NCHRP 350
Design32	(Mak et al., 1996)	G9- Thrie-beam	813	Steel W 152×229 (W6×9)	1900	1137	102.2	54.5	26.1	35	1070	640	Moderate	Failed	Extensive	Test 3-11, NCHRP 350
Design 33	(Mak et al., 1996)	Modified Thrie- beam	864	Steel W 152×229 (W6×9)	1900	1237	100.2	67.4	25.1	11.1	1020	610	Moderate	Satisfactory	Moderate	Test 3-11, NCHRP 350

Table 2-4: Summary of the occupant risk results for guardrail systems

Design Number	References	Guardrail		Post design			Speed impact (Km/hr)	Angle (deg)	Guardrail System Damage	Vehicle Trajectory		Occupant Risks Factors			
		Type	height (mm)	Type	Post Spacing (mm)	Embedment Depth (mm)				Exit	Exit	Vehicle Stability	Vehicle Damage	Longitudinal impact velocity (m/s)	Lateral Ride-down Acceleration (G's)
Guardrail system no kerb															
1	(Mak et al., 1995)	W-Beam G4 (2W)	686	St-Wood 152×203	1900	910	70.8	8.1	Moderate	Satisfactory	Moderate	7.5	11.6	5.9	11.4
2	(Mak et al., 1995)	G4(1S) W-Beam	686	Steel W150×12.6	1900	1115	58.7	5.2	Moderate	Failed	Moderate	7.6	7.8	4.9	6.2
3	(Buth et al., 1999)	Roadside-G4(1S) W-beam	710	Steel W150×12.6	1905	1118	N/A	N/A	Extensive	Failed ruptured	Extensive	9.16	15.8	4.63	8.87
4	(N.S.M. Inc, 2007)	Roadside- W-beam	686	St-Nucor post	1905	1294	N/A	4.5	N/A	Satisfactory	N/A	3.7	9.2	4.1	6.4
5	(Kennedy et al., 2006)	Guardrail W-beam	710	St- HALCO X-44	1905	940	64.8	13	extensive	Satisfactory	Moderate	3.8	10.8	5	11.6
6	(Bligh et al., 1997)	W-beam	710	W 150×13.5	1905	965	62.35	9.67	Moderate	Satisfactory	Minimal	7.38	7.76	5.21	6.54
7	(G.H. Products, March 2008)	single Face- W-beam	702	Steel W150×12.6	1905	1016	72	20	N/A	Satisfactory	N/A	4	8.7	4.6	8.1
8	(Polivka et al. 2006a)	G4(1S) W-beam guardrail	706	W 150×13.5	1905	1098	50.4	20.5	Moderate	Satisfactory	Moderate	5.38	6.92	3.99	6.61

Table 2-4 continued

9	(Trinity, 2007)	W-beam	702	Steel W150×12.6	1910	N/A	52	16	N/A	Satisfactory	N/A	5.3	12.2	4.7	13.1
10	(Bullard et al., 1996)	Roadside G4(1S) W-beam	730to 710	St- W150×12.6	1905	1100	55	16	Minimal	Satisfactory	N/A	7.1	7.9	4.4	8.4
11	(Bligh, & Menges , 1997)	G4(1S) W-beam	730 to 710	St- W150×13.5	1905	1100	46.12	13.4	Minimal	Satisfactory	Minimal	6.74	9.8	4.3	6.86
12	(N.S.M. Inc, 2007)	Roadside- W- beam	788	St-Nucor post	1905	1190	N/A	5	N/A	Satisfactory	N/A	3.4	6.2	4.2	6.4
13	(G.H. Products, 2006)	Road side- W- beam	788	Steel W150×12.6	1905	N/A	65	12	N/A	Satisfactory	N/A	5	10.7	3.2	11.5
Guardrail with kerb															
14	(Bligh et al., 2004)	W-beam	686	W 150×13.5	1905	1118	53.6	15.4	Major	Satisfactory	Major	5.7	14.6	4.5	9.1
15	(Bligh et al., 2004)	W-beam	686	178 mm dia Round wood post	1905	1118	59.4	21.2	Major	Satisfactory	Major	5.8	7.6	4.9	8.3
16	Faller et al, 2004)	W-beam Guardrail	788	W 150×13.5	1905	1172	48	6.7	Moderate	Satisfactory	Moderate	5.23	10.5	3.93	8.66
Weak-post system															
17	(Mak et al., 1995)	G2-W-beam	760	Weak-post S 3×5.7	3800	610	N/A	N/A	Extensive	Failed	N/A	5	4.2	3	4.5
18	(Buth et al., 2000a)	G2 Rodside W- beam	820	Weak-post S 75×8.5	3810	780	59.3	2	Moderate	Satisfactory	Major	3.9	5.9	4.2	6.4

Table 2-4 continued

Midwest W-beam															
19	(M.R.S. Facility, 2005)	Midwest W-beam	787	W 150×13.5	476	1019	59.5	12.9	Moderate	Satisfactory	Moderate	7.62	10.67	5.61	8.97
20	(Faller, 2008)	Midwest- W-beam	787	Round Ponderosa Pine Posts	1905	940	37.4	19.9	Moderate	Satisfactory	Moderate	6.85	5.9	7.18	4.09
21	(Faller, 2008)	Midwest- W-beam	787	Round Douglas Fir Posts	1905	940	N/A	N/A	Moderate	Satisfactory	Moderate	4.03	8.76	4.03	5.69
22	(Polivka et al. 2006a)	Midwest Guardrail System W-beam	787	W 150×13.5	1905	1016	63.7	13.5	Moderate	Satisfactory	Moderate	4.67	8.23	4.76	6.93
23	(Faller et al., 2007)	MGS W-beam	787	W 150×13.5	1905	1016	68.4	7	Moderate	Satisfactory	Moderate	5.2	8.77	4.51	5.34
24	(M.R.S. Facility, 2005)	Midwest W-beam	787	W 150×13.5	1905	1019	55.1	19.3	Moderate	Satisfactory	Minimal	5.58	9.5	3.89	6.94
25	(Polivka et al., 2004)	MGS W-beam	787	W 150×13.5	1905	1019	N/A	N/A	Extensive	Unsatisfactory	Extensive	4.98	6.51	3.15	8.19
26	(Johnson et al., 2008)	MGS	787	W 150×13.5	1905	959	N/A	N/A	Moderate	Satisfactory	Minimal	6.16	9.49	3.43	6.43
27	(Bielenberg et al., 2007)	MGS Longspan with Culvert	787	152 mm ×203 mm	7620	1016	56.7	1	Minimal	Satisfactory	Moderate	2.92	6.48	3.23	5.91
28	(Bielenberg et al., 2007)	MGS Longspan with Culvert	787	152 mm ×203 mm	7620	1016	54.3	18.8	Moderate	Satisfactory	Moderate	4.09	7.34	4.09	4.24
Thrie-beam guardrail systems															
29	(Buth, & Menges,1999)	Roadside-Thrie-beam	804	Wood 150×200	1905	1231	73.6	14.7	Minimal	Satisfactory	Minimal	6.3	8.4	5.6	9
30	(Mak et al 1995)	G9- Thrie-beam	813	Steel W 152×229 (W6×9)	1900	1137	54.5	35	Moderate	Failed	Extensive	8	7	4.9	6.3
31	(Mak et al 1995)	Modified Thrie-beam	864	Steel W 152×229 (W6×9)	1900	1237	67.4	11.1	Moderate	Satisfactory	Moderate	7.8	9.7	5.2	9

2.4 Analysis of previous guardrail system designs

This section describes literature pertaining to and analysing factors affecting the behaviour of guardrail systems; these factors are categorised according to the systems' designs. Then, a comprehensive database is created using the data from previous full-scale crash tests, which are classified according to guardrail type. Finally, guardrail systems are analysed and categorised based on their effectiveness with respect to the crash behaviour of the system according to three main parameters: the vehicle trajectory, the occupant risk factors and the structural adequacy.

2.4.1 Analysis of the vehicle trajectories of guardrail systems

The trajectory of a vehicle after a collision is concerned with the path and final position of the striking vehicle and the probable involvement of this vehicle in secondary collisions. In accordance with NCHRP Report 350, the vehicle's exit speed and angle are measured when the vehicle loses contact with the test article. These parameters are to prevent intrusions across adjacent lanes and probable secondary collisions with other vehicles in the same lane

To evaluate the performance of a guardrail system on the basis of previously conducted crash tests, those subjected to the TL-3-11 Length of Need crash test are classified, compared and analysed.

Table 2-3 presents several strong-post systems alongside other guardrail types. The system designed by Mak et al. (1995), which had a height of 686 mm and steel posts (W152×216), resulted in the test vehicle rolling over. The post was then changed to St-Wood 152×203, and vehicle was redirected back on the road in a safe manner.

Designs that used St-Nucor post and a height of 686 mm were also proven to be successful (N.S.M, 2007). The guardrail system height was changed from 686 to 788

mm. Buth et al. (1999) designed a system with a height of 710 mm with a post spacing of 1905 mm using St-W150×12.6 steel, however, the result was not successful. In contrast, a design with the same height and post spacing and with HALCO X-44 posts resulted in the extensive damage to the guardrail system, an acceptable vehicle trajectory and moderate damage to the vehicle. This could be because HALCO X-44 posts are not as strong as conventional steel I-beam posts. It could be said that post systems with lower stiffnesses might provide better performance in terms of vehicle trajectories and occupant risk factors. However, increasing the strength of the W-beam rail system and the splice configuration to prevent rails from rupturing should be considered further.

The MGS (with an embedment depth of 940 mm) by Hascall et al. (2007) and Ferdous et al. (2013) sustained moderate damage to the barrier system and the vehicles, and the tests were successful. A guardrail system with a 1016 mm embedment depth was moderately damaged, as documented by Polivka et al (2006a) and Faller et al. (2007). In contrast, an MGS designed by Karlsson (2000) and M.R.S. Facility (2005) with a 1019 mm embedment depth provided good results in terms of minimal damage to the vehicle, which is in contrast to the results of Polivka et al. (2004).

The vehicle trajectories of the guardrail systems are evaluated based on the results collected in Table 2-3 and demonstrated in Figure 2-5.

W-beams that are mounted higher improve a guardrail system's performance in terms of capturing vehicle tyres and reducing the probability of vehicle rollover. Attention should be given to small cars due to their lower centres of gravity, which cause them to become wedged under the barrier and increase the probability of their wheels snagging on guardrail posts (Sicking et al., 2002). According to Table 2-3, higher guardrails provide better crash performance in two cases: guardrails with heights of 686 and 702-

706 mm resulted in vehicle rollover (Designs 2 and 3). Design 3 caused the maximum amount of damage to the vehicle's compartment, and Designs 5 and 8 suffered from extensive guardrail damage. By increasing the guardrail height to 788 mm, the vehicle trajectory was improved and the damage to the guardrail was decreased (Designs 13, 14, 17). In other words, higher guardrails effectively contain vehicles with higher centres of gravity by redirecting such vehicles while absorbing the maximum amount of energy. However, an extensive study is needed to investigate the effects of varying the guardrail height on the stability and vehicle trajectory results of NCHRP Report 350 or the MASH criteria.

The vehicle exit angle is important because a rebounding vehicle could cause a multiple-car collision (Karlsson, 2000). The vehicle exit angle works in parallel with the vehicle angle in relation to the possibility of crashing into other vehicles. It is preferred that vehicles be smoothly redirected to the roadway with an exit angle that is less than 60 percent of the impact angle (NCHRP Report 350, 1993). Nevertheless, few designs were capable of redirecting vehicles smoothly despite having higher exit angles. By increasing the guardrail's stiffness, the probability of sharp vehicle redirection is increased.

Figure 2-5 exhibits the Thrie-beam system's maximum vehicle exit angle and the weak-post system's minimum vehicle exit angle. When the guardrails have kerbs, the greater vehicle exit angles could be due to vehicle instability after impact with the kerb. In addition, Designs 20 and 21 resulted in major damage to the test vehicles, which might be the result of multiple crashes with both kerbs and guardrail systems.

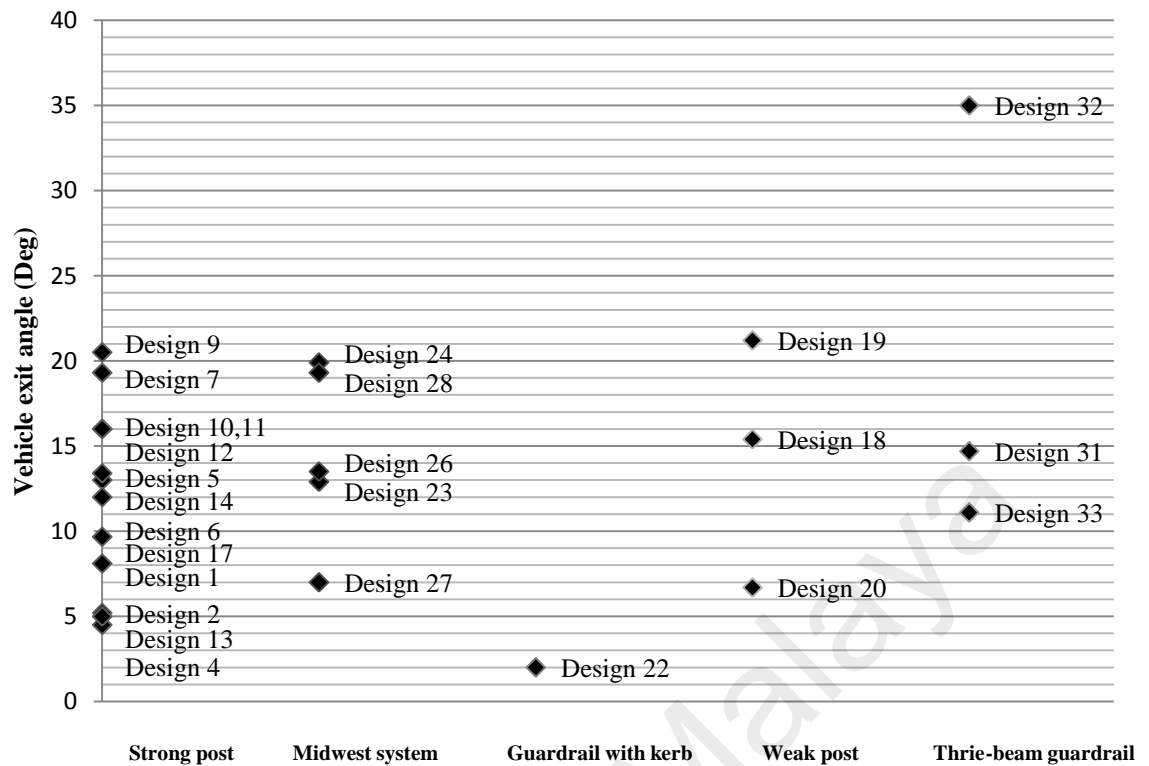


Figure 2-5. Vehicle exit angles for different guardrail systems

2.4.2 Analysis of the occupant risk factors of guardrail systems

This section addresses different levels of injury in relation to the maximum OIVs and the maximum ORAs of guardrail systems. This method is applied to guardrail systems using tests at the same level (Length of Need test 3-11).

A comprehensive occupant's response to different designs is to ensure that specific data are gathered in a systematic and routine manner. Full-scale crash tests are performed using automobiles, light trucks and passenger vehicles, and crash data reveal that there is a need to expand the study of vehicles in this class (Ross et al., 2002). The results for the occupant risk factors of guardrail systems are discussed in following sections.

Rosson et al., (1996) assessed guardrail strengthening techniques by conducting crash tests on W-beam guardrails strengthened by nesting the W-beam and reducing the post

spacing by half. The test results found that nesting the W-beam provided little benefit, whereas reducing the post spacing increased the guardrail's performance considerably. Similar results were obtained in the crash tests performed in Japan by Seo et al., (1995). The authors modified existing guardrails to reduce the possibility of barrier failure. They observed that the installed guardrails resulted in very severe injuries due to the increased mileage of national expressways and the increased speed limits adopted on these highways. The guardrails were modified by strengthening the posts, replacing weak posts by strong posts and reducing the post spacing. The modified guardrails were found to perform well and to respond favourably to high-speed impacts. However, reducing the post spacing increases the barrier's stiffness and eventually, increases the occupant risk factors. In addition, reducing the post spacing may not be a cost-effective solution.

For a guardrail system, the data from full-scale crash tests are sorted into different barrier types using same test levels to identify the less severe barrier systems. Then, a comprehensive database is created using data from full-scale crash tests, and then, the performances of different systems are compared with regard to occupant risk factors.

The results collected in Table 2-4 are illustrated in Figures 2-6 to 2-9. The results show the OIV and the ORA in two directions for the different guardrail systems.

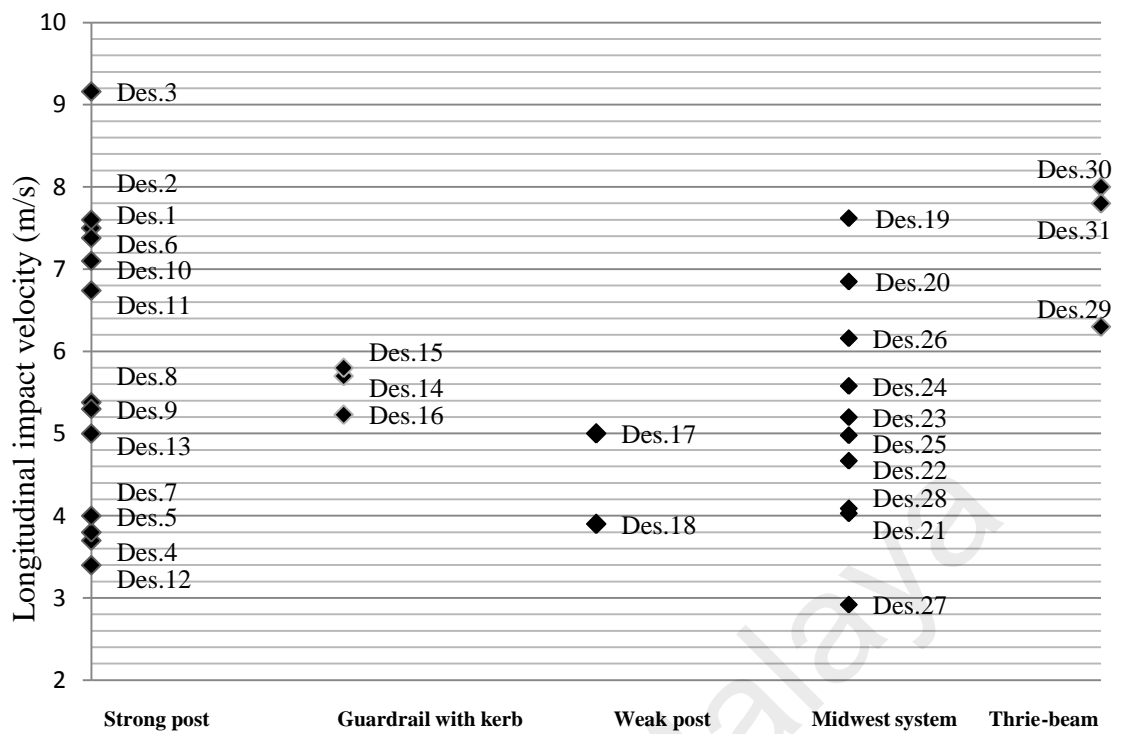


Figure 2-6. Longitudinal impact velocities for different guardrail types

A comparison of the occupant risk factors for different guardrail systems indicates that the Thrie-beam system has a higher than average longitudinal impact velocity, which could be because it is stiffer than the other systems. Weak-post systems are less severe system in terms of the longitudinal impact velocity, which could be due to their greater post spacing and weaker posts in comparison to other systems (Figure 2-6).

Four strong-post system designs showed positive results. Designs 4 and 12 (the St-Nucor post system) were the least severe, Design 5 (the HALCO X-44 post system) performed well and Design 7 (the steel W150×12.6 post system) was associated with the lowest longitudinal impact velocity.

Design 3 exhibited the highest longitudinal impact velocity. It was found that a greater embedment depth causes the system to be much stiffer than other strong-post systems.

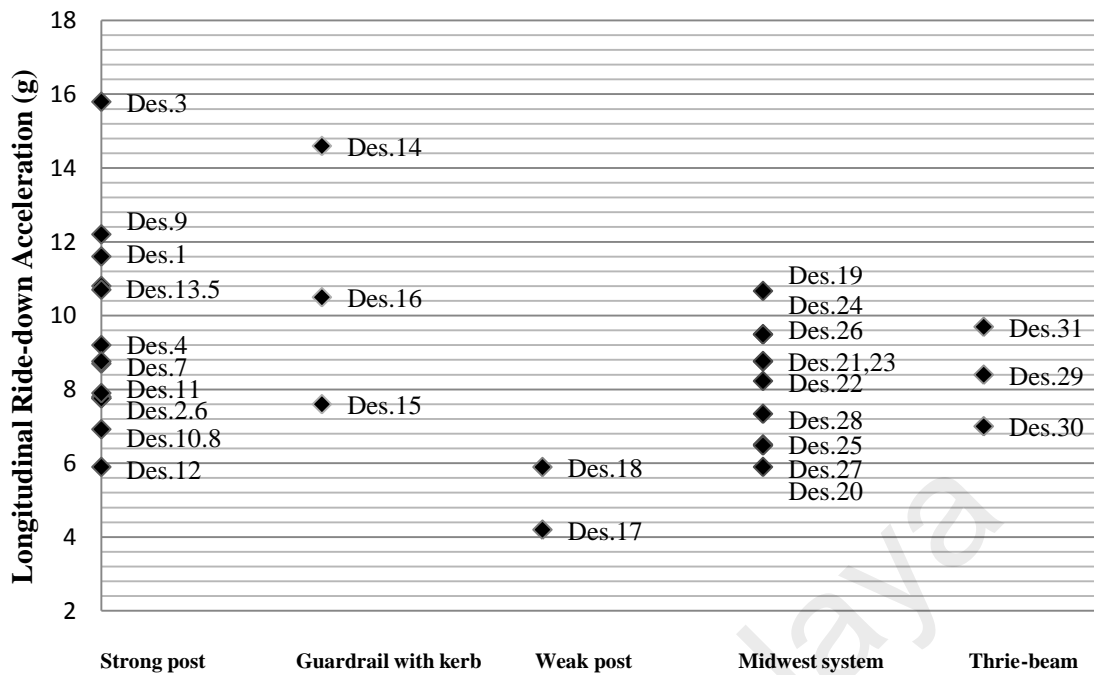


Figure 2-7. Longitudinal ride-down acceleration for different guardrail types

Figure 2-7 presents the longitudinal accelerations for different guardrail types. The weak-post system's value is the lowest, and the guardrail with a kerb has the highest average value.

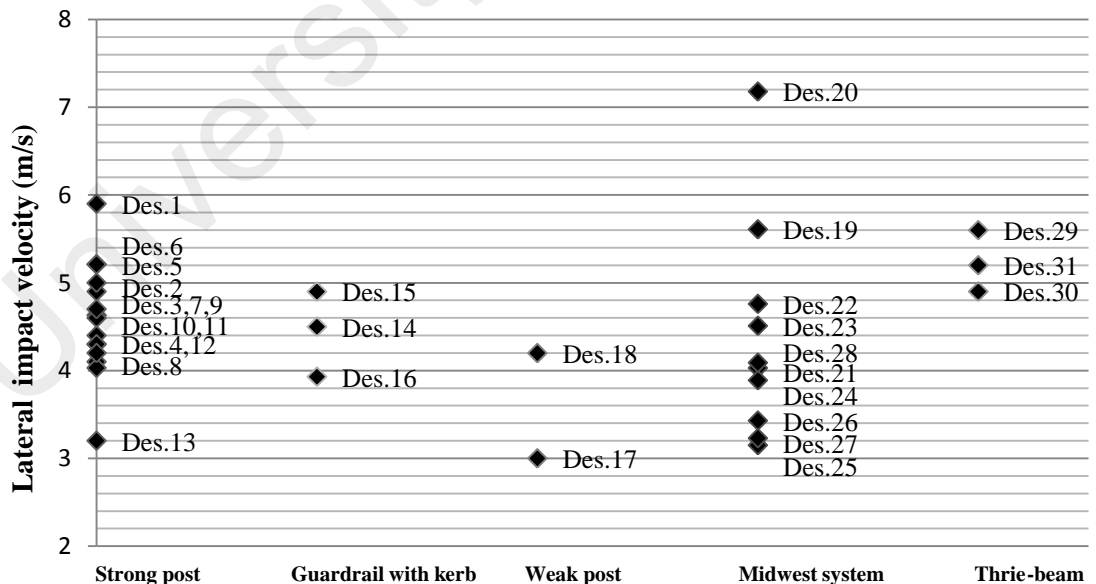


Figure 2-8. Lateral impact velocity for different guardrail types

Figure 2-8 shows that the lateral impact velocity of the Thrie-beam system is relatively high compared those of other systems. In contrast, the weak-post system has the lowest value.

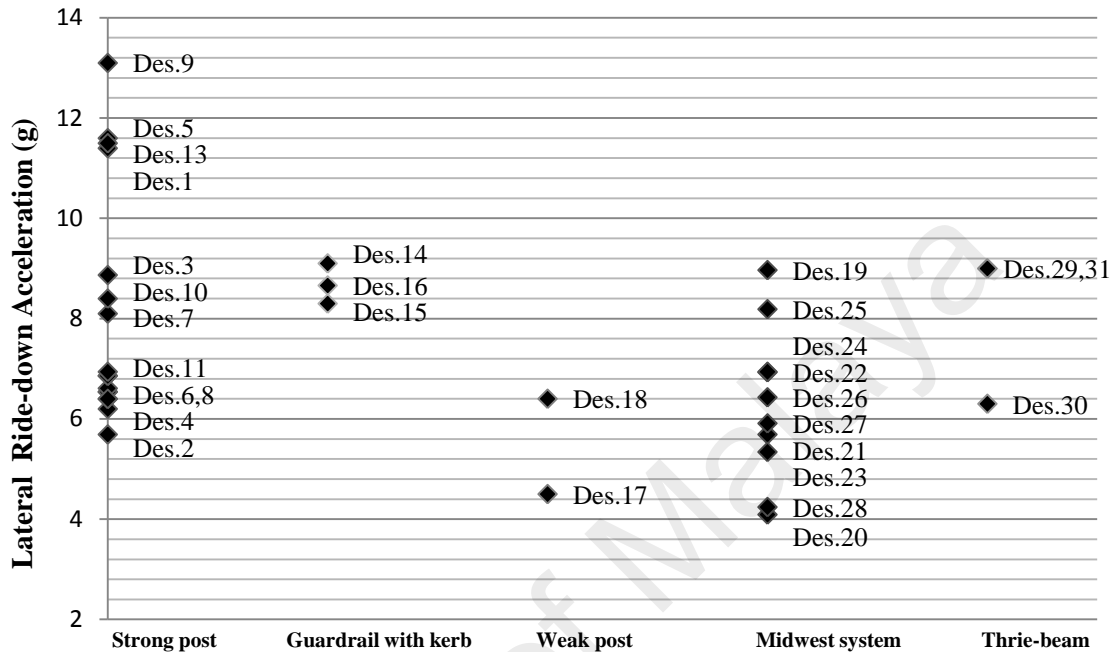


Figure 2-9. Lateral ride-down accelerations for different guardrail types

Designs 1, 5, 9 and 13 (strong-post systems) had the highest lateral ride-down accelerations (see Figure 2-9). In addition, guardrails with kerbs had the highest average ride-down acceleration in the lateral direction, which could be due to multiple crashes with the kerb and the guardrail system.

By comparing the occupant risk factor results for strong-post guardrail systems, it can be concluded that the results are very different for different designs and configurations. For the strong-post system, a small change in a design factor can change the performance of the system. Therefore, there is a need to investigate the effect of each parameter of the key design factors on the performance of the systems.

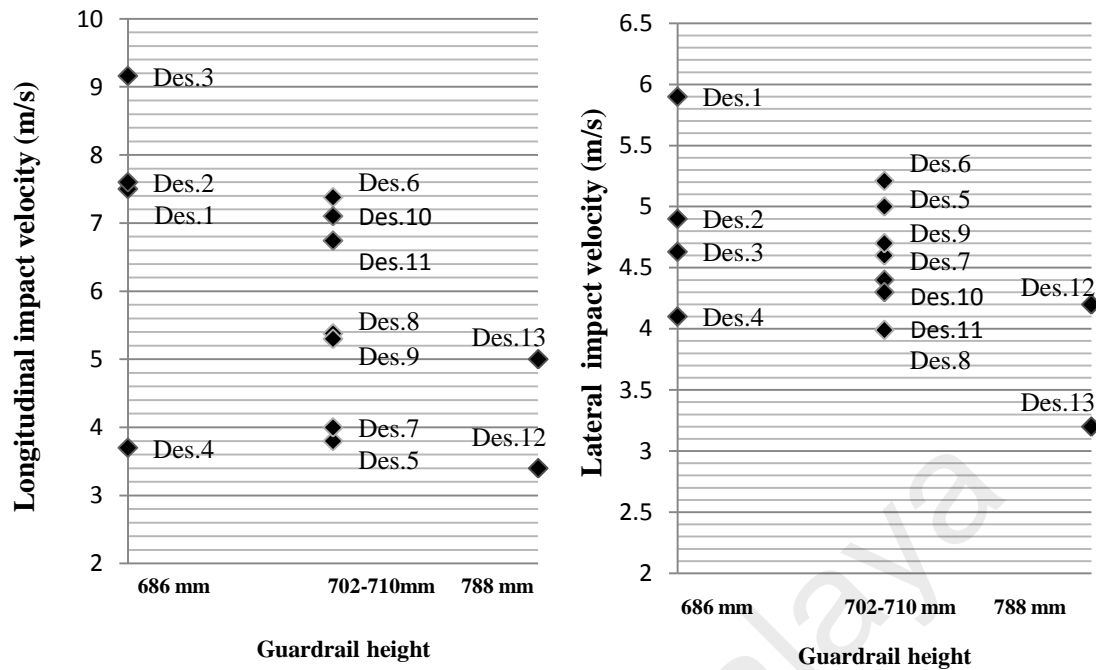


Figure 2-10. Longitudinal and lateral impact velocities for different guardrail types

In Figures 2-10 and 2-11, a comparison is made to evaluate the effect of the guardrail height on the occupant risk factors of strong-post guardrail systems. Observations of all the steel-post guardrail systems suggest that the height of the guardrail (686, 702-710 or 788 mm), which is used to categorise the occupant impact factors, plays an important role in the guardrail's performance. The results collected in Table 2-4 are used to perform this analysis.

From Figure 2-10, it was found that the maximum and the minimum longitudinal and lateral impact velocities occur for guardrail heights of 686 mm and 788 mm, respectively. The findings suggest that higher guardrails are more capable of redirecting vehicles safely and reduce occupant accelerations/velocities.

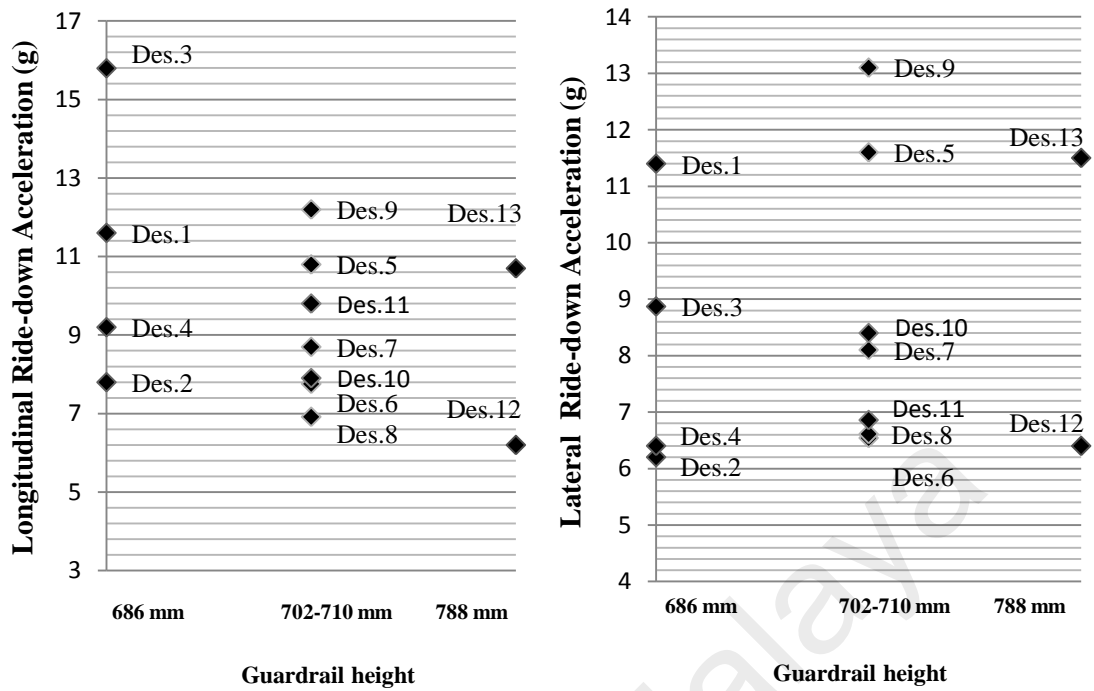


Figure 2-11. Longitudinal and lateral ride-down acceleration for different guardrail heights

Figure 2-11 shows a higher longitudinal ride-down acceleration for systems with a guardrail height of 686 mm than for those with a height of 788 mm. In contrast, a low lateral ride-down acceleration is observed for systems with a guardrail height of 686 mm, in contrast to other designs.

However, the results obtained in this section (Figure 2-10 and Figure 2-11) need to be confirmed by carrying out a parametric study using a finite element model due to the different outcomes of full-scale crash tests for different guardrail systems.

By conducting a parametric study using finite element modelling, the results of several scenarios can be considered to examine the effect of each individual design factor on the performance of a guardrail system.

2.4.3 Analysis of the structural adequacy of guardrail systems

Several studies have indicated that a guardrail system's performance is directly related to its posts (Reid et al., 2009), which serve the purpose of containing and redirecting light trucks (Sicking et al., 2002). The post embedment depth, post spacing and soil type are factors that influence the guardrail system's stiffness (Guide, 2002). Another study found that reinforced concrete is not a desirable material for guardrail posts (Cichowski et al., 1961). It also indicated that steel and wood posts are suitable for both strong- and weak-post systems; however, the strength of wood depends on its ring density, the size and density of its knots, its moisture content, and even its region of origin (Faller et al., 2009). In addition, wood properties vary over time (Seckinger et al., 2005). The deflection of a wood post is normally limited to the elastic region because it is unable to deform significantly. The energy of a vehicle impact is dissipated by the post's rotation within the soil (Kennedy et al., 2006; Mak et al., 1995).

Figure 2-12 and Figure 2-13 are based on the results of Table 2-3 and show the maximum dynamic and permanent deflections of different systems. The dynamic deflection is defined as the maximum deflection that occurs during the impact in NCHRP Report 350. Weak-post systems are subjected to the largest dynamic deflections as a result of their larger post spacings, smaller sections per set of posts and shallower embedment depths; however, guardrails with kerbs and Thrie-beam guardrail systems are subjected to the smallest deflections (Figure 2-12). In the case of a guardrail with a kerb, the vehicle's energy is reduced when it impacts the kerb. The three barriers with kerbs reviewed in this study were developed by Bligh et al. (2004) and Faller et al. (2004). The first two, which have 686 mm guardrail heights according to Table 2-3 and were designed by Bligh et al in 2004, exhibited the greatest damage to the barriers and the vehicles. Another design in this category, which had a 788 mm guardrail height and

was designed by Faller et al in 2004, performed well; moderate damage to the vehicle and the barrier was found.

The Thrie-beam system's result could be influenced by the increased depth of Thrie-beam rails. The deflections of strong-post systems varied from 700 mm to over 1500 mm. There were two categories for Midwest systems, namely, those that were greater than 1400 mm and those that were less than 1200 mm. The guardrails that deflected the most utilised embedded posts at the shallowest depths. In addition to the embedment depth, other factors, such as the post spacing and guardrail height, may affect the guardrail's deflection. However, because there is a smaller body of literature containing data from crash tests, the comparison cannot be made and the effects of these parameters cannot be evaluated.

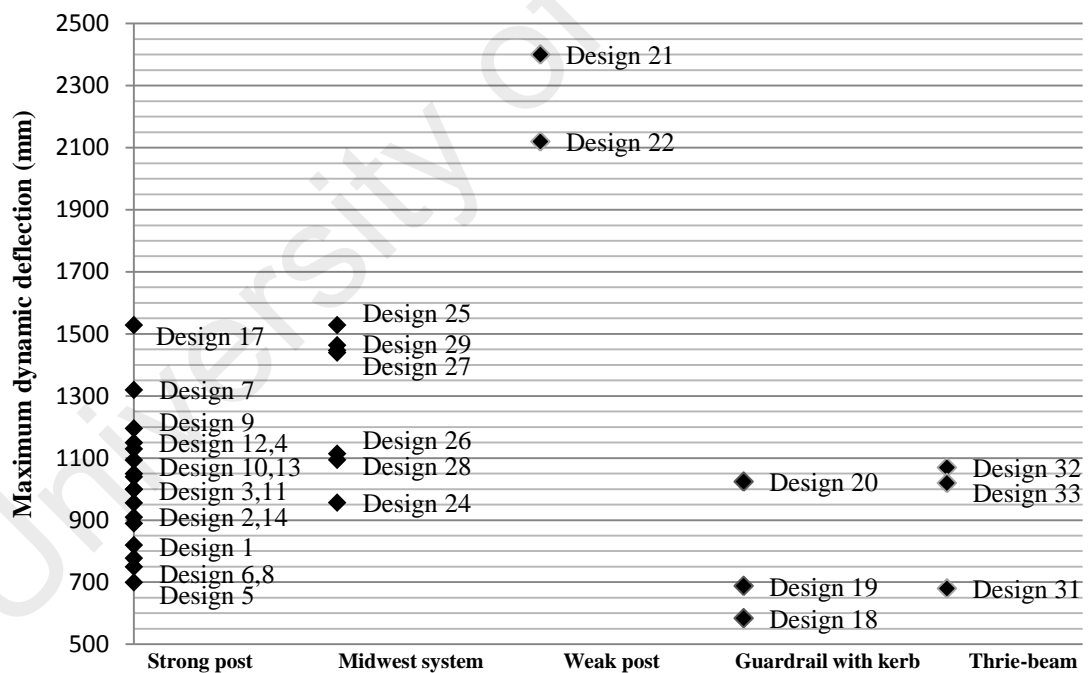


Figure 2-12. Maximum dynamic deflection for different guardrail systems

Another important parameter determining the structural adequacy of roadside barriers is the permanent deflection (NCHRP Report 350, 1983). According to NCHRP Report 350, the residual deflection remaining after impact is identified by the permanent

deflection. The permanent deflection shows the same trend as the dynamic deflection, which was previously discussed. In Designs 3 and 8, the W-beam ruptured during the crash test, and the guardrail system failed to contain the pickup truck. This raised a concern about the ability of strong-post systems to contain pickup trucks. Other than the systems that failed, Designs 4 and 17, which were strong-post guardrail systems, were subjected to the maximum amount of rail deflection, which could be due to the reduced stiffness of the St-Nucor post (N.S.M. Inc, 2009; Marzougui et al., 2010). It should be noted that this system had the highest maximum post embedment depth. In contrast, Design 5, which used a new post system (HALCO X-44), contributed a low deflection value (Kennedy et al., 2006) (Figure 2-13).

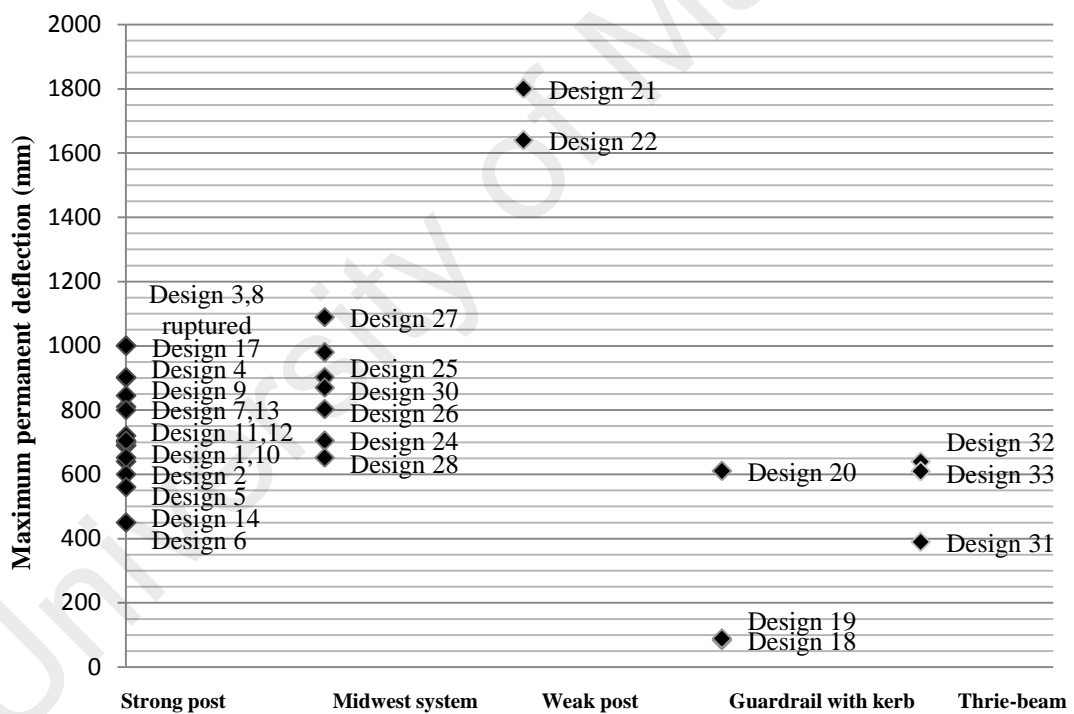


Figure 2-13. Maximum permanent deflection of different guardrail systems

The guardrail described by Faller et al. (2007), which was 706 mm high and had a post spacing of 1905 mm and an embedment depth of 1098 mm (Design 8 in Table 2-3), ruptured, but interestingly, the vehicle was successfully redirected to the roadway. Two systems (Designs 11 and 12 in Table 2-3) exhibited minimal damage (Bullard et al.,

1996; Bligh & Menges, 1997). In these systems, both heights were 710 mm, and the materials used were St-W150×12.6 steel and St-W150×13.5 steel, respectively. Interestingly, minimal damage to the vehicle was found for the second system. Following the aforementioned negative results, a barrier height of 788 mm was used, which resulted in a generally positive performance with moderate damage to the vehicle and the barrier system. Two designs for weak-post systems are reviewed in Table 2-3. The first design, which had a height of 760 mm, was unable to contain and redirect vehicles successfully and was extensively damaged during impact. Buth et al.'s (2000a) design, which used an 820 mm high barrier, performed better in terms of barrier damage, however, it resulted in serious damage to the vehicle.

Another popular system used along highways is the Midwest barrier system, which was designed at the University of Nebraska. A summary of the results for this system is provided in Tables 2-3 and 2-4. Several designs with different performance are considered in this section. All the designs have the same height (788 mm). The first Midwest barrier system design, which had a post spacing of 476 mm, exhibited an acceptable result; nevertheless, it is economically inappropriate due to its low post spacing (476 mm).

2.5 Comparison of the MASH and NCHRP Report 350

In 2009, the MASH (MASH, 2009) was issued with the recommendation that tests be conducted with heavier light trucks to better represent the pickup/van/sport-utility vehicle class. This is because some of the vehicles specified in Report 350, such as the 820C vehicles and 2000P pickup trucks, have not been manufactured since 2000 and 2001, respectively. Furthermore, the MASH increases the impact angle for most small car crash tests to the angle used in the light truck tests. These changes place greater

safety performance demands on many of the current roadside safety features. The MASH introduced a new vehicle that weighs 1100 kg, as shown in Figure 2-14.



Figure 2-14. Comparison of the passenger vehicles in NCHRP Report 350 (left) and the MASH (right)

In addition, the MASH introduced a new vehicle, which is a 2270P quad-cab pickup truck (2270 kg). A quad-cab pickup truck has a higher centre of gravity and better represents the class of large SUVs. As a result, the impact severity of crashes categorised according to the MASH increased compared that of crashes categorised according to NCHRP Report 350. A comparison of these two vehicles is shown in Figure 2-15.

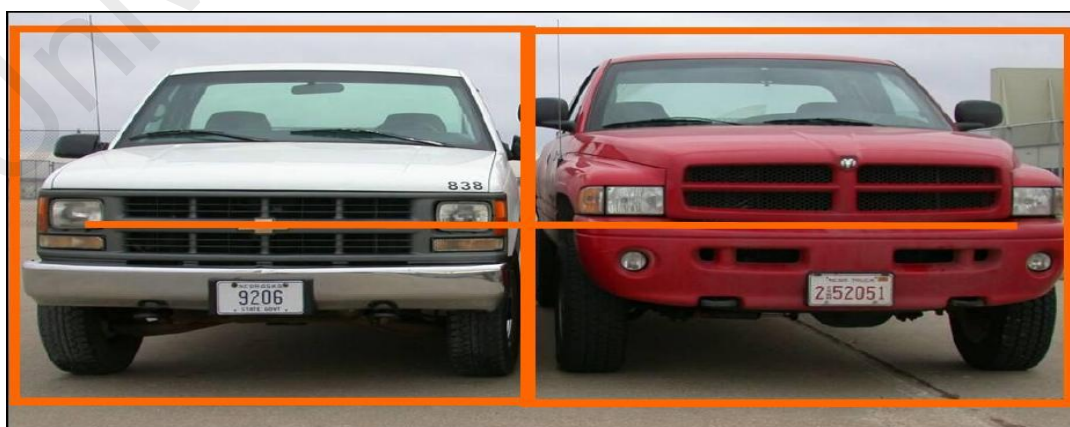


Figure 2-15. Comparison of the pickup trucks defined in NCHRP Report 350 (left) and the MASH (right)

The test procedures for the MASH and NCHRP Report 350 are shown in Table 2-5.

Table 2-5: The Length of Need test procedures for the MASH and NCHRP Report 350

Test Level	Test Designation	Impact condition (NCHRP Report 350)			Impact condition (MASH)		
		Vehicle Type	Nominal Speed (km/h)	Nominal Angle (Deg)	Vehicle Type	Nominal Speed (km/h)	Nominal Angle (Deg)
1	1-10	820c	50	20	1100C	50	25
	1-11	2000P	50	25	2270P	50	25
2	2-10	820c	70	20	1100C	70	25
	2-11	2000P	70	25	2270P	70	25
3	3-10	820c	100	20	1100C	100	25
	3-11	2000P	100	25	2270P	100	25
4	4-10	820c	100	20	1100C	100	25
	4-11	2000p	100	25	2270P	100	25
	4-12	8000s	80	15	1000S	90	15
5	5-10	820c	100	20	1100C	100	25
	5-11	2000p	100	25	2270P	100	25
	5-12	36000v	80	15	36000V	80	15
6	6-10	820C	100	20	1100C	100	25
	6-11	2000P	100	25	2270P	100	25
	6-12	36000T	80	15	36000V	80	15

2.5.1 Differences in impact severity between NCHRP Report 350 and the MASH

Currently, the FHWA requires that roadside hardware developed and tested after January 1, 2011 be evaluated according to the AASHTO's MASH, but it still allows the use of hardware designed, tested and accepted under NCHRP Report 350. In developing guidelines for selecting bridge railings, therefore, there is some ambiguity because new hardware will be evaluated under the MASH criteria, but existing hardware tested under NCHRP Report 350 can and probably will still be used in new or retrofit construction. Table 2-6 shows a list of the TL-2 through TL-5 Lengths of Need impact conditions for longitudinal barrier crash tests conducted in accordance with NCHRP Report 350 and the MASH arranged in order of increasing impact severity. One of the difficulties resolved by the MASH was that the nominal impact severity according to the TL-3 and

TL-4 Length of Need tests in NCHRP Report 350 had converged to approximately 100 ft-kips (Ray et al., 2014).

Table 2-6: Comparison of the impact conditions in NCHRP Report 350 and the MASH ordered by severity

Test	Vehicle Mass	Speed	Angle	Nominal Impact Severity	Typical Barrier Height
	lbs	mi/hr	Deg	ft-kips	in
R350 TL2	4,409	44	25	50	24
MASH TL2	5,004	44	25	57	Unk
R350 TL4	17,637	50	15	98	32
R350 TL3	4,409	62	25	102	27
MASH TL3	5,004	62	25	116	31
MASH TL4	22,046	56	15	155	36
R350 TL5	79,367	50	15	441	42
MASH TL5	79,367	50	15	441	42

With these adjustments, the severity of the TL-3 test conditions increased significantly. The weight and body style of the test pickup truck changed from a 2,000 kg (4,409 lb), ¾-tonne, standard-cab pickup truck to a 2,270 kg (5,000 lb), ½-tonne, four-door pickup truck. This approximately 13 percent change in the test vehicle’s mass was deemed to produce an impact condition that was similar to and possibly more severe than the TL-4 single unit truck (SUT) test of NCHRP Report 350.

In the case of a W-beam section, this increase in impact severity may cause the guardrail to fail. Therefore, structural adequacy and vehicle stability are both concerns that need to be addressed in terms of the MASH requirements.

2.5.2 Guardrails that fail to meet the MASH’s criteria

Because the MASH increased the impact severity to grant a higher safety level to the new standard, some guardrail designs were not able to redirect vehicles safely. Recent studies (Bligh et al., 2011) have been conducted to evaluate the performance of safety

barriers under the conditions of Length of Need test 3-11 in the MASH. For instance, a 27 5/8-inch tall modified G4(1S) steel-post W-beam guardrail was unable to perform because it ruptured when it was struck by a 5000-lb, 3/4-tonne pickup truck. In a subsequent test of the same system, the guardrail successfully contained and redirected the 5000-lb, 1/2-tonne, four-door pickup truck described in the MASH. However, the rail had a vertical tear through approximately half of its cross section, which indicates that the performance of the modified G4(1S) guardrail is limited.

As parts of NCHRP Projects 22-14 (02) and 22-14 (03), full-scale crash tests were performed using a 1/2-tonne, four-door, pickup truck (designated 2270P) under the MASH guidelines. It is learned that increasing the new pickup truck's weight from approximately 4400 lb to 5000 lb (2000 kg to 2270 kg) positively affected the impact severity part of the structural adequacy test (Length of Need test 3-11) for longitudinal barriers by 13 percent. Table 2-7 shows a summary of these barrier tests (Bligh et al., 2011).

Table 2-7: Summaries of the MASH full-scale crash tests conducted with a non-proprietary strong-post W-beam guardrail

Agency Test No.	Test Designation	Test Article	Vehicle Make and Model	Vehicle Mass (lb)	Impact Speed (mph)	Impact Angle (deg)	PASS/FAIL
2214WB-1 ^a	3-11	Modified G4(1S)	2002 GMC 2500 3/4-tonne Pickup	5000	61.1	25.6	FAIL ^c
2214WB-2 ^a	3-11	Modified G4(1S)	2002 Dodge Ram 1500 Quad-Cab Pickup	5000	62.4	26.0	PASS ^d
476460-1-5 ^b	3-11	G4(2W) W-Beam	2007 Chevrolet Silverado Pickup	5009	64.4	26.1	FAIL ^c

a) Test performed at the University of Nebraska under NCHRP Project 22-14(2)

b) Test performed at Texas A&M Transportation Institute (TTI) under NCHRP Project 22-14(3)

c) Rail ruptured

d) Rail torn through half its cross section (Bligh et al., 2011).

In test 2214WB-1, a 2268 kg GMC 2500 pickup truck (with its centre of mass at 691 mm) collided with a modified G4(1S) W-beam guardrail system at a speed of 98.3 km/h and an angle of 25.6°. The actual vehicle impact occurred 1,143 mm downstream of the centre of post 10. At 0.194 s, the rail ruptured as the vehicle began to climb over it. The damage to the guardrail system was extensive (Figure 2-16); it consisted of deformed and twisted guardrail posts, disengaged and fractured wooden blockouts, contact marks on a guardrail section, and a deformed and fractured W-beam.



Figure 2-16. Summary of the test results for the guardrail systems subjected to the full-scale crash tests (Polivka et al., 2006b)

Another failed crash test was conducted on a G4(2W) system based on Length of Need test 3-11 in the MASH's criteria at the Texas Transportation Institute. The damage (rail

rupture) to the G4(2W) W-beam guardrail is shown in Figure 2-17. The W-beam rail element ruptured at the splice on the upstream side of the bolts at post 13, and the ruptured end deformed around post 15. Posts 13 through 15 fractured below ground level, and due to fracturing and splintering, the resting places of specific posts were not identifiable. In addition, the vehicle sustained damage to its top and left side.



Figure 2-17. Rail rupture in the G4(2W) guardrail system (Bullard et al., 2010a)

Based on these results, the standard G4(2W) guardrail system (Bullard et al., 2010a) was categorised as ineffective, according to the impact conditions of Length of Need test 3-11 in the MASH, and is not able to accommodate the higher test impact speeds recommended for very high design speeds without modification. Therefore, in this study, several possibilities are considered, including improving the splice connections, the guardrail height and the post spacing, to improve the performance of this system at this test level.

2.6 Failure mechanisms of wood post systems

A main function of every guardrail system is to dissipate the colliding vehicle's kinetic energy. Such dissipation reduces the force applied to the vehicle during the redirection process and thus, reduces the risk of injury to the occupants of the vehicle. For most guardrail systems, a primary means of vehicle energy dissipation is to have the posts and soil work together to absorb that energy. Energy may be absorbed in the following ways:

- (a) By the post, which bends until it fractures,
- (b) By the soil as the post rotates in it until the post flips or is pulled out of the soil, and
- (c) By a combination of those two methods.

In many cases, the desired behaviour is that the posts rotate in the soil while the soil absorbs as much energy as possible. This process requires a trade-off between the type and size of the posts and the depth of their embedment in the soil (Pfeifer & Sicking, 1998; Reid et al., 2009).

The failure of a guardrail post drastically affects performance of the guardrail system. Post rotation, fracture, bending, or twisting of the post, or a combination of failure modes, radically affects how much energy is absorbed by a post in a guardrail system. If the post is not allowed to rotate sufficiently and fractures or yields soon after impact, the force may be weaker than what is commonly observed in full-scale vehicle crash tests of guardrail systems that include strong posts embedded in soil (Holloway et al., 1996; Reid, 1999).

In strong-post W-beam guardrail systems, if the posts do not rotate in the soil and absorb energy, the bulk of the impacting vehicle's energy is absorbed by the W-beam, which increases the tensile force in the rail. When the force increases beyond the capacity of the rail, it fails and allows the impacting vehicle to pass through it.

Therefore, the posts must have sufficient structural capacity to displace founding soils and absorb energy. In addition, the support posts in a guardrail system may also be struck by the impacting vehicle as it is redirected, which is commonly called vehicle snag. Therefore, it is also desirable to avoid the creation of hazardous conditions when the posts are directly impacted. Wood and steel posts can both perform this function, but they have inherent differences (Bielenberg et al., 2014).

There are some concerns about strong-post W-beam guardrail systems with wood posts in lieu of steel posts. For example, wood posts tend to have different strong-axis behaviour. This effect is largely due to differences in the posts' cross sections and material types. W6×8.5 steel posts have very distinct strong- and weak-axis bending capacities due to the "I" shape of their cross sections. Wood posts have larger rectangular cross sections, which can generate greater post-soil resistive forces, but wood is inherently less strong than steel. Therefore, wood posts tend to fracture if the soil's resistive force exceeds the capacity of the post and potentially absorb less energy than steel posts. Wood and steel posts embedded in soil can behave in a variety of ways when subjected to strong-axis bending; which occurs depends on the strength of the soil foundation. If the soil forces do not exceed the capacity of the post section, then, the performances of wood and steel posts in response to strong-axis bending should be fairly similar in terms of force versus deflection and the amount of energy absorbed. If the post is embedded in a very strong soil foundation (e.g., frozen soil), then the post's performance depends more strongly on its type. When the post-soil interaction force exceeds the capacity of a steel post, the post yields and deforms. However, a deforming steel post continues to dissipate energy although the forces and energy are higher than those seen in weaker soils that rotate. Conversely, a wood post fractures when the post-soil interaction forces are high enough to exceed the capacity of the post. Consequently, the reduced energy dissipation of the support posts due to fracturing can increase rail

loading and potentially cause rails to rupture (Bielenberg et al., 2014). In the next section, some examples of failures in guardrail systems due to this issue are highlighted.

2.6.1 Splice connection failures

According to the results of Length of Need test 3-11 in NCHRP Report 350, whenever a W-beam guardrail is installed in a critical situation, such as over a kerb (Polivka et al., 2000) or at a terminal end (Ray et al., 2001b), the rail element can rupture at a splice connection. Polivka et al. (2000) observed that the splice connection is the weakest point of a rail element (Sicking et al., 2002).

In the study of Plaxico et al. (2000), the impact performance of two strong-post W-beam guardrail systems, the G4(2W) and G4(1W) systems, were compared. After a finite element (FE) model of the G4(2W) guardrail system was developed using data from a full-scale crash test, a FE model of the G4(1W) guardrail was developed. The deflection, vehicle redirection, and occupant risk factors of the two guardrail systems were compared. The two systems were found to perform similarly in collisions, and both satisfied the requirements of NCHRP Report 350 under the conditions of Length of Need test 3-11 in LS-DYNA simulations and laboratory experiments. However, the same G4(2W) system failed due to rail rupture according to the criteria for Length of Need test 3-11 in the MASH (Bullard et al., 2010a). In another study, Plaxico et al. (2003) investigated the failure mechanism of a bolted connection between W-beam and a guardrail post; the results indicated that the splice connection's design could have a significant effect on the performance of a guardrail system (Fang et al., 2013).

In another study, seven NCHRP crash tests were successfully simulated to provide extended validation of a new finite element model of a Chevrolet Silverado pickup truck as a surrogate for the 2270P test vehicle. Analyses of six modifications to the G9 Thrie-beam barrier, three variations of the G4(1S)) guardrail median barrier and G4(2W)

guardrail system were undertaken. For the G4(2W) guardrail system, failure was characterised by a tear or rupture of the rail during the test. It was possible to simulate this result by embedding a material failure algorithm in the model of the barrier, but this significantly increased the complexity of the simulations. Because rail rupture is a significant design issue for G4(2W) barrier systems and project resources were limited, it was determined that further retrofit analysis would not be performed in this study (Marzougui et al., 2012).

In conclusion, increases in impact severity seem to be more critical in terms of requirements for the structural adequacy of guardrail systems. Therefore, the use of more effective guardrail systems with higher load bearing capacities to contain heavier and faster errant vehicles is deemed pragmatic.

The previous study revealed that most of guardrail failures occurred near splice connections. However, there is not a significant body of work on this issue. A study conducted by Rosson et al. (1996) suggested that the strengthening technique of nesting W-beams should not be used because it produces only a marginal reduction in the lateral deflection. Instead, the strengthening technique of using a single W-beam with half the usual post spacing is recommended.

Reducing the post spacing may increase the chance of wheel snagging as well as the occupant risk factors caused by stiffer guardrails. Strengthening the splice connection would be very beneficial because with the splice connection's stiffness reinforced, the W-beam is able to support higher tensile and bending forces. With stronger splice connections, greater post spacing or lower post cross sections can be considered in the designs of guardrail systems, which can help reduce the occupant risk factors significantly.

2.7 Numerical analyses of guardrail systems

There have been limited numbers of studies that evaluate the performance of guardrail systems using the MASH's criteria due to the high costs of full-scale crash tests. Therefore, predicting the behaviour of this component using the finite element method and discovering relationships between factors helps designers and engineers reduce construction costs and the number of tests required.

Computer simulations and full-scale crash tests are the most general methods of evaluating barrier systems. Because it is not cost-effective to use physical testing to test all possible crash scenarios, computer simulation using, for instance, FE analysis, is a useful technique for exploring guardrail impact performance and developing new designs for systems subjected to different impact conditions. Over the last 20 years, a number of FE models of various vehicles and roadside barrier systems have been developed by researchers at the National Crash Analysis Centre (NCAC); which can be used to investigate different crash scenarios.

In this section, an overview of numerical simulations of guardrail systems is provided.

A W-beam guardrail system requires a more complex structural model than a concrete barrier does in roadside crash simulations. Modelling a W-beam barrier is more challenging because a finer mesh size is required to describe the rich details of the barrier's components and capture their deformations. In early years, due to limits on computing resources, significant efforts were made to reduce the sizes of models while maintaining accuracy and computational efficiency. For example, Hendricks et al. (1996) modelled a G2 weak-post W-beam guardrail system in which a small portion of the rail was meshed and the soil was excluded because it was computationally expensive. In their model of a G4 strong-post system, Tabiei & Wu (2000b) tackled the rail to blockout connection, soil-post interactions and guardrail ends using spring

elements whose properties and positions were based on the results of a more detailed small-scale FE model. To address the interactions between the posts and the soil, Wu & Thomson (2007) measured the strength of a single post embedded in gravel and used the data to validate a computer model for investigating soil-post interactions. While modelling rail splice connections and their failures, Ray et al. (2001b) found that the most common mechanism for a splice connection failure was that the rail was stretched and subjected to plastic deformation and then, the bolt slid through the hole or a rupture occurred. Because the bolt almost never failed, it was represented by a computationally efficient rigid material in the model.

In a study conducted by Hendricks et al. (1996), a G4(2S) weak S3 × 6 steel-post W-beam guardrail system was developed using a finite element model. Weak-post guardrail system modelling techniques were described, and the results of finite element simulations of impacts were presented. A comparison was made between the simulations in the study and the results of a crash test. The results show that the impact of a small 820 kg vehicle on a G4(2S) guardrail system was successfully modelled using LS-DYNA.

Reid et al. (1997) used a model of a C-1500 pickup truck in their analysis of impacts on strong-post guardrail systems. The purpose of the study was to develop a finite element simulation of a new guardrail system based on recommendations in NCHRP Report 350. The results showed that the strong-post guardrail system could satisfy the requirements of NCHRP Report 350. In addition, a model of a strong-post guardrail system with 150 mm wide × 200 mm deep wood posts spaced at 1905 mm agreed well with crash tests results.

In another study, Tabiei & Wu (2000b) developed a finite element model (FEM) to verify a strong steel-post W-beam guardrail during a full-scale crash test. Springs were

used to simulate the crashworthiness of components. In conclusion, a roadmap was introduced to model the steel-post guardrail system, and the claim that this roadmap can be used for other road restraint systems was made.

Furthermore, in a study conducted by Seckinger et al. (2004), the crashworthiness of two different types of post were investigated. The FE method was used to model strong G4(2W) wood post and G4(1S) steel-post guardrail systems along pavement mow strips. Varying the stiffness and developing a standard mow strip design were the most important objectives of that study, which was based on the criteria for roadside hardware in NCHRP Report 350 (NCHRP Reports 350, 1993).

Borovinšek et al. (2007) used shell elements with five integration points to model parts of a barrier. Linear Hughes–Liu beam elements were used to model the bolt connections with failure criteria based on filtered forces. The maximum strength and deformation of the safety barrier were determined. The results of both experiments and simulations showed that the safety barrier was able to contain and redirect the truck to the roadway in a safe manner.

The FE method was used by Ferdous et al. (2011) to study a modified G4(1S) W-beam guardrail to analyse its performance with different guardrail heights. The AASHTO's Guide to Standardised Highway Barrier Hardware (AASHTO, 2000) was used to specify the components of the system in the model. Belytschko-Tsay shell elements were used to model the W6×9 posts. The embedment was adjusted to 1100 mm (43") in soil. The results showed that the modified G4(1S) W-beam guardrail model was in good agreement with full-scale vehicle impact tests as well as the results of a previously conducted crash test of the system.

Wright & Ray (1996) described the techniques for modelling steel materials that LS-DYNA uses to model guardrail materials. To validate the finite element model, quasi-

static laboratory tension tests were conducted on guardrail steel coupons, and the results were compared to the results of finite element simulations. Two different material models were used to model the steel used in the guardrail: the kinematic/isotropic elastic-plastic Material model no. 3 and the rate-dependent tabular isotropic elastic-plastic Material model no. 24. The authors came to the conclusion that Material no. 3 and no.24 are not adequate for modelling strain rate effects for AASHTO M-180 guardrail and therefore, they did not include strain rate effects in the models.

Wu & Thompson (2007) investigated the interactions between gravel and posts through experiments and computer simulations. A parametric study was subsequently conducted to investigate the effect of the gravel's stiffness on soil-post interactions through computer simulations using LS-DYNA. The numerical results showed that the LS-DYNA models of soil and concrete and the Cowper-Symonds model of steel effectively captured the soil-post interactions because the calculated strength of the post agreed with the range of the test data. Input parameters for the material models of soil and concrete for roadside gravel in crash analyses were recommended.

Parametric computational simulations were used by Borovinšek et al. (2013) in the process of developing a new class of steel-reinforced wood road safety barrier with particular attention to optimising the behaviour of pre-stressed bolt connections. The results of the parametric simulations of the bolt connections were used in full-scale vehicle impact simulations. The new steel-reinforced wood road safety barrier design was first tested according to the regulations of the EN1317 standard using dynamic parametric explicit computational simulations. A simplified model of the wood parts was used to ensure that the time required by the parametric simulations was acceptable. The results of the computational simulations showed that the proposed road safety barrier design fulfils all the requirements of the EN1317 standard.

In another study conducted by Sassi (2011), the effects of different test parameters on the interaction of a post and the soil were evaluated. Five parameters, the impactor's speed, the impactor's mass, the post's embedment depth, the blockout's crushability and the soil density, were evaluated and analysed. A finite element model of a guardrail post was used to conduct the study, which suggested design guidelines for improving the soil-post interaction for a full-scale crash test. The results of the study indicated that the friction is the most important factor in a guardrail post's reaction to a lateral impact and plays a major role in the peak load, the average load and the maximum post displacement.

Furthermore, Wu & Tabiei (2002) investigated the behaviour of a G4(1S) guardrail system using a parametric study and presented a feasible approach to improving its structure. The study provided a roadmap for simulations of highway safety structures. The effect of reducing the embedment depth of the posts was investigated using both FE simulations of components and full-system crash simulations. The results obtained from the parametric study indicated that an appropriate reduction of the embedment depth of the posts could weaken the soil-post interaction and result in a greater displacement of the posts in the web direction. This would decrease the lateral stiffness of the guardrail system and allow the W-beam to absorb more energy during an impact. The yaw and roll of the vehicle should therefore be efficiently reduced by the modified guardrail system. However, the decrease in the lateral stiffness causes the tensile and bending forces to increase, which may cause the splice connection to fail or the W-beam rail to rupture.

Adequate parametric data on vehicle responses for use in simulations of crashes with G4(2W) guardrail systems are generally lacking. Except the study conducted by Wu & Tabiei (2002), which studied the effect of the embedment depth on yaw and roll of

vehicles, no study has investigated the responses of vehicles that crash into guardrail systems parametrically.

In addition, by implementing the MASH's criteria, more research needs to be conducted to improve the performance of guardrail systems. One important case is the G4(2W) guardrail system; little attention has been paid to improving this system.

An important issue is the lack of a strong parametric study that examines the effects of individual factors, including the configuration of splice connections, the guardrail height and the post spacing, on the performance of guardrail systems. This parametric study should be capable of examining the important factors and their effects on all the required criteria, including the structural adequacy, the vehicle trajectory and occupant risk factors, based on the MASH.

In the next section, a static test is considered to verify the results of a simulation of a section of a W-beam, and literature on the most recent tests performed on W-beam is collected. In addition, an overview of static tests of guardrail systems and general applications of this method are discussed.

2.8 Static tests

The W-beam system is the part of a guardrail structure that has the primary function of attenuating the effects of a collision in direct contact. The majority of studies of guardrail designs have considered the whole system, and fewer studies have characterised W-beams. To verify a model of a W-beam, a simple experiment has been conducted; in it, the load-deflection characteristics of a W-beam under a variably located, quasi-static applied load are measured.

2.8.1 General applications

The early stage of the development of safety features for a roadside barrier may require an evaluation of the barrier's strength and deflection because it must bear a considerable load. Therefore, static tests are often specialised and do not conform to the American Society for Testing and Materials (ASTM) standard. Most static tests have one of the following objectives:

- 1) To demonstrate the performance of a safety feature under simulated environmental loading.
- 2) To evaluate the ultimate strength of the critical connections.
- 3) To determine load and deflection properties for subsequent computer simulations.

Static testing is used to evaluate components of safety features; therefore, developers should address problems involving the sensitivity of the material load rate, such as energy absorption. Static testing generally allows a component to fail at the lowest possible load. However, this often does not correspond to the failure mode with the lowest energy (NCHRP Reports 350, 1993). Table 2-8 lists applications of static tests.

Table 2-8: Applications and limitations of safety feature development techniques
(NCHRP Report 350, 1993)

Development Technique	Principal Area of Application	Possible Limitations
1. Structural (Design Methods)	<ul style="list-style-type: none"> • Preliminary and final design of feature for environment and non-collision performance. • Preliminary design of feature for vehicle collision performance. • Analysis of connections, material properties requirements and foundation design. 	<ul style="list-style-type: none"> • Dynamics and kinematics of feature and collision vehicle are not addressed. • Collision severity in terms of occupant injuries and fatalities is not addressed.

Table 2-8 continued

2. Static Tests (quasi-static)	<ul style="list-style-type: none"> • Mechanical properties of unique shapes, connections, new materials. • Validation of structural design features. • Quality control of critical material properties. • Develop input values for computer programs. 	<ul style="list-style-type: none"> • Dynamic properties not examined. • Generally applicable to samples, connections, and small subassemblies; entire system is not accommodated.
--------------------------------	---	---

In 2012, Chen provided a numerical model of a W-beam and found that the load decreased when the W-beam section became flatter. The flattened shape can be quantitatively expressed in terms of the radii of curvature of the top and bottom of the cross section. A new method was proposed for predicting the relationship between load and deflection (Chen, 2012).

Hui et al. (2002) downscaled W-shaped guardrail samples (using a scale of 1:3.75) and tested them under quasi-static and impact three-point bending. Two different types of end restraint systems were adopted. The energy absorption characteristics and the large deformation mechanism were studied by looking at load-deflection curves, flexural profiles, cross-sectional distortion and different supporting conditions and end constraints. The experimental results were compared with their static counterparts, and it was determined that the load-carrying capacity of a W-beam and the corresponding plastic dissipations are affected by the material's strain hardening and structural softening due to the local cross-sectional distortion and to the tension factor due to the axial constraints.

Most of the guardrail systems in use today are semi-rigid systems, which generally allow a large deflection of the guardrail before the colliding vehicle is stopped or redirected. If a vehicle hits the system, energy is mainly dissipated in three ways:

- (1) Through plastic flexural deformation of the guardrail beam,
- (2) Through the deformation of posts and/or blockouts and
- (3) Through the removal of the posts from the soil or concrete.

Significantly fewer studies have been conducted to evaluate just the shape of a W-beam. To fully understand the deformation mechanism of a W-beam system, this study attempts to test only the most basic unit of the guardrail system, i.e., the W-beam, to verify the model of the W-beam section. The beams were tested statically in an experiment, the results of which are compared with the numerical results. The load-carrying capacities and the local cross-sectional distortion of a W-beam under a loading wedge are recorded. Subsequently, a model of a W-beam section during a static test is prepared using the finite element method. The goal of this is to determine the optimum mesh size that provides reliable results due to lack of information on suitable mesh sizes for W-beams in the literature.

2.9 Research gaps

Studies in the literature have found that the G4(2W) strong-post systems tested were not able to accommodate a pickup truck according to the conditions of Length of Need test 3-11 specified in the MASH's criteria, and there has not been sufficient work on the development of a suitable wood post system. Therefore, in this study, several conditions are considered, including improving splice connections, the guardrail height and the post spacing, to improve the performance of this system.

Most failures of guardrail systems occur in the splice connections and the rails. Most of the strengthening techniques focus on nesting the W-beams and reducing the post spacing. However, none of these methods improves or strengthens the splice connections. With stronger splice connections, greater post spacing or a smaller post

cross section could be considered in guardrail system designs, which could significantly reduce the occupant risk factors.

To study the splice connections in a W-beam system, developing an accurate model of the W-beam section is essential. However, no information about suitable mesh sizes for W-beam sections is provided in the literature. Therefore, static tests using three-point bending are conducted to verify and validate the model of a W-beam section. This is to provide an accurate model of a W-beam with the optimum mesh size.

Another issue is the lack of a strong parametric study that examines the effects of individual factors on the performance of the guardrail system. This parametric study should be capable of examining all the factors and their effects on all the required criteria, including the structural adequacy, vehicle trajectories and occupant risk factors in accordance with NCHRP Report 350 or the MASH.

2.10 Chapter summary

In this study, the common guardrail systems, including strong-post systems, guardrails with kerbs, weak-post systems, Midwest systems and Thrie-beam rail systems, are reviewed. This is to examine their structural adequacy, vehicle trajectories and occupant risk factors.

Increasing safety levels by implementing the new standard (from the MASH) highlights the weakness of current guardrail systems, several types of which, including G4(2W) systems, were not able to satisfy the requirements of the MASH's criteria. Therefore, the failure modes of the guardrail systems are discussed, and areas that require development in the field of guardrail design are presented as research gaps.

To address the research gaps presented in the previous section, the present thesis aims to examine the G4(2W) guardrail system through a parametric study by adopting a finite

element model in LS-DYNA. The results could provide valuable guidance for improving guardrail systems. The research methodology used is presented in the following chapter.

University of Malaya

CHAPTER 3: RESEARCH METHODOLOGY

3.1 Introduction

This chapter discusses the methods of analysis that are used in this study, including modelling the G4(2W) guardrail system, performing the static tests and validating the LS-DYNA model. Computer simulation is the most versatile approach for investigating a wide range of possible impact scenarios (e.g., vehicle type, guardrail type, and impact conditions). Computer simulation can also be very useful for determining the precise effects of a crash with a barrier on a vehicle's performance. Experiments and finite element analysis (FEA) are two methods that were considered for use in this study. In an experiment, a static test is performed to validate the model of the W-beam rail section, and the FEA model is used to model different crash scenarios. FEA has been used in several studies involving the impacts of vehicles with roadside safety hardware and has proven to be very effective. In this chapter, the methodology used to assess the performance of guardrail systems in this study is presented (Figure 3-1).

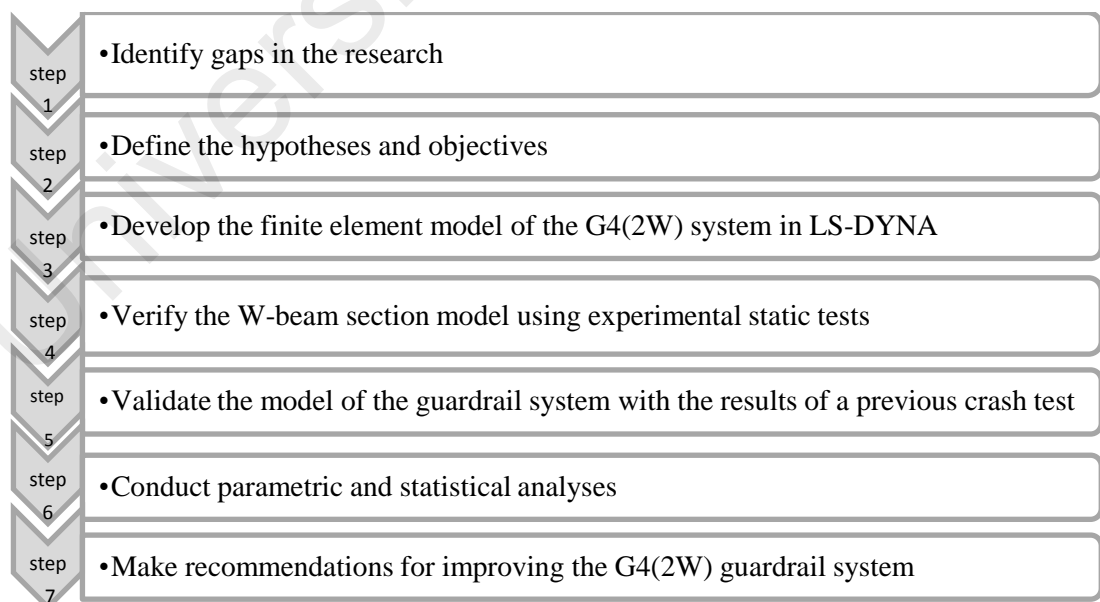


Figure 3-1. Steps in the study

3.1.1 LS-DYNA modelling

Improving the impact performance of roadside guardrail systems has been one of the major topics in transportation engineering because these systems can save lives when collisions occur. A great deal of effort has been put into evaluating existing guardrail systems and seeking alternative materials or structures that enhance their energy absorbing capacities. However, because there are many possible combinations of rail and post materials, a thorough investigation of all possible combinations would be very expensive and almost impossible. For that reason, a mathematical model that can estimate the global deformation of a guardrail and the energy dissipated by a vehicle impacting a guardrail system and its impact on the vehicle's occupants is a good screening tool for selecting promising combinations of rails and posts for further full-scale testing and full-scale finite element simulation. This modelling could be performed by conducting a series of finite element analyses, using a fully validated empirical model derived from the results of extensive tests, or using a simple model that incorporates the equations of motion and the structural behaviour, which may not provide high accuracy. Therefore, with high-performance computers, finite element modelling is used to predict the impact response of a guardrail system during a real vehicle impact. In the following sections, the method of modelling a vehicular impact on a W-beam guardrail is presented. Ideally, the performance of a strong-post W-beam system would be clear from the results of the crash tests, but only a few crash tests of G4(2W) guardrail systems have been conducted using the MASH's criteria. Due to the high cost of crash tests in terms of both money and time, finite element modelling was used. The existing literature on tests of guardrails is valuable because it provided data with which the finite element model could be validated.

3.2 Strong-post W-beam guardrail model

The basic steel-post guardrail model used in this study was provided by the NCAC (<http://www.ncac.gwu.edu/vml/models.html>). This guardrail model was made available online by the NCAC for use by researchers in crash modelling. The model was designed to be used with LS-DYNA, a finite element simulation package. The guardrail system is 53.6 metres (175.8 feet) in length from end to end. It includes a total of 29 posts, 21 of which are standard W150 × 13.5 (W6 × 9) steel I-beams. Each rail section is 3.81 metres (12.5 feet) long and 2.66 mm (0.1 in) thick, except at each end, where the rails are twice as long. The material properties of all the components are provided with the model. Both ends of the guardrail are supported by four wooden terminal posts leading to breakaway cable terminals (BCTs). Each wood post is 140 mm wide, 190 mm deep, and 2200 mm long (5.5" × 7.5" × 7.2') and embedded in a steel foundation tube, which is embedded in the ground.

Near the area of contact, i.e., near posts 9 – 21, the bolts that hold the rails and posts together are explicitly modelled as rigid bodies. The bolts and nuts are held together with spring elements. Outside of the area of contact, i.e., near posts 1 – 8 and 22–29, the connections are modelled as rigid nodal constraints. This simplification was made under the assumption that the connections outside of the area of contact would experience minimal deformation and remain connected during the crash tests.

The specific components of the basic steel-post guardrail model were not validated; however, the overall guardrail system was validated using a full-scale crash test performed at the Texas A&M Transportation Institute. Because no model of the G4(2W) guardrail system has been provided by the NCAC, one is developed in this study.

3.3 Development of a model of a G4(2W) wood post guardrail system

Wood posts are commonly used in guardrail systems around the world. Wood has nonlinear material properties and is an anisotropic complex fibrous material. In addition, the material properties of wood vary with temperature, time, loading rate and moisture content.

Because the behaviour of wood is commonly less elastic, the sudden fracture of a wood post could cause a vehicle to be pocketed and increase the tensile stress in the W-beam. Therefore, a numerical model of the wood posts must accurately predict their failure. Although wood is anisotropic, it is a fibrous material that has three major directional axes. For analysis and design purposes, wood can be considered orthotropic. On reviewing the available material models in LS-DYNA, six potential models are identified for the wood posts (Table 3-1). The material models are selected based on their support for solid elements, orthotropic constitutive relationships, and element failure criteria. The material models listed in Table 3-1 that contain the word “*Option*” in their names are able to model various constitutive relationships, such as orthotropic, anisotropic and isotropic relationships. Except for excluding Material no. 13, each of the material models is valid for modelling the orthotropic material behaviour of elements described as solid (Table 3-1). Isotropic Material model no. 13 has a simple plastic strain failure model (LS-DYNA, 2013). Plaxico et al. (2000) developed equivalent isotropic characteristic to model wood guardrail posts using experimental data. In general, an isotropic material model is unable to capture the actual failure mechanism of a wood post subjected to bending; however, equivalent isotropic characteristics can be used to approximate the complex behaviour of wood. Orthotropic material behaviour can be modelled with the other five material models presented in Table 3-1.

Table 3-1: LS-DYNA material models considered for wood posts

Material Number	Material Name
2	Option tropic Elastic
13	Isotropic Elastic-Plastic with Failure
22	Composite Damage
26	Honeycomb
59	Composite Failure Option Model
126	Modified Honeycomb

Materials no. 26 and no. 126 are considered suitable for use with metallic honeycombs and could be used to model with 3 independent, uncoupled axes. The extensive property required to model materials of this type is not available for wood. In addition, honeycomb materials contribute to several problems, including hourglass formation and numerical instability. For these reasons, Materials no. 26 and no. 126 were not considered. Three other materials, no. 2, no. 22, and no. 59, are used to represent orthotropic, solid elements. Orthotropic elastic Material no. 2 is a model that is able to represent the linearly elastic behaviour of wood. To consider the failure of an element made from Material no. 2, an *Add Erosion* card can be added to the LS-DYNA input file. This option could impose element failure properties on any material model that does not already include such criteria. The limitation of the *Add Erosion* card is its requirement that elements fail due to principal stress or strain, equivalent stress or strain, shear strain, or pressure. These failure criteria are not readily available for wood and neglect to consider the differences in strength along each of the material's axes.

Materials no. 22 and no. 59 support linearly elastic orthotropic material behaviour as well as orthotropic brittle failure. The compressive, tensile, and shear strengths for each

principal axis are input, and failure is determined using the Chang-Chang criterion (LS-DYNA, 2013).

The difference between Materials no. 22 and no. 59 is in their implementations of element failure. Material no. 59 erodes failed elements, whereas Material no. 22 leaves failed elements in the model. Because element erosion provides a more accurate visual representation of the actual failure mechanism of a wood post, Material no. 59 was chosen over Material no. 22 (Figure 3-2). Support for Material no. 59 is not fully integrated; therefore, eight-node constant stress solid elements are used in the simulations. The behaviour of the wood posts is closely monitored for hourglass instabilities during the simulations.

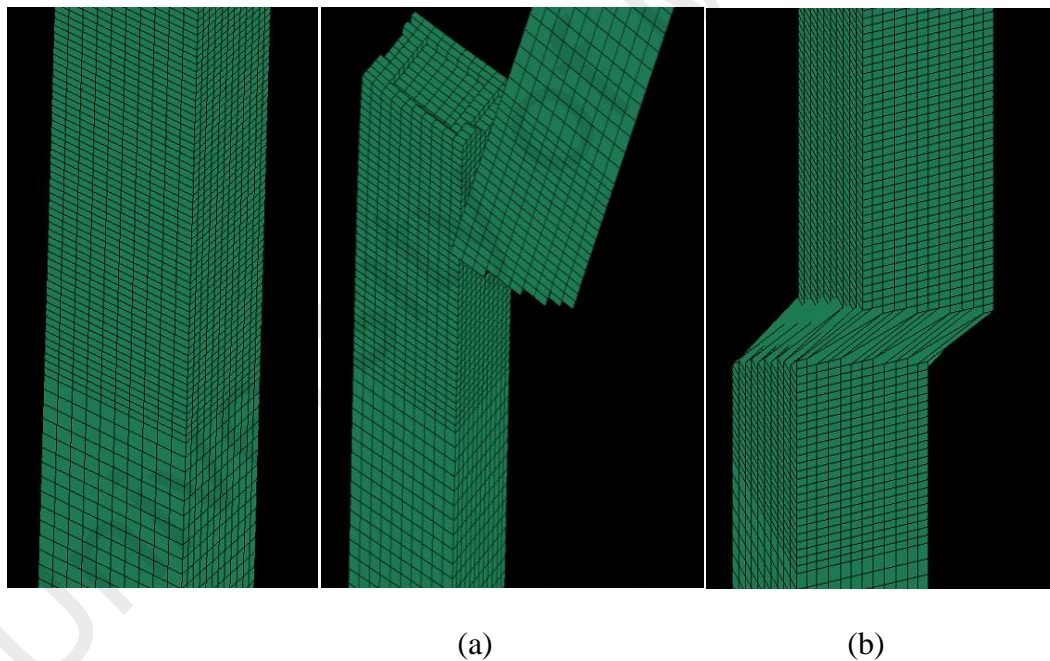
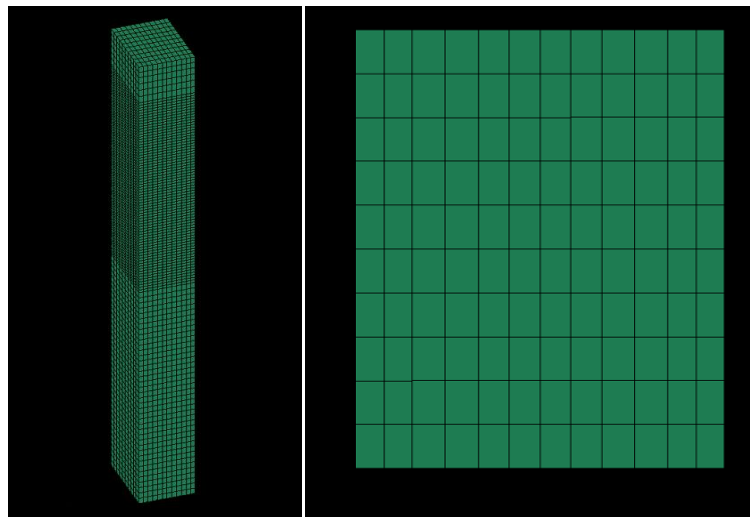


Figure 3-2. Wood post failure: (a) Material no. 59; (b) Material no. 22

The model of a 203.2 mm deep 150 mm wide wood post shown in Figure 3-3 consists of 1376 elements and 2220 nodes. The wood post is 1828.8 mm long.



(a)

(b)

Figure 3-3. Finite element mesh of a wood post: (a) Isometric and (b) Bottom views

3.3.1 Post assembly

The strong-post design uses wood posts. The posts are meshed with a 36.83 mm mesh. The region near ground level is given a finer mesh, and Material no. 13 is used to allow fracture in that region. However, the upper part of the post is modelled as being constructed of an elastic material for simplicity, and a coarser mesh is used to reduce the computation time. This configuration improves the model of the wood posts. A failure criterion is also defined to allow fracture in that region.

3.3.1.1 Post-blockout connections

To avoid possible instabilities caused by the difference in the mesh sizes, the mesh of the upper parts of the posts matches that of the blockouts in size (Figure 3-4).

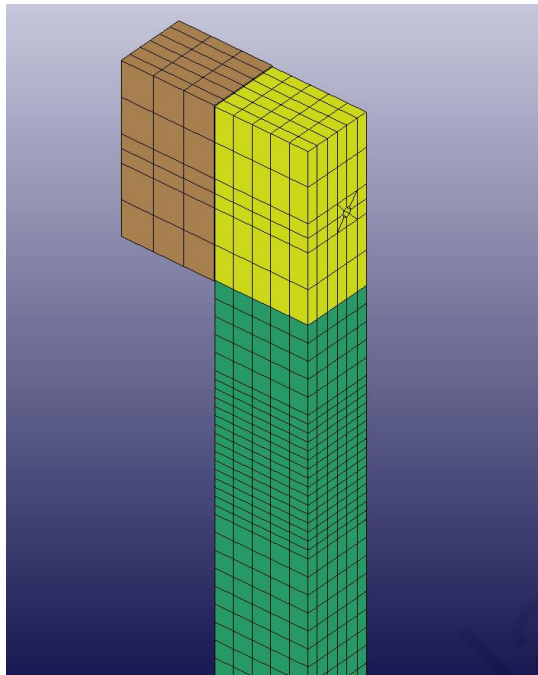


Figure 3-4. The mesh of a blockout and the upper part of a post

3.3.1.2 Assembling the bolt connections

In the original model, bolts and nuts only attach the rail to the blockout. Now, the model is extended by attaching the rail to the blockout and the blockout to the post. Therefore, each bolt now connects three parts: the rail, a blockout and a post (Figure 3-5).

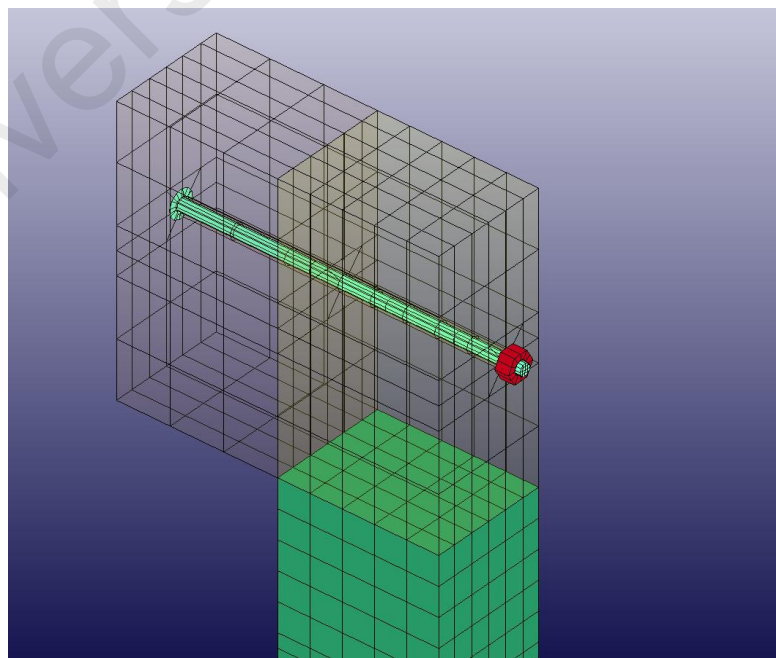


Figure 3-5. Post-Blockout attachment modification

3.3.1.3 Fracture region of the wood posts

In Figure 3-6, two posts with different mesh sizes are compared. When the mesh is coarser, the behaviour of the post is stiffer. Therefore, it does not fracture as expected. To solve this problem, the mesh of the post is refined at the region in which it is expected to fracture due to bending.

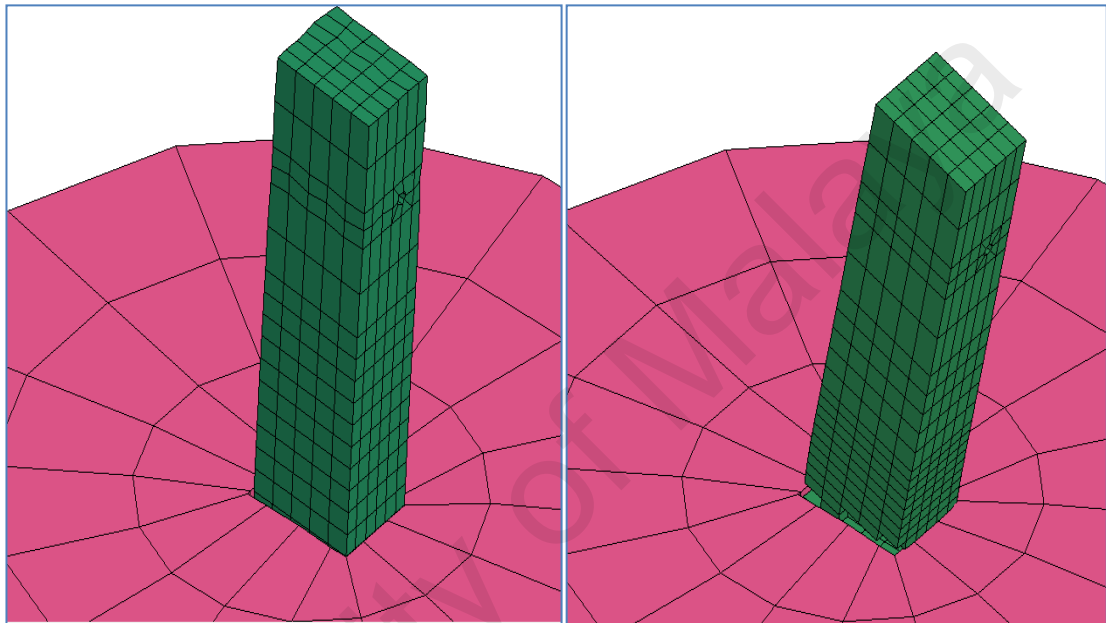


Figure 3-6. Fracture region of a wood post

3.3.1.4 Guardrail bolt and nut

The guardrail bolt and nut meshes are generated from solid elements based on the specifications of physical guardrail bolt FBB06, which are outlined in the AASHTO's Guide to Standardised Highway Barrier Hardware (AASHTO-AGC-ARTBA, 1995). Profile views of the guardrail bolt and nut mesh are shown in Figure 3-7. The mesh size used for the bolt is constant because a rigid material model is used. In general, guardrail bolts and nuts are simplified and modelled as rigid parts because they do not usually fracture in guardrail systems.

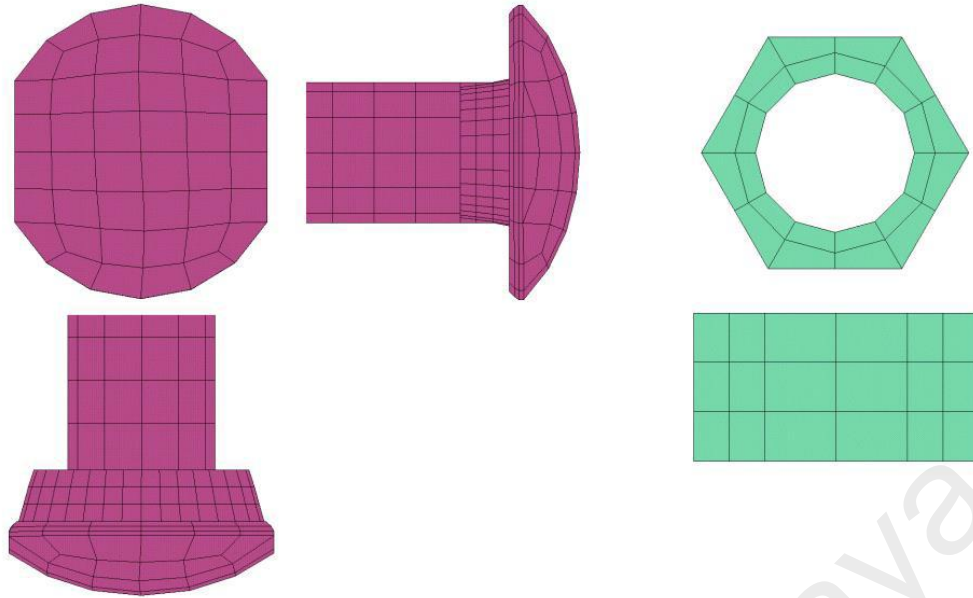


Figure 3-7. Profile of guardrail bolt and nut solid element mesh

3.3.2 Blockout

The blockouts are meshed with a 25 mm solid element mesh. The blockouts are not expected to fracture or deform as severely as the posts; therefore, their mesh elements are not refined further to reduce the computational cost (Figure 3-8).

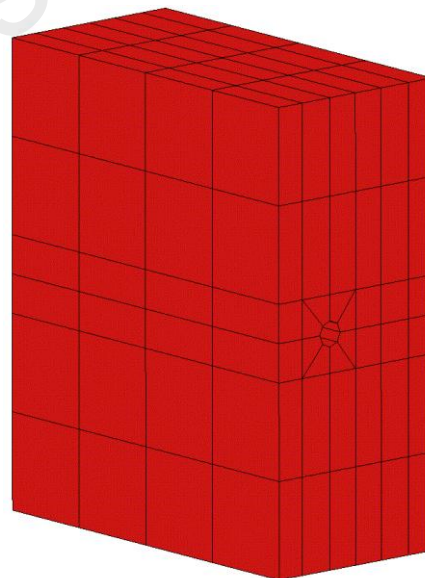


Figure 3-8. Blockout mesh size

3.3.2.1 Guardrail bolt and blockout interference

The blockouts are simulated using an elastic-plastic failure material model, and the properties of the wood are set in the input card. In contrast, the bolts and nuts are modelled as rigid materials with the properties of steel. Therefore, the contact between these two parts results in instabilities due to the significant difference between the Young's moduli of elasticity (due to contact between a very stiff material and a comparably soft material). There are many contact types available in LS-DYNA, however, to reduce the computational time, the common `AUTOMATIC_SURFACE_TO_SURFACE` is used with the help of NULL shell elements that cover the blockout. These shell elements are solely used for contact purposes and have no effect on the geometry of the blockouts (Figure 3-9).

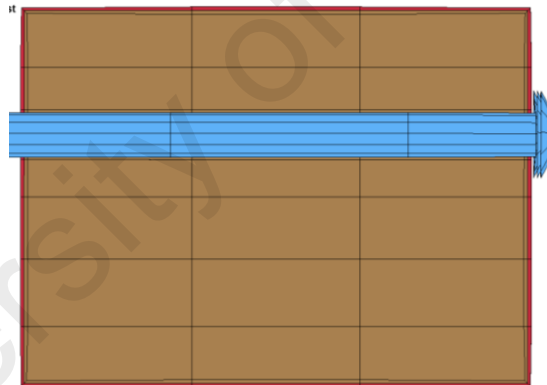
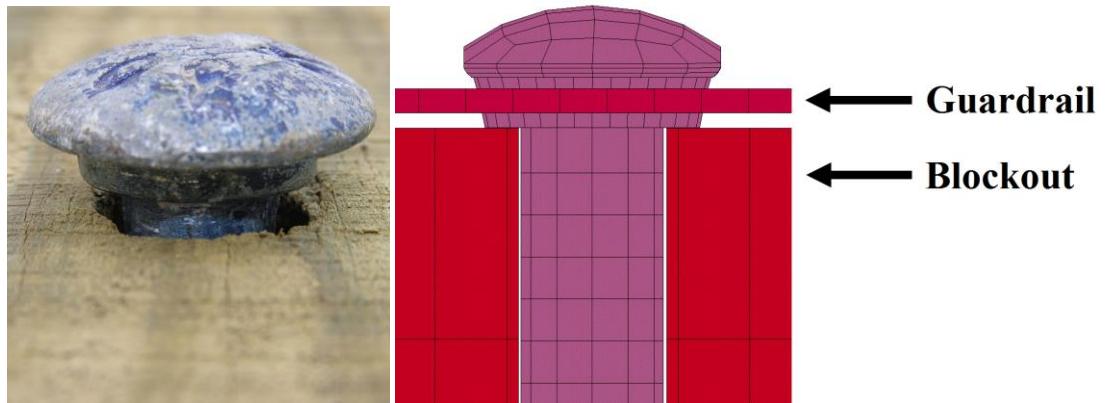


Figure 3-9. Introducing a layer of NULL shell elements

Interactions between the blockouts and the guardrail bolts during the clamping phase pose a challenge due to the geometry of the guardrail bolts. A guardrail bolt contains an oblong neck region just below the bolt head that measures 25 mm×16 mm ×6 mm, which helps prevent rotation of the bolt during tightening. The wider portions of the neck interfere with the face of the blockout directly surrounding the circular bolt hole, as shown in Figure 3-10.



(a) Physical System

(b) FEM Model

Figure 3-10. Guardrail bolt and blockout interference in the physical system and the FEM model

3.3.2.2 Contact interference between the bolt and post

Another method for preloading bolts is to use a technique developed for modelling shrink-fitted parts. In this method, initial geometries are defined such that there are finite initial penetrations between parts. The `*CONTACT_..._INTERFERENCE` option is invoked in the definition of the contact between the interpenetrating parts.

The contact interference option is available with the following contact definitions (LS-DYNA, 2013):

1. `CONTACT_NODES_TO_SURFACE_INTERFERENCE`
2. `CONTACT_ONE_WAY_SURFACE_TO_SURFACE_INTERFERENCE`
3. `CONTACT_SURFACE_TO_SURFACE_INTERFERENCE`

However, for simplicity, this model only includes the rigid bolt and nut; no discrete springs are used in this method. The guardrail bolt and nut are constrained together so that the nut is not permitted to move along the shaft of the bolt. The geometry of the guardrail nut is then defined so that it initially penetrated the back side of the post as shown in Figure 3-11. When the contact forces developed, the initial penetrations were

removed, forcing the nut to separate from the post flange. Thus, a clamping force develops within the bolted connection.

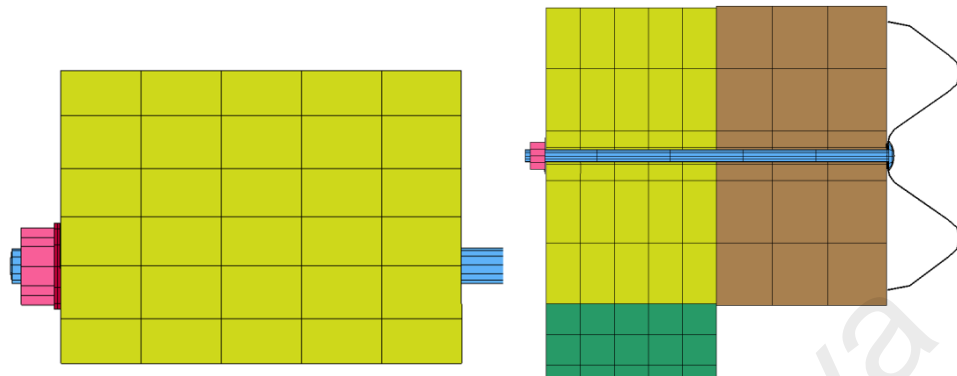


Figure 3-11. Interactions between guardrail nuts and posts

3.3.3 Soil model

The performance of a guardrail system is highly affected by the soil's ability to deform to absorb energy during a vehicle impact. Variations in the soil strength have a considerable influence on guardrail performance (Eggers & Hirsch, 1986). Therefore, an accurate numerical model of the soil and its behaviour in contact with the guardrail post is necessary to develop a reliable model. Developing numerical models of the contact between soil structures and guardrail posts is discussed by Seckinger and Roschke; a summary follows (Seckinger & Roschke, 2002).

The standard soil used in crash testing of roadside guardrails is basically an AASHTO-designated base material for roads (AASHTO, 1990).

A summary of the material properties of the soil used in the simulations performed in this study is given in Table 3-2. These properties attempt to be relatively similar to the soil conditions of the full-scale crash test conducted by Bullard et al. (2010a), which is used in this study to describe the soil's material properties.

Table 3-2: Summary of the material properties used in the soil model

Mass Density (kg/m ³)	Elastic Shear Modulus (MPa)	Poisson's Ratio	Failure Surface Shape Parameter	Internal Friction Angle (rad)	Cohesion	Dilation Angle (rad)
1,922.0	9.00	0.40	0.80	0.75	0.00	0.00

In the past, due to the significant computational time required to process a continuum of solid soil elements, researchers used less expensive approximations for modelling soil-structure interaction. For example, Patzner et al. (1998) used a subgrade modulus approach to model contact between wood guardrail posts and a cohesionless soil. Figure 3-12 shows the finite element representation of this model, including the nonlinear springs used to represent the soil. While this technique could represent the interaction of soil and posts well, variations in the overburden pressure or confinement during the simulation, for example, during an impact on a guardrail encased in a mow strip, can decrease the accuracy.

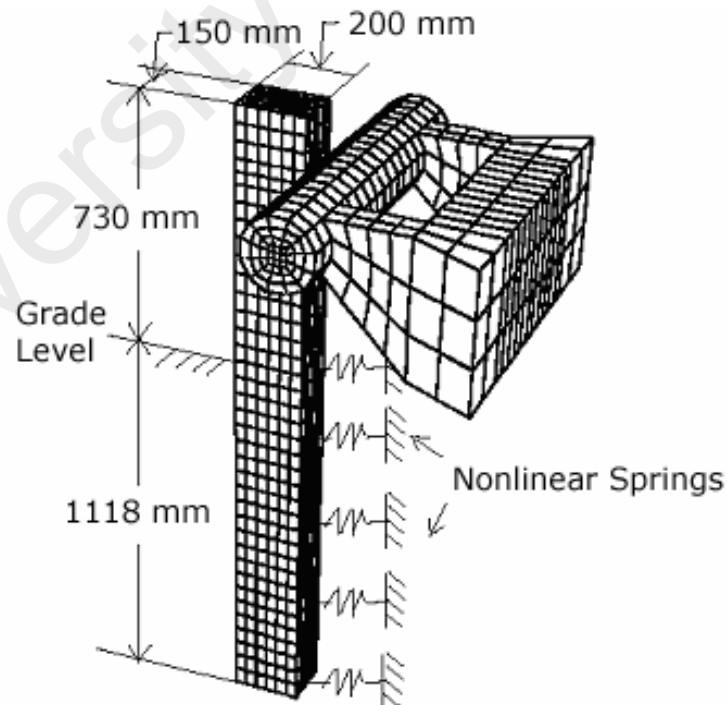


Figure 3-12. Post-impact model using the subgrade modulus for soil discretisation

To represent solid Lagrangian elements, several material models that have the characteristics of soil are available in LS-DYNA (LS-DYNA, 2013). The material models used in this study are listed in Table 3-3.

The majority of the material models of soil are intended for deep-foundation, high-confinement problems. Generally, these materials behave as fluids, and it is necessary to confine them within geometric boundaries. However, low confining stresses generate numerical instabilities. This restriction is present in materials no. 5, no. 14, and no. 78.

An isotropic elastic-plastic constitutive model (Material no. 12) is available in LS-DYNA (2013) to model a continuum of soil elements. However, the yield surface used for this model is pressure independent (Figure 3-13), which can lead to inaccuracies when the confinement or normal stress in the soil changes during an impact.

Table 3-3: LS-DYNA material models considered for the soil

Material Number	Material Name
5	Soil and Foam
12	Isotropic Elastic-Plastic
14	Soil and Foam with Failure
16	Pseudo Tensor Geological Model
25	Inciscid Two Invariant Geological Cap
26	Honeycomb
72	Concrete Damage
78	Soil Concrete
79	Hysteretic Soil
126	Modified Honeycomb
192	Soil Brick
193	Drucker-Prager

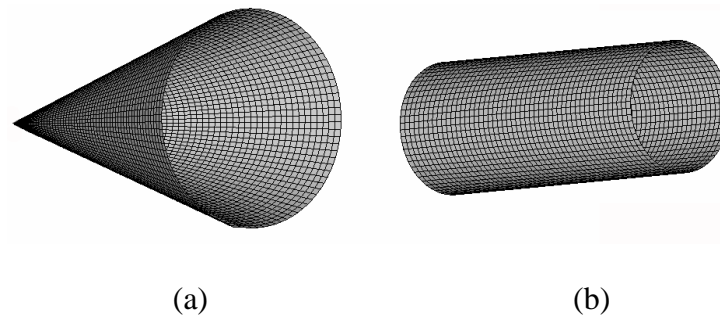


Figure 3-13. Yield surfaces in plasticity models: (a) Drucker-Prager (pressure dependent); (b) Von Mises (pressure independent)

To capture the increase in strength of a sandy soil under normal stress, Drucker and Prager proposed a modification of the Mohr-Coulomb criterion (Drucker & Prager, 1952).

The yield surface is calculated using Equation. 3.1,

$$3\sigma_m \sin(\phi) + J_2 - c = 0, \quad 3.1$$

Where J_2 is the second stress invariant, σ_m is the mean stress, c is the cohesion, and ϕ is the angle of internal friction of the material.

A Drucker-Prager material property is available in LS-DYNA (2013) and requires input parameters that are readily available in previous studies. Due to its computational efficiency and ability to model essential soil characteristics accurately, this material model is used for the numerical simulation of soil in this study. The other material models, require complex algorithms or experimental data that are not readily available. Soil can be numerically modelled by considering its behaviour as linearly elastic up to a state of stress at which slip or yield occurs.

To model a cylinder of soil, a continuum of 704 solid elements with 938 nodes is created. The mesh is shown in Figure 3-14. The soil cylinder is 2.104 m high and provides sufficient depth below the post.

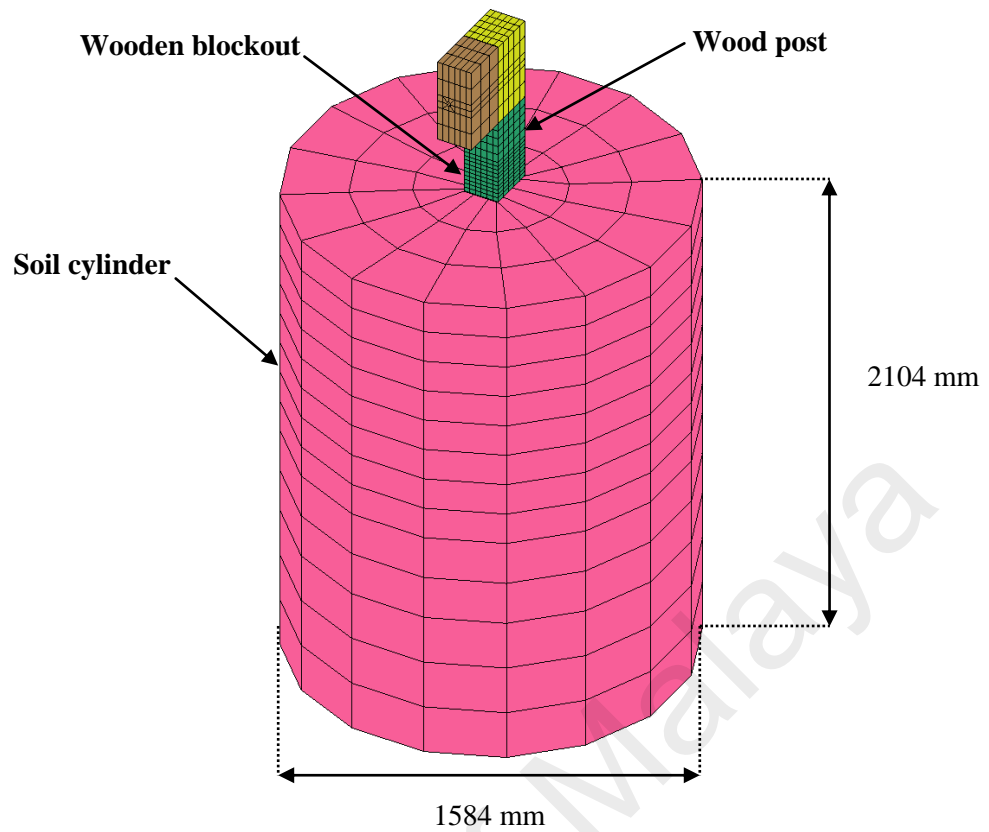


Figure 3-14. Finite element model of a steel post in soil

The behaviour of the elements must, therefore, be carefully monitored for the presence of such modes during the simulation.

To define the contacts between posts and soil, null shell elements are used (LS-DYNA, 2013) (Figure 3-15).

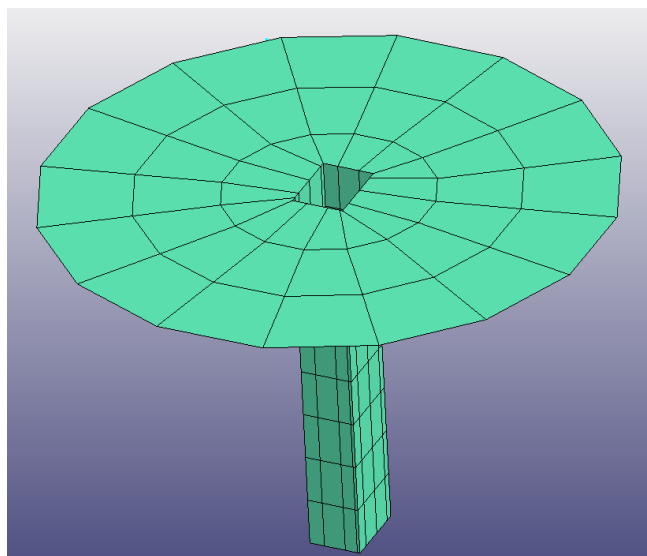


Figure 3-15. Null shell elements for simulating contact between a wood post and soil

Null shell elements are only included for contact purposes and are not included in structural element processing. The selection of contact algorithms available in LS-DYNA is case-specific. To capture the contact between the surface of the soil and a wood post, it is necessary to select surface to surface contact.

3.3.4 W-beam model

The most common longitudinal barrier system in use today is the strong-post guardrail system, which consists of a corrugated steel beam supported by either wood or steel posts. Since the mid-1950s, several countries around the world have developed and tested their own corrugated steel beam shapes. For many years, the United States has relied heavily on corrugated steel beams with only one shape, W-beams. The shape of a W-beam was developed and evaluated for both weak- and strong-post guardrail systems and was based primarily on the results of a significant amount of full-scale vehicle crash testing with both sedans and small cars.

The analysis of the rail shape considered several factors, including the geometry, structural capacity and aesthetics of W-beams. The common 2.66 mm W-beam thickness described in the AASHTO's M180 Class A specification is considered in this study.

3.3.4.1 Computer simulations

Nonlinear FEA is used to aid the design process. The code used for the simulations is LS-DYNA. This section briefly describes the simulations.

The W-beam guardrail model used in this study consists of corrugated sheet steel beams, as shown in Figure 3-16. The W-beam section is 312 mm high, 81 mm wide and 2.66 mm thick. The model W-beam guardrail system is 3820 mm long and has 320 mm overlaps between each pair of adjacent beams. The guardrails located in the central portion are subjected directly to the impact of the vehicle.

Splice bolt holes are meshed at each end of the rail segment for splicing adjacent rails. It is particularly important to model these splice bolt holes because this is the region of the rail that is subjected to the greatest stress and is, therefore, the most likely location for the rail to fail.

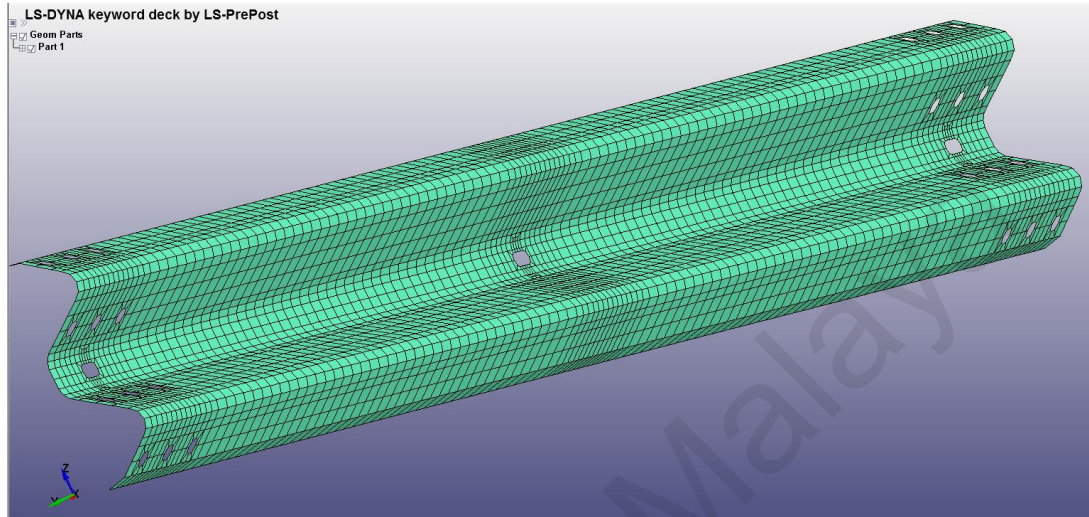


Figure 3-16. Finite element mesh of the W-beam guardrail

The numerical model of each rail segment consists of 3851 elements and 4006 nodes. Under-integrated Belytschko-Tsay shell elements are used with two Gauss integration points through each element's thickness. Among the many material models in the LS-DYNA library that describe the behaviour of steel rails, the piecewise linear plasticity material (LS-DYNA, 2013) is found to be the most compatible with the experimental results.

Failure of a steel W-beam is identified based on its nominal yield strength, ultimate strength, and ductility.

In this section, the internal energy is considered equal to the total energy absorbed. A typical cross section of a W-beam guardrail is shown in Figure 3-17.

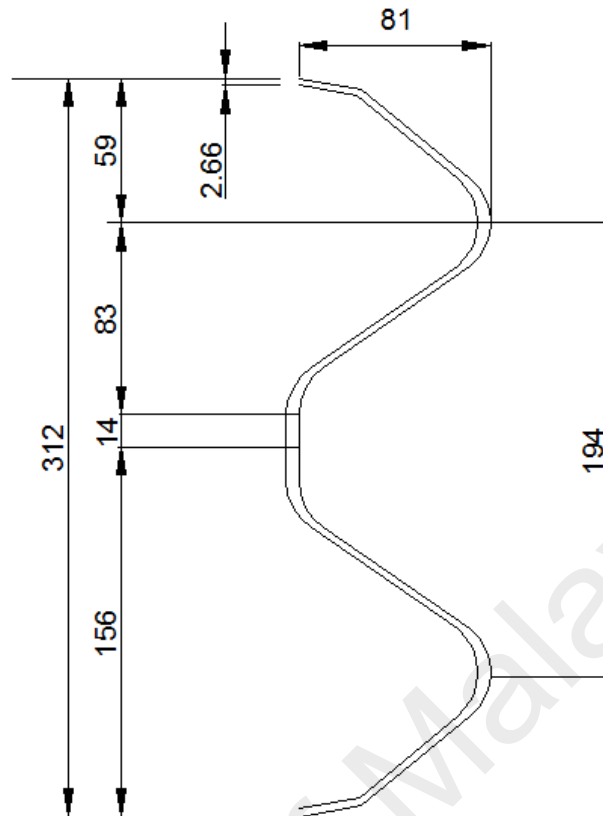


Figure 3-17. Cross section of a W-beam guardrail according to the AAHTSO (2000)

It is acknowledged that the strain rate effect influences the dynamic impact behaviour of steel significantly. The yield criterion that governs the plastic flow in the structural problem is dependent of the rate of strain (Jones, 1989). Material no. 24, a piecewise-linear-plastic material, is used in LS-DYNA. Table 3-4 lists the data points with the eight stress-strain and other factors used to describe the characteristics of the material that makes up the W-beam section (Wright & Ray, 1996). In addition, a failure criterion based on an ultimate strain is used to define the material. The computational efficiency of the Belyshko-Tsay shell element formulation is a key factor underlying its selection. A sketch of a typical 2-D shell element with four nodes and integration points is shown in Figure 3-18.

The mesh size of the W-beam is established based on the results of a sensitivity study. The results of the mesh sensitivity study conducted to verify the W-beam section are explained in the next chapter.

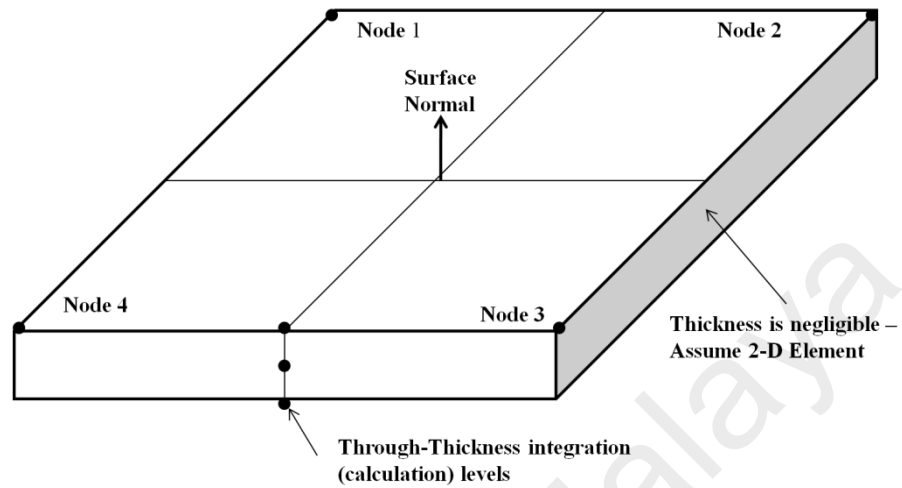


Figure 3-18. A sketch of a two-dimensional four-node shell element used in this study with three levels of integration across its thickness (Atahan, 2002)

Table 3-4: LS-DYNA material inputs for the W-beam section

Properties	W-Beam Material
Material type	Piecewise-linear-plastic with failure
Element type	Shell
Density	7850 kg/m ³
Modulus of elasticity	200,000 MPa
Poisson's ratio	0.3
Yield stress	450.0 MPa
Failure plastic strain	0.22
Effective Plastic Strain	True Stress (MPa)
0.000	450.0
0.025	508.0
0.049	560.0
0.072	591.0
0.095	613.0
0.140	643.0
0.182	668.0
0.750	840.0

3.3.4.2 Verifying the model of a W-beam segment

The main focus of this study is mainly on the W-beam rail. Due to its corrugated shape and nonlinear behaviour, an accurate model is needed. To improve the model of the W-beam section, additional considerations are described in this part.

The optimum mesh density is determined using a mesh sensitivity study to verify the model of the W-beam rail. LS-DYNA is an explicitly nonlinear finite element software; therefore, the time step used in the analysis is highly affected by the size of the elements, and a very small mesh size would make the model impractical due to its high computational demand.

Three different mesh sizes are considered: 40 mm, 20 mm, and 10 mm. The 40 mm mesh is used in the basic model of the W-beam sections of the strong-post guardrail system. A series of experimental tests is conducted to verify the finite element model of the W-beam section, and the results are discussed in the following subsections.

3.3.4.3 Experimental studies of W-beam guardrail systems

Figure 3-19 shows a schematic of the test matrix, which consists of a simple rigid base girder onto which support columns are placed. The W-beam is simply supported to allow for variations in the lengths of W-beam rail. The supports are considered adjustable along the length of the base unit. Initially, the W-beam is loaded at midspan.

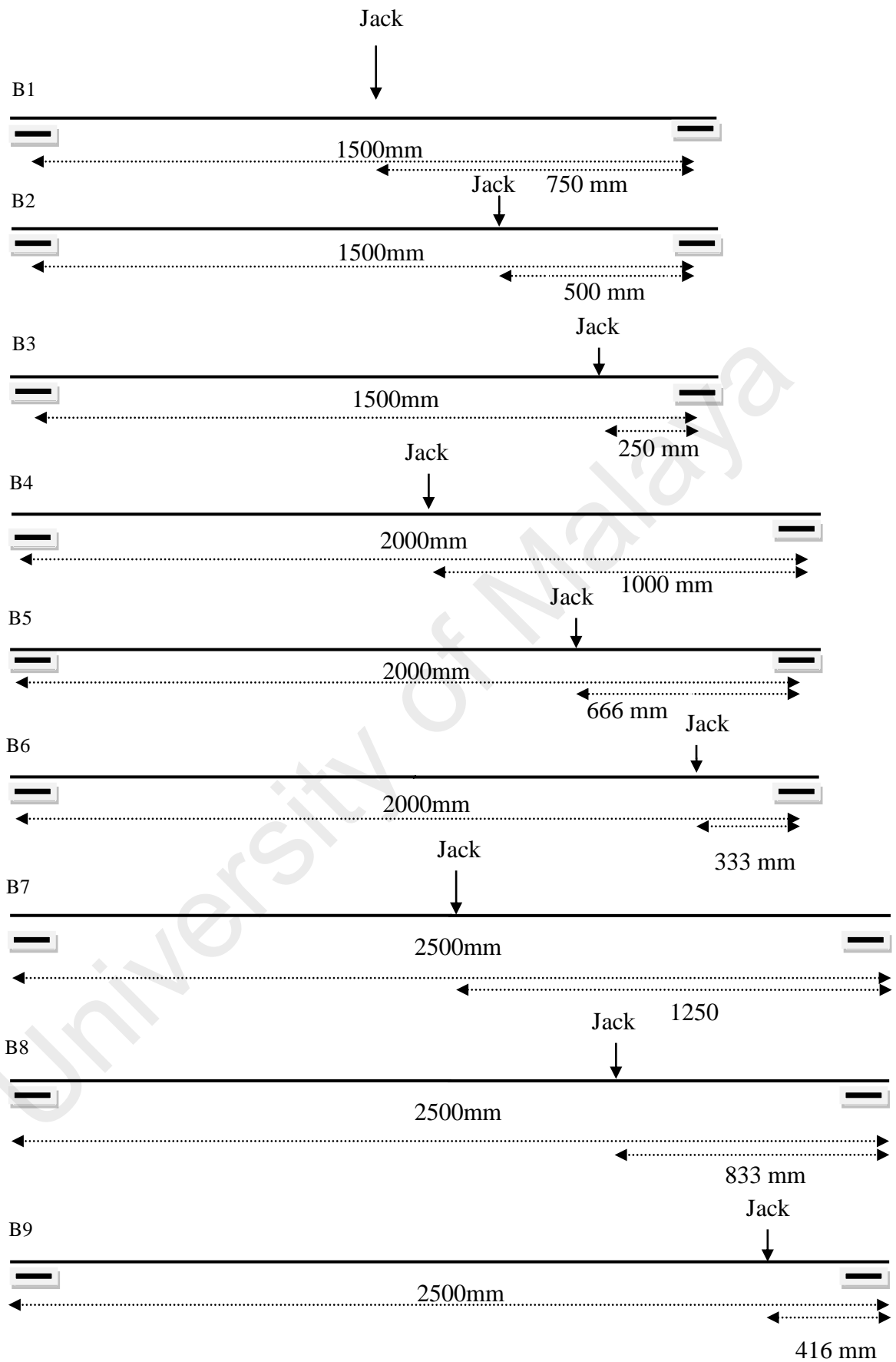


Figure 3-19. Schematic of the test matrix

Nine steel W-beams with the specifications listed in Table 3-5 are tested in the lab to calculate the force-deflection distribution along the beams for different lengths and loading points. Loading continues after the load is decreased to 80 percent of the maximum load. The W-beam preparation process includes surface preparation and positioning the W-beam at the supports. A C-flange support is chosen to create the conditions used on highways, where the beam is simply supported at both ends.

The dynamic effects serve to increase the magnitude of the force corresponding to any measure of deflection obtained in static tests, this is considered significant because W-beam rails are essentially thin-walled structures, and the mass of an impacting car is large in comparison to the guardrail system. Therefore, dynamic loading by means of full-vehicle modelling is also considered to simulate the dynamic behaviour of the system in real-world crash tests.

Table 3-5: Specifications of sample W-beam guardrails

No.	Specimen	Specimen's Length (m)	Specimen's Thickness (mm)	Loading Position (from the right support)
1	B1	1.5	2.66	750mm
2	B2	1.5	2.66	500mm
3	B3	1.5	2.66	250mm
4	B4	2.0	2.66	1000mm
5	B5	2.0	2.66	666mm
6	B6	2.0	2.66	333mm
7	B7	2.5	2.66	1250mm
8	B8	2.5	2.66	833mm
9	B9	2.5	2.66	416mm

3.3.4.4 Test configuration and instrumentation

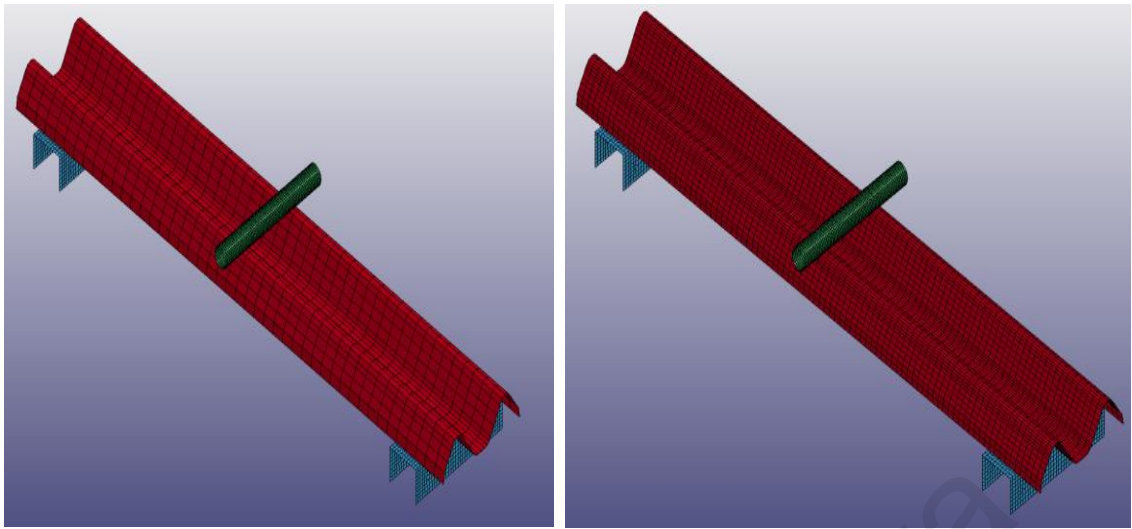
A fully equipped loading machine is required for the experiment. A load cell and a linear variable differential transformers (LVDT) are attached to the loading machine at the point of loading. When a force is applied to the specimen, the acquisition system captures data from the load cell. Subsequently, the data obtained from the load cell and LVDT are used to create load-deflection diagrams for the W-beam.

3.3.4.5 Loading and support conditions

The specimens (which are between 1.5 and 2.5 metres long) are simply supported with box elements (BS). Specimens are symmetrically placed on the supports and loaded at three different locations. Quasi-static tests are conducted using a universal testing machine (UTM) with a loading rate of 2 mm/min (0.000033 m/s) until a final transverse displacement occurs.

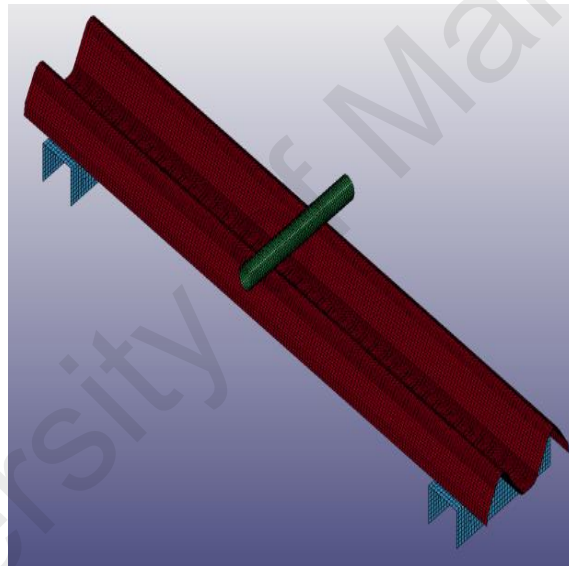
3.3.4.6 Modelling a W-beam rail using a static test

The goal of this section is to verify and validate the model of the W-beam section. Three different load positions on the W-beam are considered. To simulate a static test, the jack and support are modelled following the experimental setup (Figure 3-20). In addition, the loading is performed in accordance with the experiments. The speed of displacement of the rigid rod is 2 mm/min. Subsequently, an LS-DYNA model of a static test of the W-beam section is developed. This is performed to conduct a mesh size sensitivity test to evaluate the effect of the mesh size and to examine the first hypothesis. Finally, the optimum mesh size is selected because it agrees best with the results of the experimental tests. The validated W-beam section is used in the model of the G4(2W) guardrail system for the MASH's Length of Need test 3-11.



(a)

(b)



(c)

Figure 3-20. Different mesh sizes used to verify the W-beam rail (a) 40 mm, (b) 20 mm, and (c) 10 mm

3.3.4.7 Redirection forces

A properly designed and installed barrier system should gradually redirect vehicles towards the roadway without piercing them. During impact, the horizontal members (which work in tandem with the end anchors and the posts) should bear against the

bumper and the front fender of the vehicle. In simple terms, during impact, a properly designed and installed barrier should develop sufficient lateral forces and bending resistance to redirect the vehicle.

Strong-post W-beam guardrail systems redirect impacting vehicles through post deformation and translation in the soil, membrane action due to axial strain, and beam bending. Therefore, W-beam guardrails carry significant amounts of tension through their cross sections, including the critical section where the holes for the splice bolts are. A W-beam guardrail also provides a flexural capacity. However, the flexural capacity can decrease when the vehicle passes across the beam and flattens because hard parts of the vehicle press against the beam. Static tests may help demonstrate how the redirective load changes with the rail configuration.

The basic structural law governing the force of a guardrail system is presented in this section. The way the forces combine is shown presented in Figure 3-21.

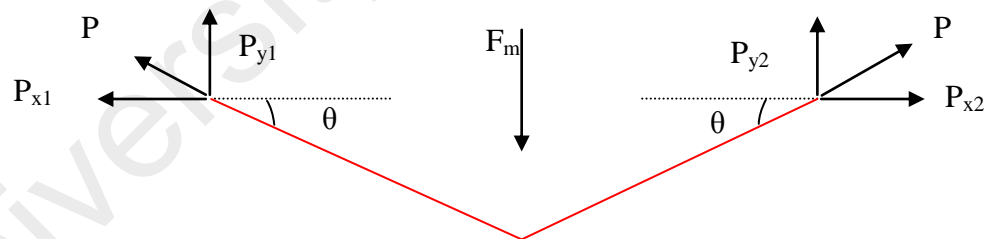


Figure 3-21. Forces due to membrane action (P_{x1} and P_{x2})

In Figure 3-21, F_m is the lateral force (Eq. 3.2) resulting from membrane action and P_{x1} , P_{x2} , P_{y1} and P_{y2} are the components of the reaction force (P). P_{x1} and P_{x2} are forces that are generated when a force is applied to the W-beam section.

$$\sum F_y = 0.$$

$$\text{Then, } F_m = P \sin \theta + P \sin \theta.$$

Consequently, $F_m = 2P\sin\theta$. (3.2)

Although FEA was not the leader in the guardrail design used for this application, the simulation provided valuable insight into the guardrail's behaviour with regard to calculating the redirection force. This insight, although not quantifiable, plays a significant role in the rail's design. The simulation results are presented in the next chapter.

3.3.5 Pickup truck model

The Silverado vehicle model was originally developed by the NCAC of the George Washington University and was later modified by MWRSF personnel for use in roadside safety applications. This particular vehicle model is a reduced version of the Silverado model that contains 248,915 elements instead of the 930,000 elements in the detailed version of the model (Figure 3-22).

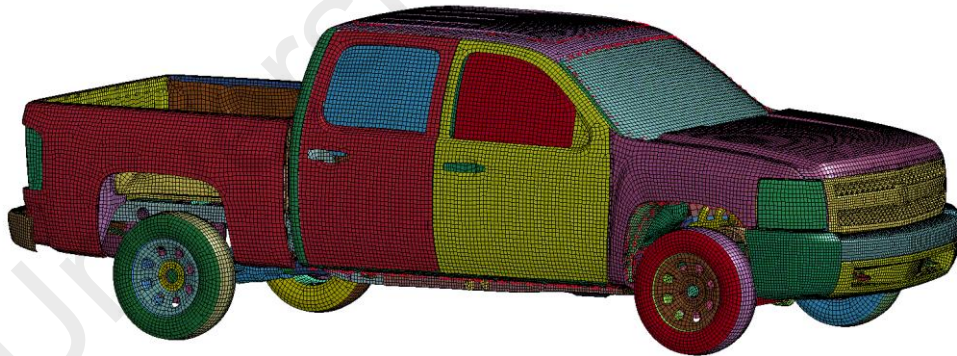


Figure 3-22. Reduced Chevrolet Silverado finite element model

3.4 Test designations and actual impact conditions

Length of Need test 3-11 in the MASH involves a 2270P vehicle weighing 2270 kg impacting a guardrail at a speed of 100 km/h and an angle of 25 ± 1.5 degrees. The target impact point was determined using information provided in the MASH and is

3.55 metres upstream of the splice at post 13. The 2007 Chevrolet Silverado four-door pickup used in the test weighs 2272 kg (Figure 3-23). The results of the crash test (Bullard et al., 2010a) conducted by the TTI are used in this study to validate the LS-DYNA model of the G4(2W) guardrail system.



Figure 3-23. Vehicle and installation geometry for test RF476460-1-5 (Bullard et al., 2010a)

3.4.1 Test description

The 2007 Chevrolet Silverado pickup, which was travelling at an impact speed of 103.64 km/h, impacted the G4(2W) W-beam guardrail 3.48 metres upstream of post 13 at an angle of 26.1 degrees. At 0.034 s after the impact, the left front corner of the vehicle contacted post 12, which began to rotate in the soil. The left front tyre and wheel rim contacted post 13, which fractured below the ground at 0.053 s. The vehicle contacted post 14 at 0.065 s and was slightly redirected at 0.078 s, after which time the vehicle was pocketed in the guardrail. At 0.122 s, the W-beam ruptured, and at 0.129 s, the vehicle began to yaw clockwise. The vehicle contacted posts 15, 16 and 17 at 0.173 s, 0.252 s, and 0.378 s, respectively. At 0.630 s, the vehicle lost contact with the W-beam and was travelling at an exit speed and angle of 54.39 km/h and 4.3 degrees, respectively, towards the field side of the installation. At 0.824 s, the left front area of

the vehicle became visible and it was noted that the left front tyre and wheel assembly had separated from the vehicle. The vehicle began to roll at 1.263 s as the rims of the wheels on the left side dug into the soil. The vehicle rolled 180 degrees counterclockwise and subsequently came to rest upside down, facing the field side of the barrier, and 4.87 metres away on the field side between posts 21 and 22 (21.03 metres downstream). A summary of the results is shown in Figure 3-24 (Bullard et al., 2010a).

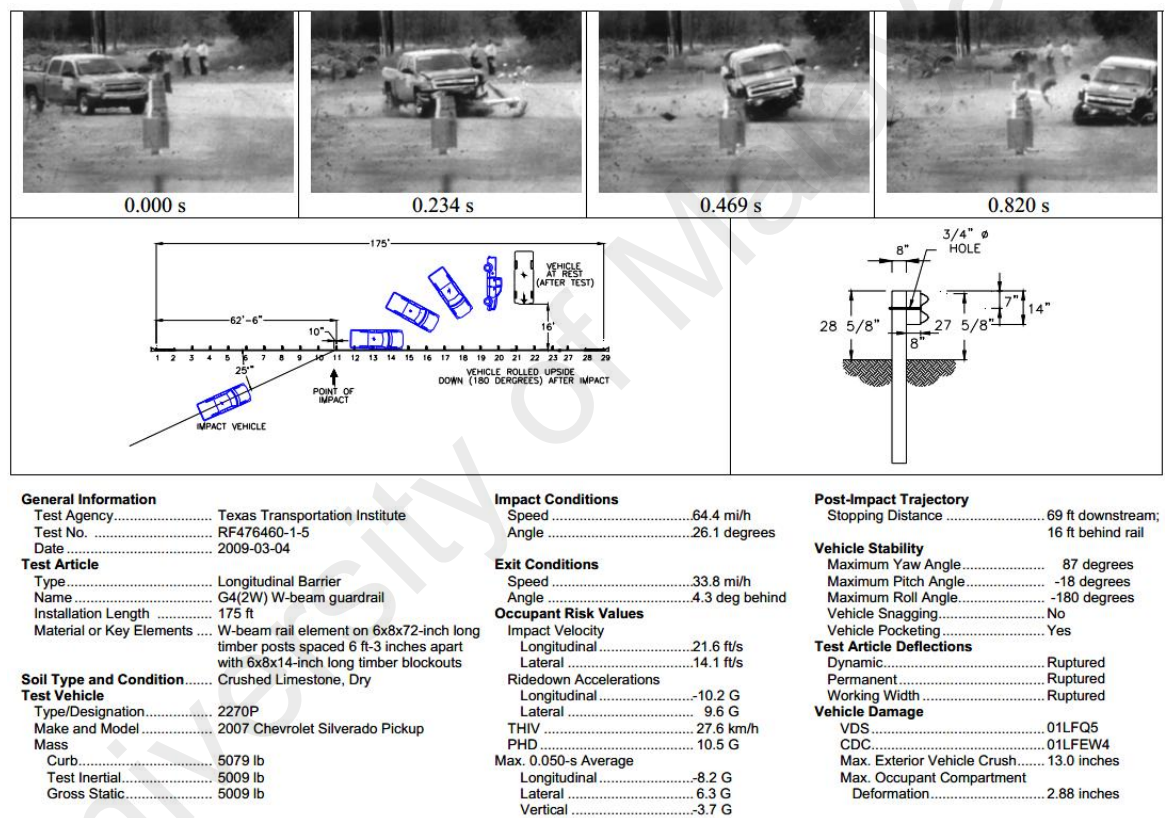


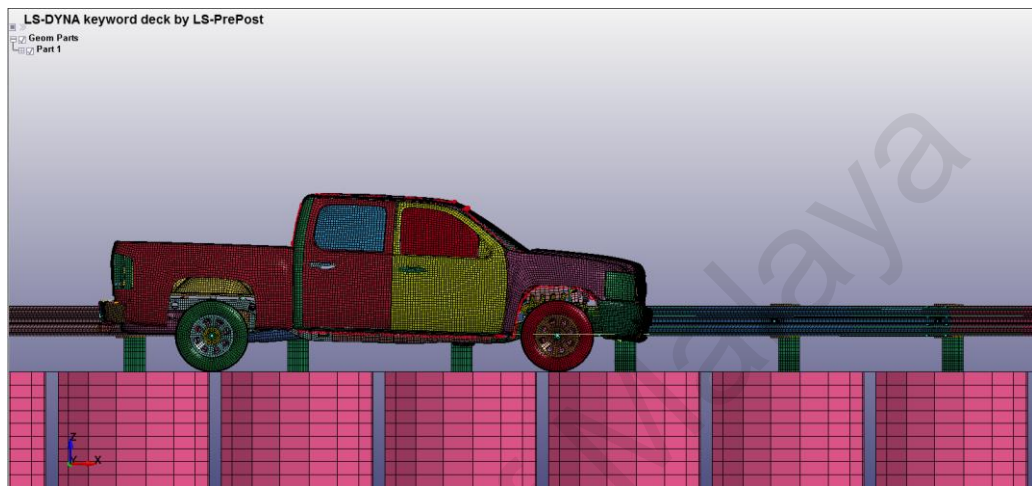
Figure 3-24. Summary of the results of Length of Need test 3-11 in the MASH for the G4(2W) W-beam guardrail system

3.4.2 Impact of the pickup truck with the guardrail system: Baseline model

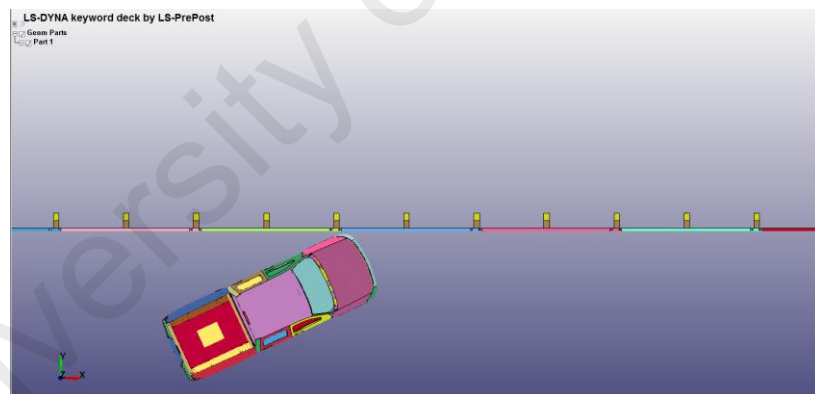
A finite element model of a G4(2W) guardrail system impacted by a Chevrolet Silverado was developed using the method described in the previous sections. The model consists of 30 posts spaced 1.905 m apart and embedded at a depth of 1.100 m

and connected to guardrail W-beams that are 3.810 m long. Figure 3-25 illustrates the position of the pickup truck with respect to the guardrail system.

The simulation follows the procedure described in the MASH's criteria for Length of Need test level 3-11 with full-scale crash test conditions.



(a)



(b)

Figure 3-25. Finite element model of the pickup truck impacting the guardrail system:

(a) side view and (b) top view

3.4.3 Qualitative validation

A comparison of sequential photographs (overhead views) is performed to provide detailed information on the LS-DYNA model and the full-scale test results.

In this study, the results of FE simulations are compared with the results of previously conducted crash tests (Bullard et al., 2010a). The comparative figures capture the basic sequence of events and correlate the finite element simulation with the full-scale crash test.

3.4.4 Quantitative validation

Quantitative validation necessary for the model used in the simulations; it can be performed at the same time as qualitative validation of the developed FE model. This can be completed by comparing the acceleration of the vehicle's centre of gravity in the simulation and the full-scale test.

Ray et al. (2007) recently developed the Roadside Safety Verification and Validation program (RSVVP), which can calculate metrics that compare the signals of simulations and crash tests that help with the quantitative validation of models of roadside hardware. The programme compares the vehicle response and attitude signals obtained from simulation and crash tests to calculate two comparison metrics: (a) the Sprague and Geers metric and (b) an ANOVA of the signals. The Sprague and Geers metric is an integral comparison that combines time integrals of the response waveforms (Schwer, 2007). The magnitude (MSG) and phase (PSG) components of the metric are calculated using Equations (3.3) and (3.4):

$$M_{SG} = \sqrt{\frac{\sum C_i^2}{\sum m_i^2}} - 1 \quad (3.3)$$

$$P_{SG} = \frac{1}{\pi} \text{COS}^{-1} \frac{\sum c_i m_i}{\sqrt{\sum c_i^2 \sum m_i^2}} \quad (3.4)$$

The ANOVA metric is based on the residual between the measured and computed curves. Ray (1996) proposed the method shown in Equations (3.5) and (3.6) for determining the average residual error and its standard deviation.

$$\bar{e}^r = \frac{\sum(c_i - m_i)/m_{max}}{n} < 0.05 \cdot m_{max} \quad (3.5)$$

$$\sigma^r = \sqrt{\frac{\sum(e^r - \bar{e}^r)^2}{n - 1}} < 0.35 \cdot m_{max} \quad (3.6)$$

In these equations, m_i and c_i are the measured and computed values, respectively. The average residual error (\bar{e}^r) and its standard deviation (σ^r) in the ANOVA metric are normalised by the peak value of the measured curve (m_{max}). The acceptance criteria for both metrics, which were suggested by Mongiardini and Ray, are shown in Table 3-6. The RSVVP is used to validate the numerical model of the guardrail system in this study.

Table 3-6: Acceptance criteria used in the RSVVP (Mongiardin & Ray, 2009)

Sprague and Geers metric		ANOVA metric	
MSG	≤ 40	Mean	≤ 0.05
PSG	≤ 40	Standard deviation	≤ 0.35

3.5 Parametric studies

Improving G4(2W) guardrail systems is an important issue, according to the FHWA. The aim of this section is to explore the system's behaviour through a parametric study and to develop an approach that improves its structural capacity. Generally, the method used to increase a guardrail's structural adequacy is to increase the intensity of the posts and the W-beam panel. Decreasing the post spacing or increasing the embedment depth could increase the intensity of the posts.

Increasing the intensity of the W-beam panel can result in less significant damage to the guardrail system and reduce its maximum deflection. Increasing the number of beams could help improve the intensity of the W-beam section. However, due to significant costs, options other than nested rails must be considered. However, guardrails can still cause vehicles to roll over. This issue is more challenging for large trucks and other vehicles with high centres of gravity, which may climb the face of the guardrail.

All these concerns should be considered when the position and the height of a guardrail system is being determined, particularly when truck traffic is significant. In conclusion, to improve the performance of the G4(2W) guardrail system, the distance between the posts, the guardrail height and the splice configuration are selected as the design variables.

Once it has been validated, the model can be further considered and developed. Therefore, parametric studies are performed to improve the G4(2W) wood strong-post system in ways that cannot be identified through experimental studies.

3.5.1 First step: strengthening the connection areas

After reviewing the results of full-scale crash test, it appears that the rail ruptured at its splice connections. Several ideas are considered to strengthen these areas because these are the most critical areas of the guardrail system. An analysis of the effects of increasing the number of bolts from 8 to 10 and 12 bolts is performed. The aim of this section is to examine hypothesis 2 to evaluate the effect of increasing the number of bolts in each splice connection on the structural adequacy of guardrail system.

- *Choosing two areas in which to increase the number of bolts*

Two locations (category 1 and 2) are considered for increasing the number of bolts in a splice connection to 10; these are shown in Figure 3-26.

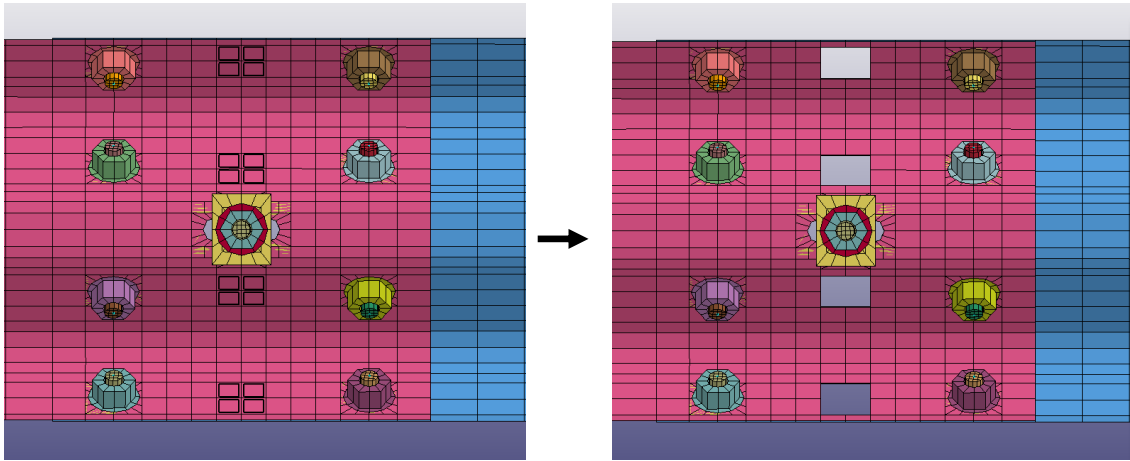


Figure 3-28. Deleting the element to place the bolts elements

To ease this process, the shell beam elements around the bolt connections are copied in the suggested area. Once the elements have been copied, the nodes are merged to connect them. This procedure is shown in Figure 3-29.

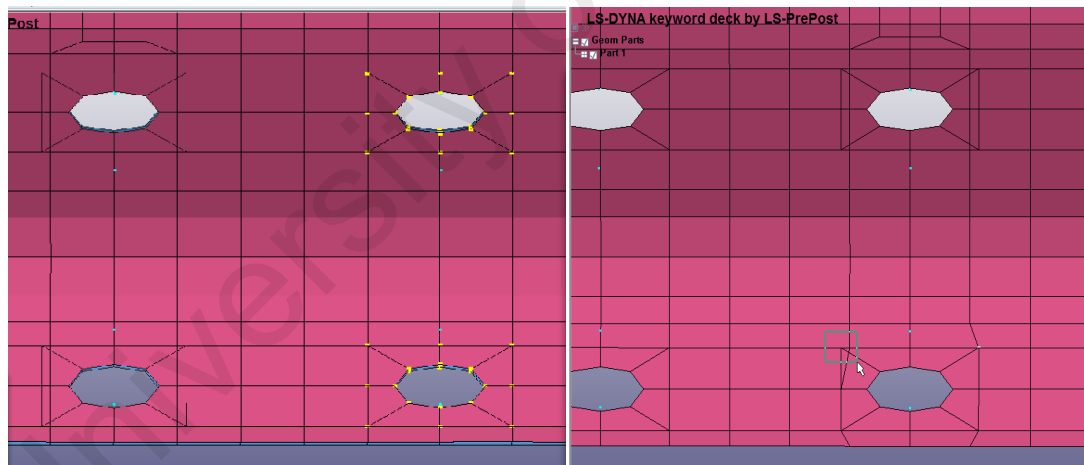


Figure 3-29. Merging the new copied elements into the rail elements

Once the rail has been prepared, the bolts are placed in the proposed locations (Figure 3-30).

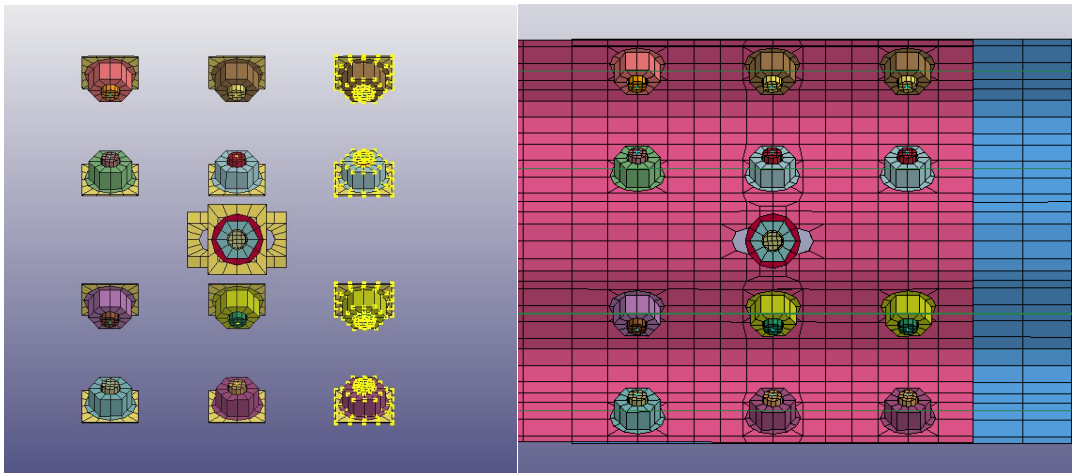


Figure 3-30. Placing the bolts in the proposed locations

3.5.2 Investigating the effect of guardrail height on safety performance

The guardrail height is one of the important factors in the design of a guardrail system. In this study, 3 different guardrail heights, 28, 30 and 32 inches, are considered in the FEM model to examine hypotheses 3, 4 and 5 and to investigate how varying the guardrail height affects the performance of the guardrail system. The posts' embedment depth is kept the same as it is in the original model (Figure 3-31).

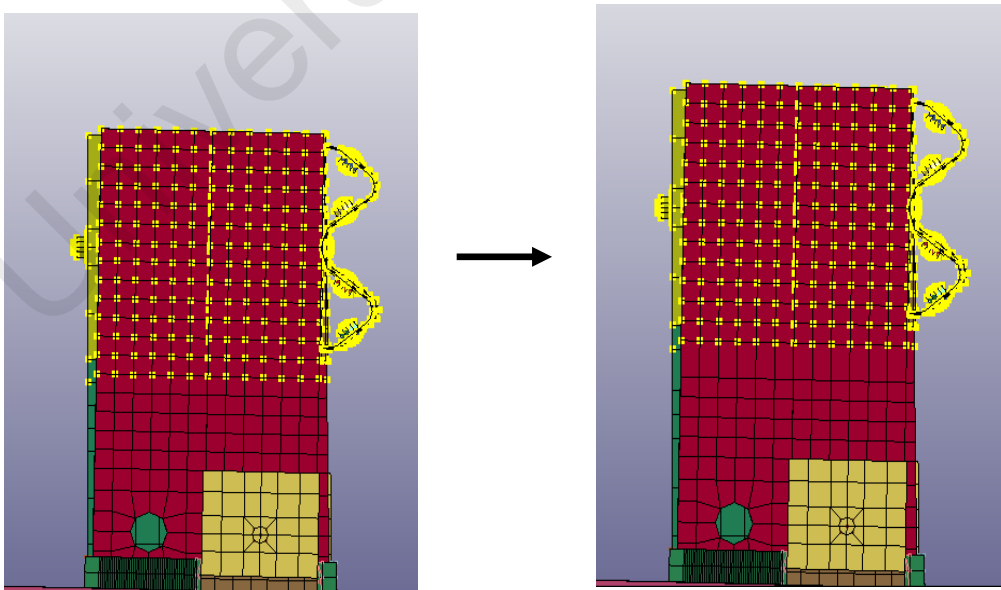


Figure 3-31. Increasing the height of the guardrail

3.5.3 Investigating the effect of the post spacing on safety performance

Variations in the post spacing are also considered in the parametric finite element study to investigate the effect of this parameter on the guardrail's performance. This is performed to examine hypotheses 4 and 5. The response of the guardrail post is measured for three different post spacings, 1.5, 2 and 2.5 metres, to evaluate the system's structural adequacy, the vehicle trajectory and the occupant risk factors. The parameters, including the sand density and the undrained shear strength of the clay, are considered constant for all the simulations.

In this modification, the post spacing of the guardrail system is changed. An increase in the post spacing can increase the time required for the vehicle to travel from one post to another.

First, the beam is cut to reduce the post spacing to 1.5 metres, as shown in Figure 3-32. Then, the part of the guardrail system is shifted to reach the desired post spacing (Figure 3-33).

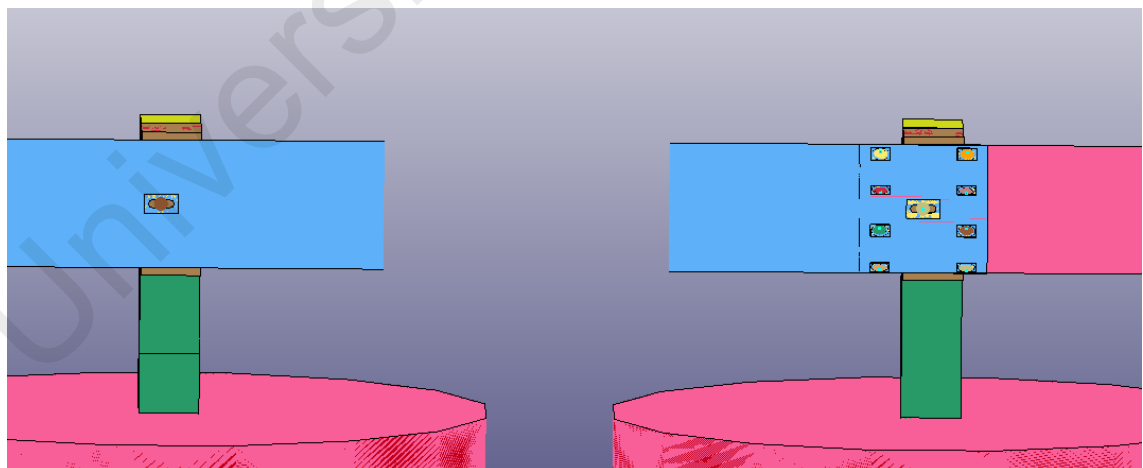


Figure 3-32. Cutting the W-beam to change the post spacing

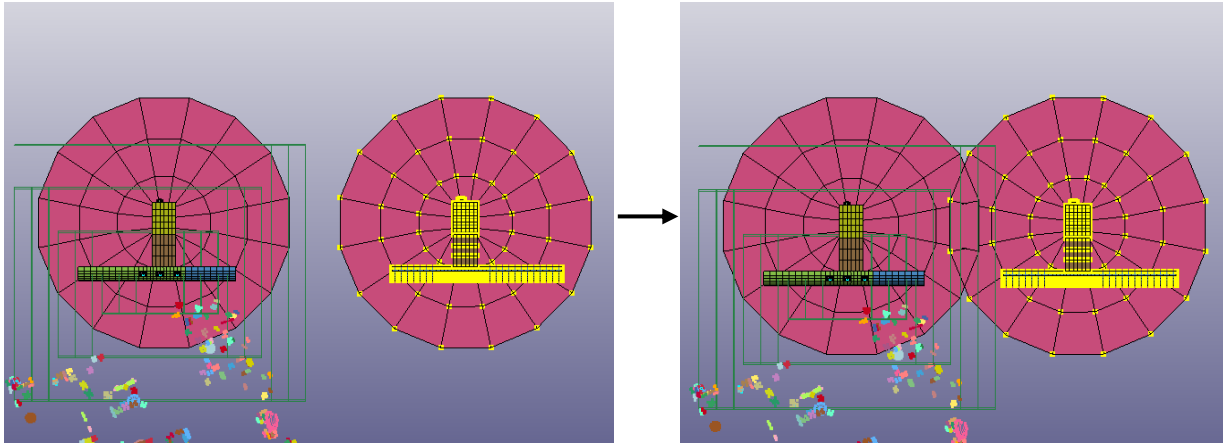


Figure 3-33. Shifting a post to reach the desired post spacing

The interacting elements are deleted, as shown in Figure 3-34. After the outer layer is deleted, a new soil box must be created to keep the soil elements stable (Figure 3-35).

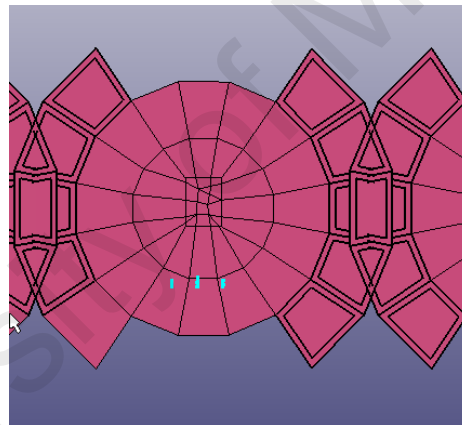


Figure 3-34. Deleting the interacting elements

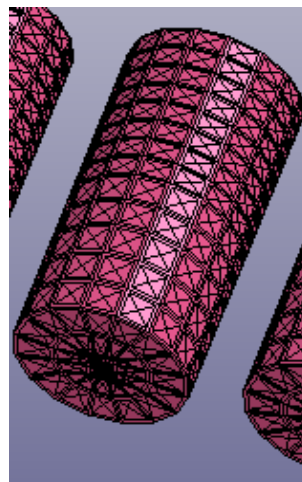


Figure 3-35. Modifying the soil box's boundary to create the boundary of new soil box

3.6 Statistical analysis

Design of experiments (DoE) is a powerful statistical technique for studying the effects of multiple variables simultaneously. This technique can be used to solve problems whose solutions lie in the proper combination of factors or variables rather than in a single identifiable cause (Roy, 2001).

DoE is a better alternative to the best-guess approach and one-factor-at-a-time experiments, which are not only costly but also not always efficient.

The best-guess approach is used in practice by engineers and could work because the experiments are designed to investigate certain technical, theoretical and practical aspects of the system. The best-guess approach has two main disadvantages. The first is that it is time-consuming, especially if the initial best-guess does not produce the desired results, and the second is the necessity of experimental planning, especially if the first test produces acceptable results. The one-factor approach involves selecting a baseline set of factors and then, studying the response of the system as each factor is varied over its range while the other factors are kept constant. The major disadvantage of this strategy is that it fails to consider any possibility of interaction between the factors (Montgomery, 2005).

DoE can be used to investigate the interactions between different parameters and the contribution of each parameter to the guardrail system's performance. This method can be used to investigate the effects of interactions among the control factors. The response surface method (RSM) was selected from the various practical DoE methods available to study the effects of the parameters. This method, which is used extensively in industry, has the advantages of optimising many factors and extracting quantitative information by conducting a reasonable but sufficient number of tests. Figure 3-36 shows the steps involved in the RSM.

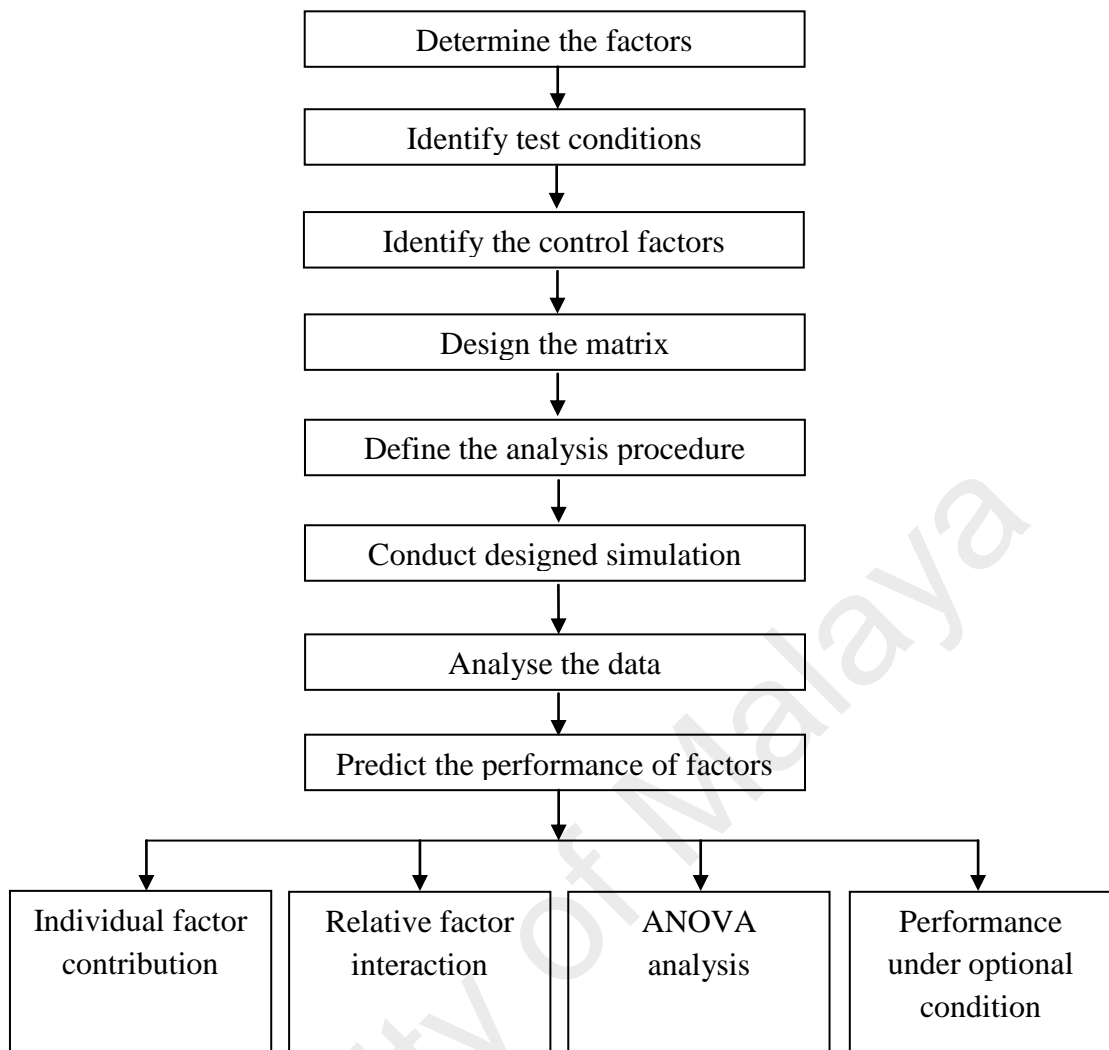


Figure 3-36. Steps involved in the RSM

Design-Expert Software 9.0.2.0 is used to design experiments, perform statistical analyses, and create regression models. A central composite design (CCD) with a quadratic model is combined with the RSM to statistically design experiments and analyse data.

Instead of the one-factor-at-a-time (OFAT) method, this study uses the statistical RSM to analyse the interactions among the parameters (Myer & Montgomery, 2002; Azargohar & Dalai, 2005) because the OFAT method is time-consuming and incapable of identifying the effects of possible interactions among the variables.

In the present study, the effects of two numerical variables (the guardrail height and the post spacing) are investigated using a CCD. Simulations are performed to identify a narrower range for the post spacing and the guardrail height.

The simulation results shown are the lateral deflection and the longitudinal and lateral accelerations are evaluated to determine the relationship among the factors, including the guardrail height (A) and the post spacing (B).

The quadratic model for predicting the optimal conditions is shown in Equation. (3.7),

$$Y = \beta_0 + \sum_{i=1}^n \beta_i x_i + \sum_{i=1}^n \beta_{ii} x_i^2 + \sum_{i=1}^n \sum_{j=1}^n \beta_{ij} x_i x_j + \epsilon \quad , \quad (3.7)$$

In this equation, Y is the predicted response, β_0 is a constant, x_i and x_j are the coded values of the independent variables, β_i is the coefficient of the linear term, β_{ii} is the coefficient of the quadratic term, β_{ij} is the coefficient of the interaction term, ϵ is the random error, and n is the number of factors studied.

An ANOVA is used to evaluate the model's fitness and to identify interactions between the amination variables and the responses. The polynomial model's goodness of fit is expressed by the coefficients of determination, R^2 and R^2_{adj} , shown in Equations. (3.8) and (3.9), respectively (Körbahti & Rauf, 2008).

$$R^2 = 1 - \frac{SS_{residual}}{SS_{model} + SS_{residual}} \quad (3.8)$$

$$R^2_{adj} = 1 - \frac{SS_{residual} / DF_{residual}}{(SS_{model} + SS_{residual}) / (DF_{model} + DF_{residual})} \quad (3.9)$$

In these equations, SS is the sum of squares and DF is the number of degrees of freedom. The statistical importance of the model was checked by determining the model's adequate precision ratio using Equation. (3.10) and by applying the F-test supplied with the software (Körbahti & Rauf, 2009):

$$\text{Adequate Precision} = \frac{\max(Y) - \min(Y)}{\sqrt{V(Y)}} \quad (3.10)$$

In these equations, Y is the predicted response, p is the number of parameters in the model, σ^2 is the residual mean square, and n is the number of experiments.

Three-dimensional response surfaces are created to visualise the individual and interactive effects of the independent variables.

ANOVA is used in graphical analyses of the data to identify interactions between the process variables and the responses. The quality of the polynomial model's fit is expressed by the coefficient of determination, R^2 , and its statistical significance is checked using the Fisher's F-test supplied with the same software. The model's terms are evaluated using the P-value (probability) at a 95% significance level. Three-dimensional plots are created for all responses based on the effects of the post spacing and the guardrail height.

The R^2 coefficient represents the proportion of the total variation in the response predicted by the model, which indicates the ratio of the sum of squares due to regression (SSR) to the total sum of squares (SST). A high value of R^2 , one that is close to 1, is desirable, and reasonable agreement with the adjusted value of R^2 is necessary. A high R^2 coefficient ensures that the quadratic model is satisfactorily adjusted to the experimental data. The adequate precision (AP) compares the range of the predicted values at the design points to the average prediction error. Ratios greater than 4 indicate adequate model discrimination.

3.7 Chapter summary

One aspect of the study is to verify the W-beam guardrail system to ensure the accuracy of the results. Due to the corrugated shape of the W-beam, a large mesh may provide

less promising results. To solve this problem, a series of static tests is proposed to verify and validate the W-beam model. Subsequently, the verified model of the W-beam section is used in the complete G4(2W) guardrail system. A finite element model of the G4(2W) guardrail system is developed in LS-DYNA. The procedures for qualitative and quantitative validation with data from a previously conducted full-scale crash test obtained from the literature are described; they are based on the MASH's criteria for Length of Need test 3-11. The previously conducted crash test involving a G4(2W) guardrail system and a Silverado pickup truck demonstrated that there is an increased risk of vehicle instability due to a lack of structural adequacy and failures of splice connections.

A parametric study is conducted on the basis of the results of the LS-DYNA simulations to investigate the guardrail system's key design factors, including the splice configuration, the post spacing and the guardrail height. This is to improve the performance of the system as measured by the MASH's criteria for Length of Need test 3-11. Eventually, statistical results highlight the effects of the main parameters, including the guardrail height and the post spacing, on the system's structural adequacy and occupant risk factors. The aim is to examine the significance of each factor for the system's behaviour.

CHAPTER 4: RESULTS AND DISCUSSION

4.1 Introduction

This chapter presents the results and discussion. The present study includes a verification of the W-beam section (Objective 2), a model that is validated by finite element simulations (Objective 3), a parametric study (Objective 4) and a statistical analysis (Objective 5). Analyses of the experimental work and the finite element modelling conducted using LS-DYNA are presented, including a discussion of the key findings. The following hypotheses were evaluated and discussed:

Hypothesis 1: The mesh size of the W-beam guardrail is related to an increase in the accuracy of the results.

Hypothesis 2: Increases in the stiffness of the splice connections are related to increases in number of bolts.

Hypothesis 3: Higher guardrails are related to increases in guardrail deflection.

Hypothesis 4: Higher guardrails and greater post spacings are related to increases in pickup truck stability and improved trajectories.

Hypothesis 5: Lower occupant risk factors are related to increases in the guardrail height and the post spacing.

As discussed in previous chapters, strong-post W-beam guardrail systems are used extensively around the world as roadside barrier systems. This is the most widely used type of steel roadside barrier; it is more than prevalent alternative systems such as the Thrie-beam, weak-post, and three-cable systems. It is one of two types of guardrail system that use W-beams, which are named for their distinctive “W” shape (the other

type is the weak-post guardrail system). There are two main types of strong-post guardrail system: steel and wood strong-post systems. As mentioned earlier, guardrail systems are evaluated using full-scale crash tests. Since the implementation of the MASH's new standard in 2009, the performance of this guardrail system has been considered unsatisfactory. In this chapter, a series of experimental studies and finite element simulations conducted to improve the performance of strong-post systems to satisfy the requirements of the MASH's criteria are described.

To avoid the significant cost of a large set of crash tests, finite element modelling was used to evaluate the crash performance of guardrail systems. While this provided significant savings in both time and cost, it also required additional effort to demonstrate that the resulting finite element model was capable of producing realistic results. The best way to show that this was true was to use the finite element model to reproduce the results of an existing crash test. If the finite element model was successful in predicting the test's outcome and the values of the MASH's test criteria, then, the finite element model was considered a valid alternative to full-scale tests. Therefore, finite element models representing full-scale crash tests should be successfully correlated with physical tests before they are applied to new design proposals.

The crash test that was selected for this purpose was a full-scale crash test conducted by the TTI to demonstrate the safety of the modified G4(2W) guardrail system. The crash test was not successful according to the criteria for the MASH's based on Length of Need test 3-11 because the guardrail ruptured at a splice connection. The damage to the guardrail was considered extensive (Bullard et al., 2010a).

Due to the limited amount of research conducted to validate the section of the W-beam guardrail used, a series of static tests was performed to validate this part. After validation, the model W-beam guardrail was used in the guardrail system, and further validation was performed with the results of a previously conducted full-scale crash test.

To improve the G4(2W) system, different parameters, including the conditions at the splice connections, the post spacing and the guardrail height were evaluated, and a finite element model of a guardrail system impacted by a Silverado pickup truck that was consistent with the MASH's Length of Need test 3-11 was built and used to investigate the effects of the different guardrail design parameters.

4.2 Validation of the W-beam section

To examine hypothesis 1 and to achieve objective 2, further consideration is performed in this section. A series of experimental static tests was performed to verify the finite element model of the W-beam section, and the results are discussed in the following subsections.

4.2.1 Comparison of the numerical model with experimental studies

During the static tests, prior to collapse, the load decreased, which was mainly due to flattening of the cross section (Figure 4-1), which can be approximately represented by the curvature of the upper and lower sides. The load increased very quickly to a peak and then, decreased gradually. Along with the global flexural distortion and flattening, there was local cross-sectional distortion directly under the loading wedge. The local cross sections flattened at the top and then, the entire cross section collapsed as bulges formed at the top. However, there was no increase in the width of the local cross section of a simply supported beam near the support.

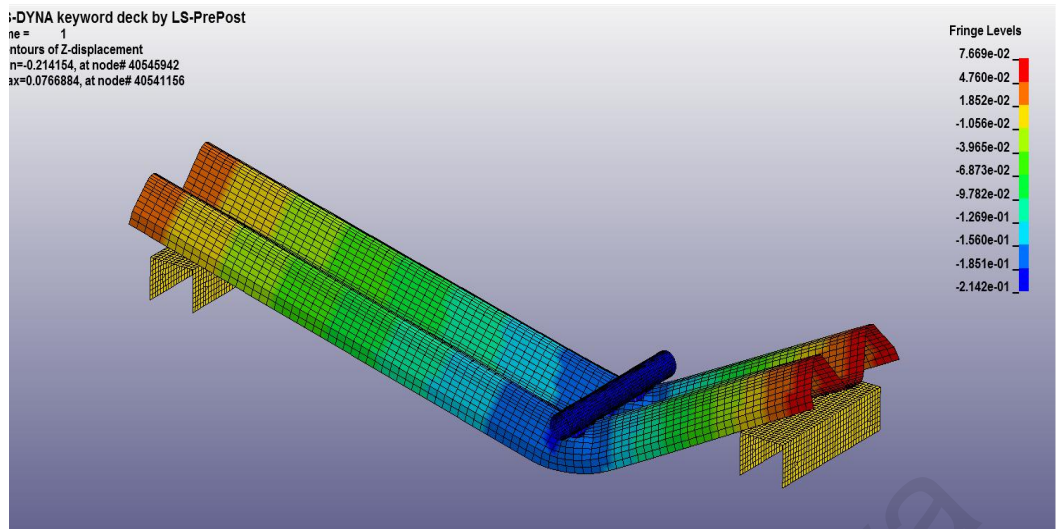
To compare the results of the finite element model with the experimental results, a setup exactly like the one used in the experiments was modelled using LS-DYNA. Three different loading points and the W-beam guardrail's length were used in the determination of the proper mesh size (10, 20 or 40 mm) for the W-beam section.

The results for the 40 mm mesh (the NCAC's basic model of a W-beam guardrail) were not accurate because the beam flattened unrealistically, as shown in Figure 4-1C. Further investigation was performed to compare to the load bearing capacity of the experimental model with that of the finite element model to determine a suitable mesh size for the W-beam section.

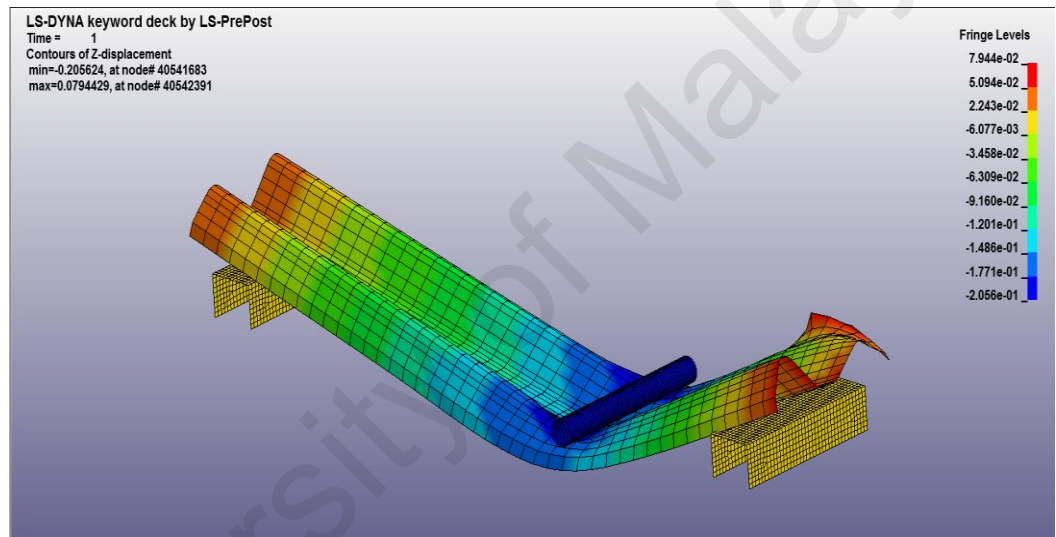
From the above analysis of the quasi-static three-point bending of the sample W-beams, it is seen that there are basically three major factors affecting the load-carrying capacity of a W-beam and the associated energy dissipation, namely, the material's strain hardening, its structural softening due to local cross-sectional distortion and the tensile force due to the axial constraints. The material's strain hardening contributed to the increase in the load-carrying capacity.



(a)



(b)



(c)

Figure 4-1. Comparison of the bulking and flattening of the cross section under a static load. (a) Experiment, (b) simulation with a 20 mm mesh, and (c) simulation with a 40 mm mesh

4.2.2 Evaluating the load-displacement curves

In this section, the mesh sensitivity of the load-displacement curves is analysed to validate the W-beam guardrail system. The results shown in Figures 4-2 to 4-10 reveal that using a mesh size of 40 mm leads to unrealistic results for the bending test.

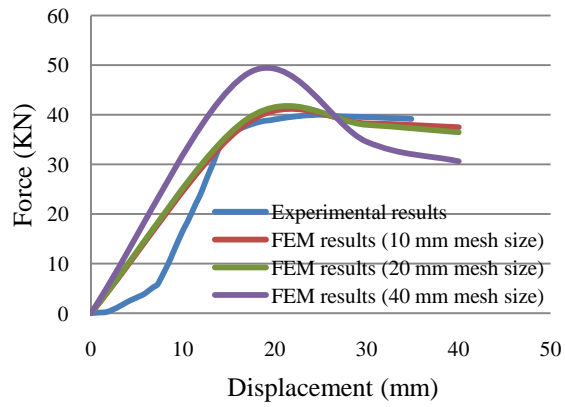


Figure 4-2. FEM and experimental results showing the force on a 1.5 metres length with a load at 0.16 of its length (2.66 mm thickness)

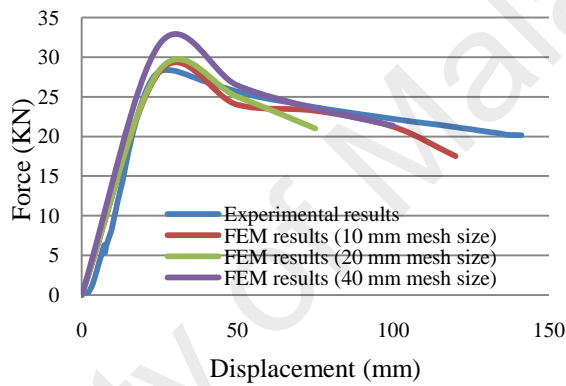


Figure 4-3. FEM and experimental results showing the force on a 1.5 metres beam with a load at 0.33 of its length (2.66 mm thickness)

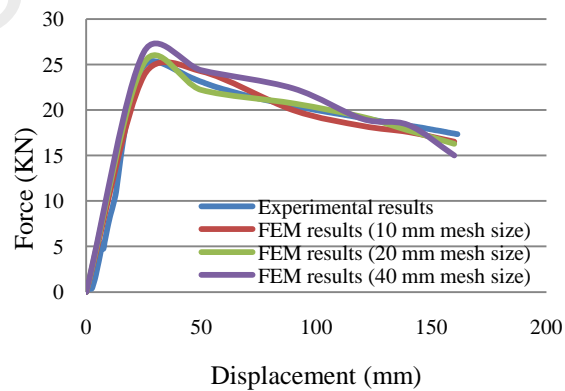


Figure 4-4. FEM and experimental results showing the force on a 1.5 metres beam with a load at midspan (2.66 mm thickness)

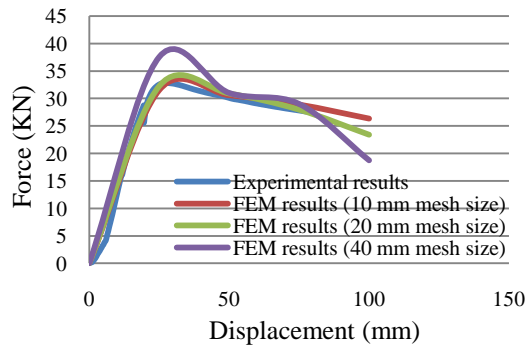


Figure 4-5. FEM and experimental results showing the force on a 2 metres beam with a load at 0.16 of its length (2.66 mm thickness)

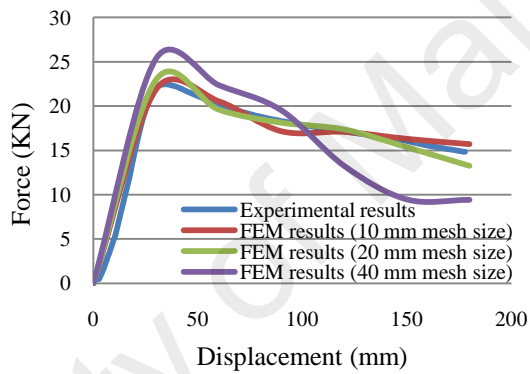


Figure 4-6. FEM and experimental results showing the force on a 2 metres beam with a load at 0.333 of its length (2.66 mm thickness)

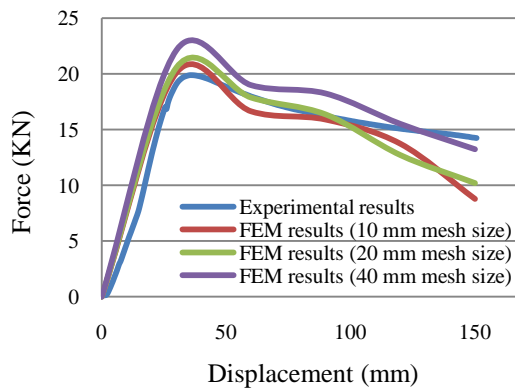


Figure 4-7. FEM and experimental results showing the force on a 2 metres beam with a load at midspan (2.66 mm thickness)

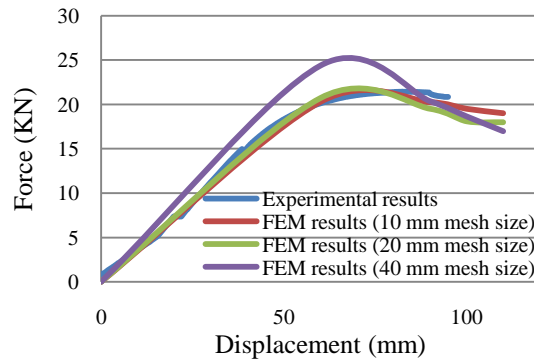


Figure 4-8. FEM and experimental force comparison showing the force on a 2.5 metres beam with a load at 0.16 of its length (2.66 mm thickness)

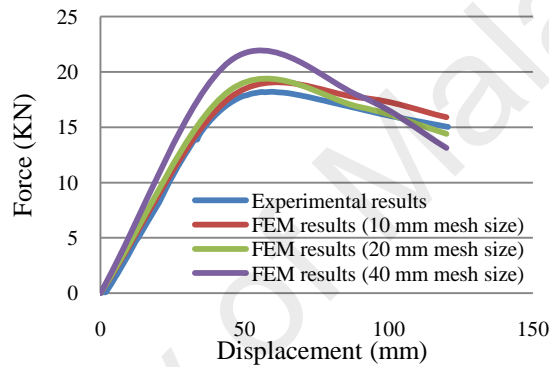


Figure 4-9. FEM and experimental results showing the force on a 2.5 metres beam with a load at 0.333 of its length (2.66 mm thickness)

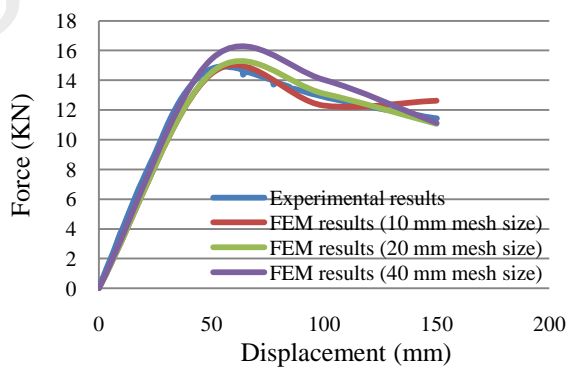


Figure 4-10. FEM and experimental results showing the force on a 2.5 metres beam loaded at midspan (2.66 mm thickness)

Figure 4-2 to 4-10 show comparisons of the experimental and finite element results of static tests. W-beams that were 2.66 mm thick were used in the experiments.

By comparing the results, it can be concluded that the 40 mm mesh, which was used in the NCAC's basic model of a guardrail system, exhibited the highest values in all the simulations. The results for the 40 mm mesh were more unrealistic when load was placed near the supports. However, when the load was moved to midspan, the results for the 40 mm mesh became closer to the experimental results.

In contrast, the results obtained for 20 and 10 mm meshes were very similar to the experimental results. To reduce the computation time, the 20 mm mesh size was chosen for the simulations of full-scale crash tests.

4.2.3 Calculating the forces during applying the load

The validated model of the W-beam section using a 20 mm mesh was used to investigate the performance of W-beam guardrails to investigate the amount of redirective force generated by a W-beam guardrail. This helps us understand how this force changes as the length of the beam and the location of the load are changed. Figure 4-11 shows a schematic of the redirective force.

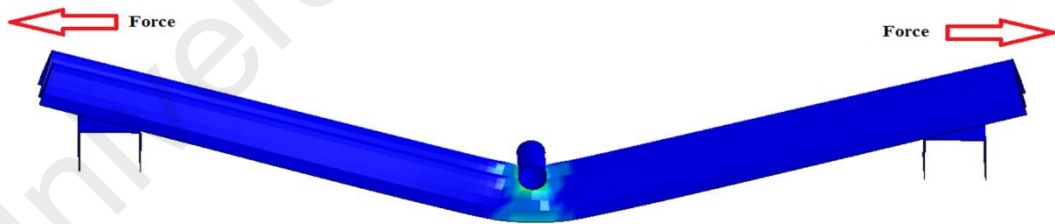


Figure 4-11. Schematic of the forces during applying the load

The amount of force generated by a section of the W-beam guardrail was calculated based for loads at different points using LS-DYNA; the results are presented in Figures 4-12 through 4-14.

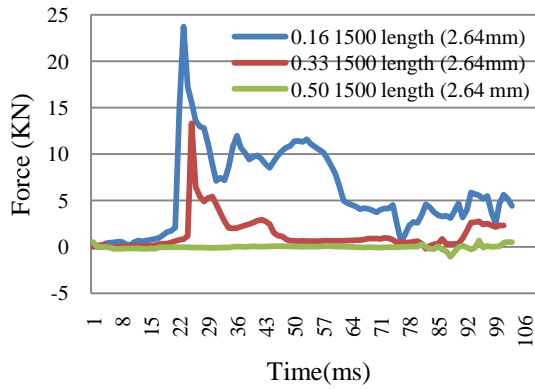


Figure 4-12. Redirective forces for loads at different points

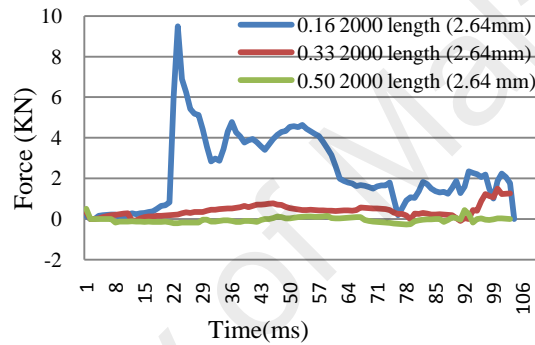


Figure 4-13. Redirective forces for different loads

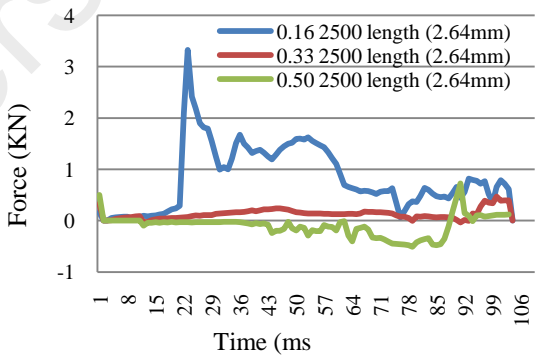


Figure 4-14. Redirective forces for loads at different points

As shown in Figures 4-12 through 4-14, the force is strongly affected by the position of the load. When the load is applied at 0.16 of the length, i.e., near a support, the highest force is obtained. It can be said that when the load is applied near a support, the highest

force is generated in the support area, which may provide more critical support to sustain the guardrail system during the loading process.

4.3 Simulations of a pickup truck impacting the guardrail system

Once a suitable mesh size had been identified, the G4(2W) W-beam section was replaced with the verified model. The model of the G4(2W) system was defined according to the procedure described in chapter 3. Subsequently, the simulation model was produced in accordance with the requirements outlined in the MASH's criteria for Length of Need test 3-11. The finite element simulation shows the pickup located in front of the guardrail barrier at 0 ms. The vehicle impacts the guardrail at a speed of 100 km/h and an angle of 25°. An isometric view of the model is provided in Figure 4-15.

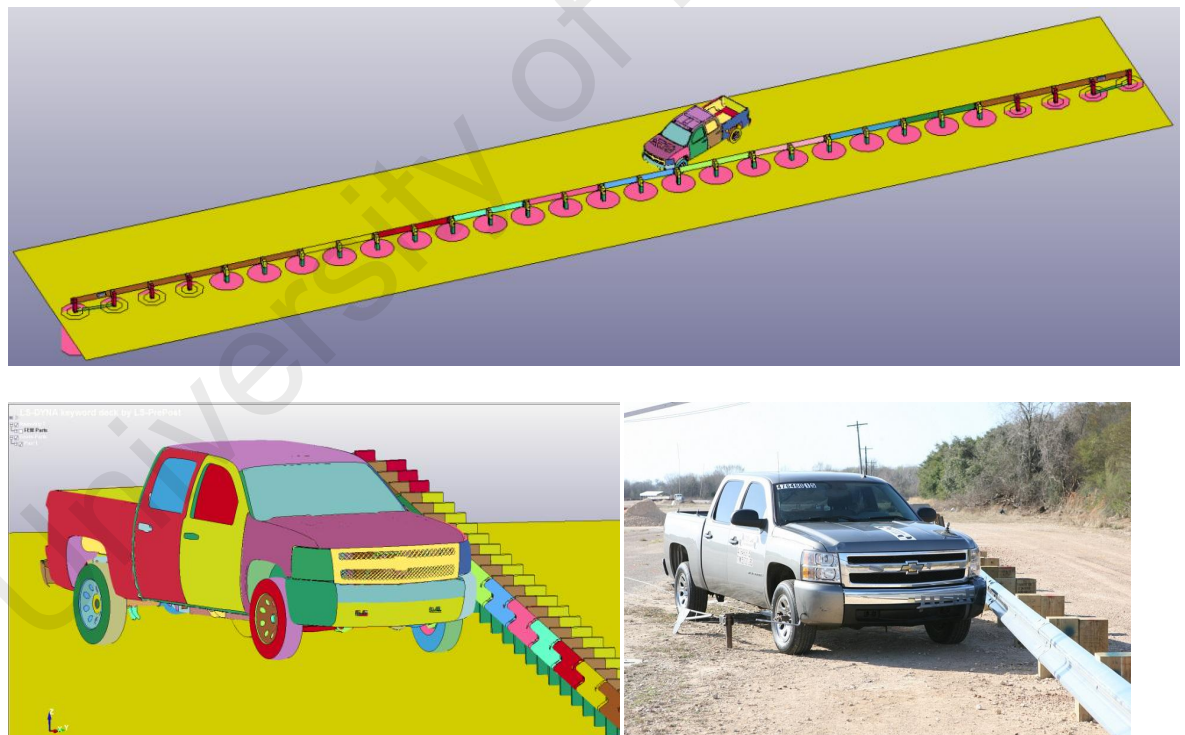


Figure 4-15. The pickup truck in a real crash test and in the LS-DYNA model

4.3.1 Validation of the finite element crash simulation

To validate the G4(2W) strong-post guardrail system to achieve objective 3, the full-scale crash test described by Bullard et al. (2010a) was considered for model validation and to assess the accuracy of the simulation of a truck impacting the guardrail system as in the test. In the finite element model, the wood posts were spaced 1.9 metres apart, and all the design parameters were the same as those of the G4(2W) system used in the full-scale crash test.

Both qualitative and quantitative validation are used to compare the FE model and the full-scale crash tests. In the qualitative method, the FE model should be able to capture the basic sequence of events. The validated model can be used to improve the crashworthiness of the G4(2W) guardrail system.

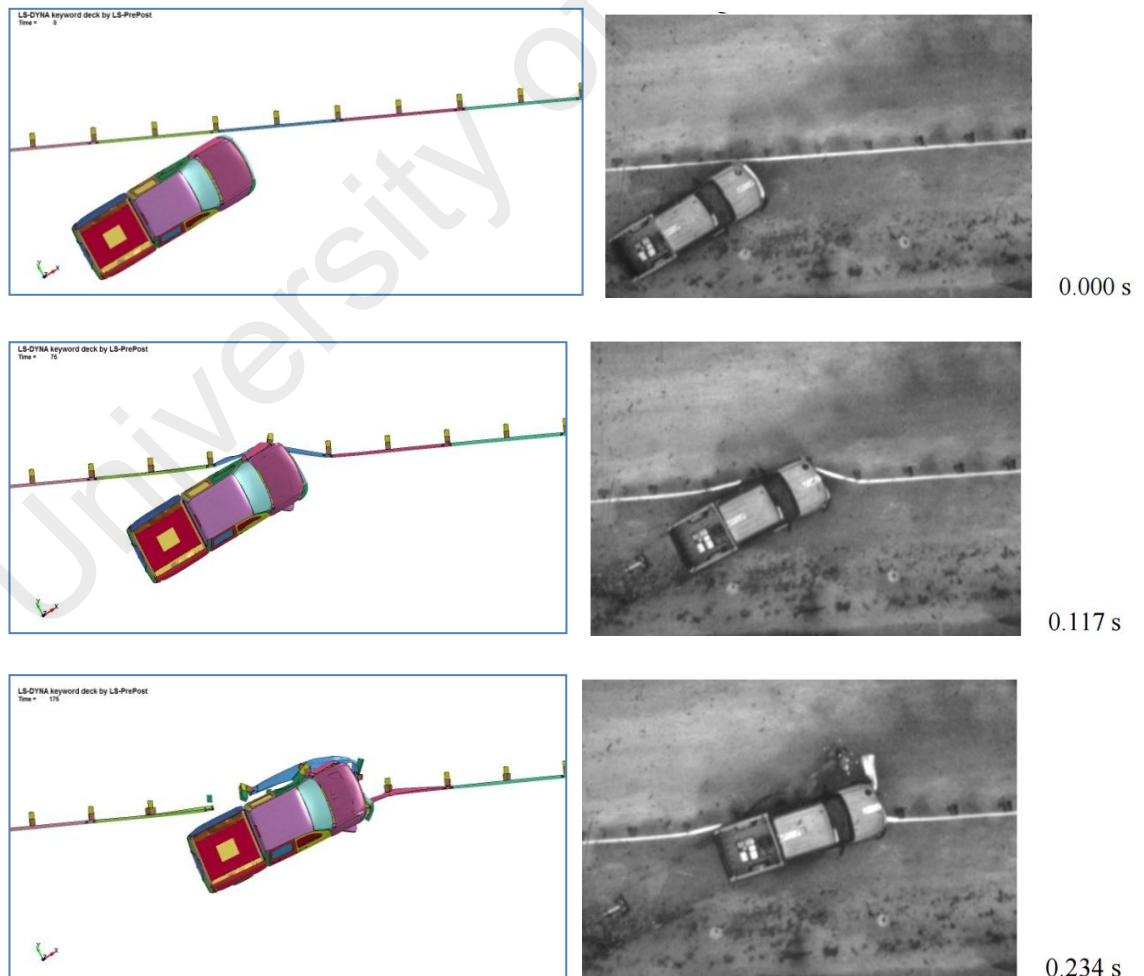
The crash simulation was performed on a computer workstation at the Centre for Transportation Research of the University of Malaya. Sequential photographs from the test and the simulation were compared for qualitative validation. The comparison indicated that the finite element simulation reasonably captured the basic sequence of events during the impact. The W-beam guardrail's rupture and post-fracture phenomena were observed in the finite element simulation. Quantitative validation was performed by comparing the acceleration at the vehicle's centre of gravity in the full-scale test and the simulation. The NARD quantified validation measures used in the study are described in the following sections.

4.3.1.1 Qualitative validation

The front bumper was the first component to impact the guardrail and began to deform at 40 ms. The left tyre contacted post 13 at 90 ms and post 14 at 180 ms. The tyre began to deform and the left fender showed severe deformation after 170 ms. The vehicle

became completely aligned with the guardrail with an intrusion of 525 mm at 250 ms. The speed was reduced to 60.5 km/h and the roll angle was 8.5°. Comparable sequences of photographs (overhead views) are shown in Figure 4-16. The vehicle penetrated the guardrail 0.20 seconds after the impact. The simulation results predicted that the guardrail would rupture at that time.

The left front tyre of the vehicle first snagged on post 15 and turned towards the W-beam guardrail. This caused the vehicle to decelerate strongly. In an actual impact, this would cause the tires to deflate and may cause the wheel assembly to separate from the vehicle. According to these pictures, the finite element model is in good agreement with the dynamic test in terms of the vehicle's position with respect to the guardrail and its interaction with the barrier.



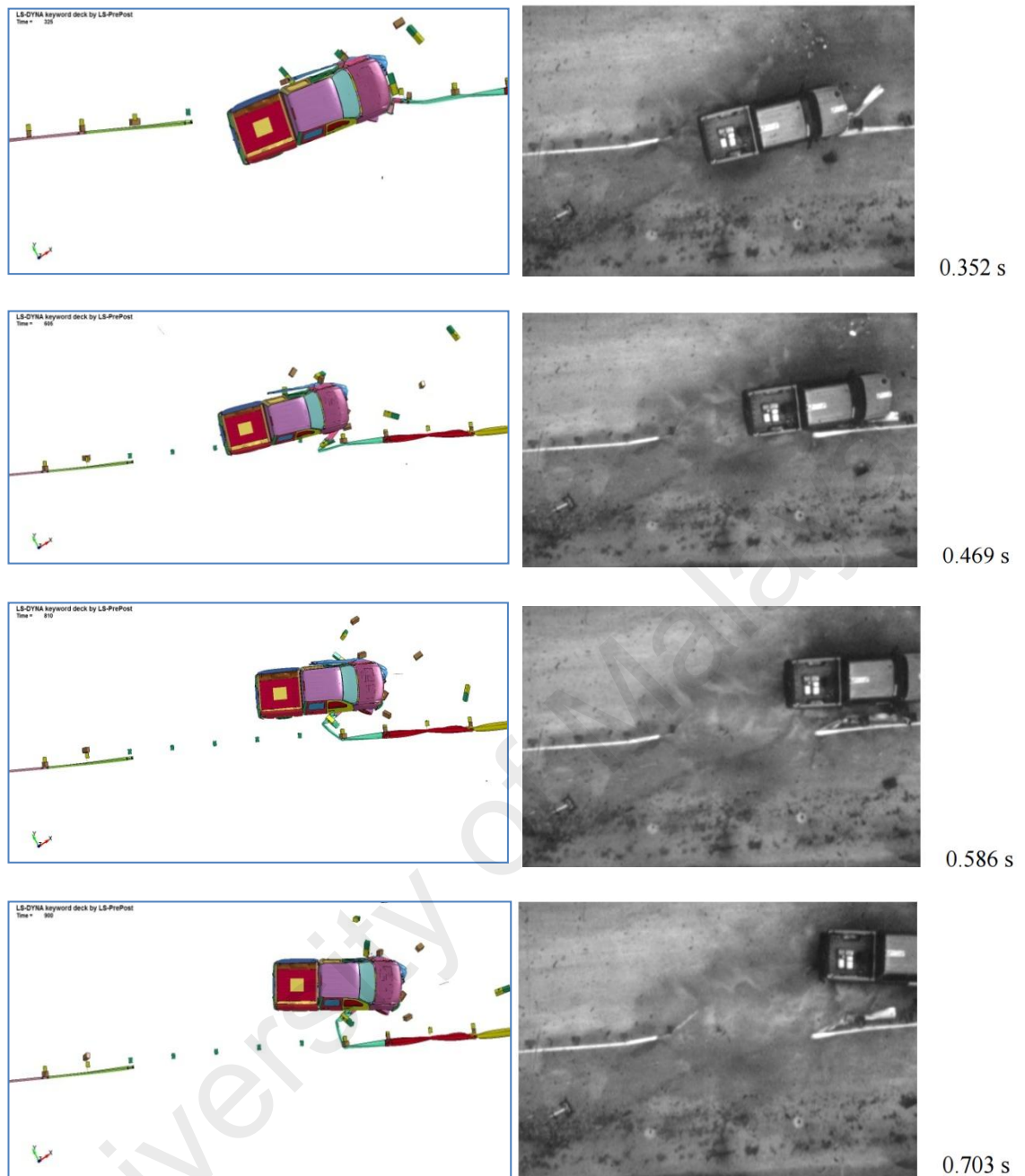


Figure 4-16. Sequences of photographs from the full-scale crash test and the LS-DYNA simulation

4.3.1.2 Quantitative analysis

The verification and validation procedure recommended by NCHRP Project 22-24, “Guidelines for Verification and Validation of Crash Simulations Used in Roadside Safety Applications”, was used to compare the results of the crash with those of the computer simulation.

This quantitative validation procedure involves the use of the RSVVP, a software package that compares paired sets of time series data, performs the necessary adjustments, and then, applies a series of statistical tests to the data sets to determine how comparable they are. The software allows various types of data to be used, including common crash test and simulation data, which are as follows:

- X- acceleration –Acceleration in the longitudinal direction, i.e., along the vehicle
- Y- acceleration –Acceleration in the lateral direction, i.e., perpendicular to the direction of travel
- Z- acceleration – Acceleration in the vertical direction

For this evaluation, the RSVVP, which was developed as part of NCHRP Project 22-24, was used to synchronise and compare the results of the simulation and the test. This software allows single- and multi-channel comparisons of the above types of data, which are collected by the instruments used in crash tests, and the metrics that can be generated by the simulation software. The accelerations measured in the crash test were provided by the TTI for use in the quantitative validation of the G4(2W) guardrail system in this study.

The comparisons between the acceleration in each direction (X, Y and Z) measured in the crash test and calculated in the simulation are shown in Figures A-1, A-2 and A-3 in Appendix A. All the tests conducted show that the guardrail model accurately reproduces the behaviour of the real system, and therefore, this model is used as a component of the full safety barrier model. The graphs created by the RSVVP provide information about the relative differences in the data in multiple ways and provide statistical comparisons using the Sprague-Geers metric and an ANOVA. The output also indicates whether the results meet the acceptance criteria. The software produced a graph for each of the 3 accelerations. The metrics calculated when the time histories of

the crash test and the simulation of the G4(2W) guardrail system were compared, which are shown in Table 4-1, satisfied the criteria found by the Sprague-Geers metric and the ANOVA.

Table 4-1: Time History Evaluation Table for the MASH-based Simulation of a G2(2W) guardrail system

Channel Type	Sprague-Geers		ANOVA		Pass
	Metrics		Metrics		
	M	P	Mean Residual	Std. Deviation	?
	≤ 40	≤ 40	≤ 0.05	≤ 0.35	
X- acceleration	-7.8	30.5	0.024	0.146	Yes
Y- acceleration	8.4	35.1	-0.003	0.13	Yes
Z - acceleration	5.2	39.5	-0.011	0.222	Yes

4.4 Parametric study

The displacement results from the deflection of the beam element, the bending of the steel posts or fracture of wood posts and the lateral displacement of the posts in the soil. The benefit of a finite element simulation is that once a model has been developed and validated, the impact conditions, as well as the basic design and geometry of the installation, can easily be varied to examine different crash scenarios. Subsequently, the results can be evaluated using a parametric study.

To achieve objective 4, the essential factors that directly affect the guardrail's performance are considered in this study to balance the number of possible scenarios with the number of simulations that can be performed.

4.4.1 Evaluating structural adequacy

The full-scale crash test of the G4(2W) guardrail system indicated that this guardrail system was unsatisfactory according to guidelines given in the MASH because the W-beam ruptured. Based on a validated FE model, a parametric study is described in the following section. It explores the effects of modifying components of the G4(2W) guardrail system. This is useful for improving the G4(2W) guardrail system to ensure that it redirects vehicles back onto the road in a safe manner.

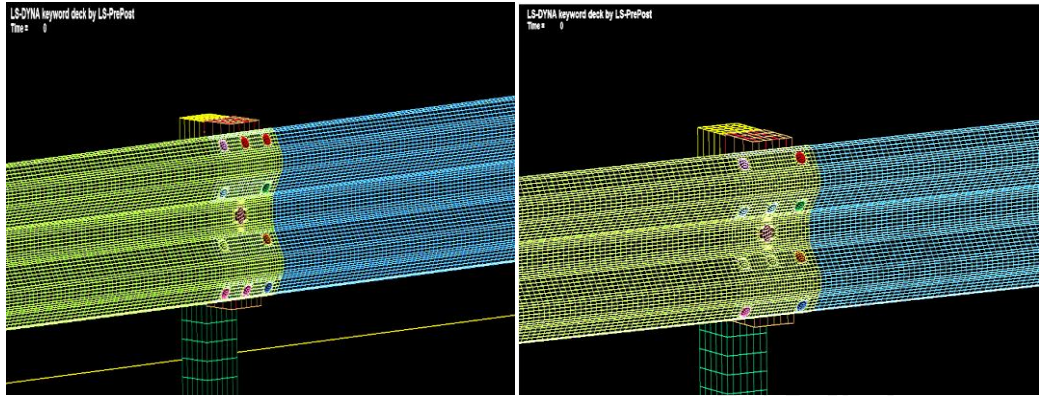
4.4.1.1 Evaluating the strength of the connection area (spliced W-beams)

One potential failure mode of the guardrail system is rupture. After reviewing the outcome of the full-scale crash test and the finite element model, it seems as though the guardrail was forced to absorb an additional amount of energy with each additional missing post, and which increased the deflection. At that point, the maximum tensile capacity of the guardrail increased and caused it to rupture at the splice connections. Several ways to strengthen this area were considered because this is the most critical area of the guardrail system's design.

The first parameter considered in this study is the structural adequacy of guardrail system. To test hypothesis 2, increasing the number of bolts in each splice connection is considered in this study. The effect of increasing the number of bolts from 8 to 10 and 12 at each splice connection is analysed. This is performed to determine whether increasing the number of bolts increases the guardrail's stiffness enough to absorb the energy of an impacting vehicle. The results of this modification are discussed in the following sections.

- *Increasing the number of bolts to 10 (Categories a and b)*

Two locations in each splice connection are considered for increasing the number of bolts to 10 (Figure 4-17).

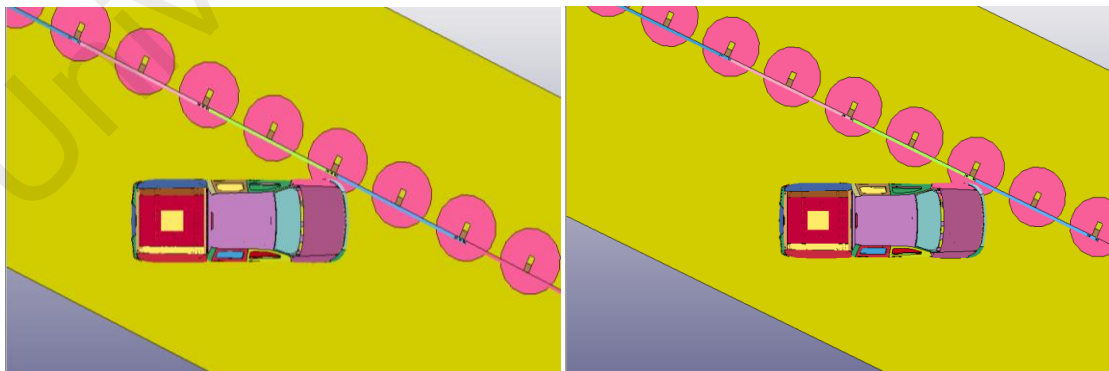


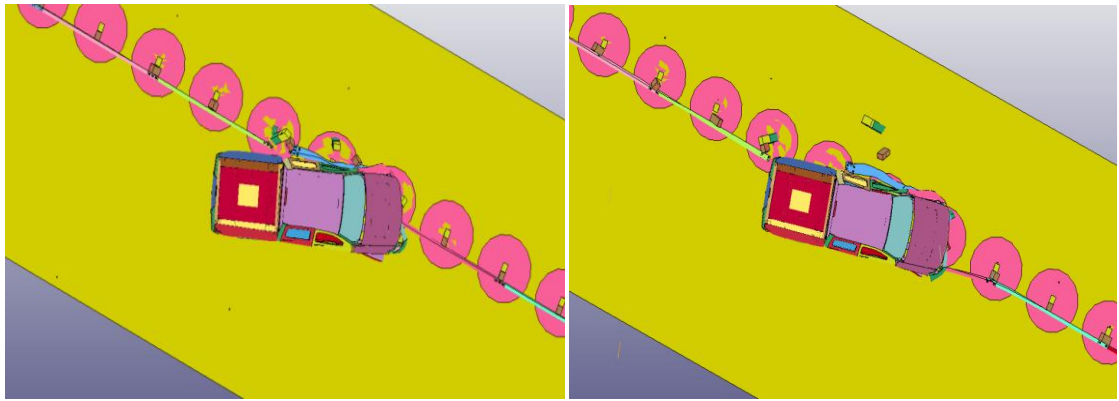
(a)

(b)

Figure 4-17. Proposed splice connection locations to increase the number of bolts to 10
a, (Category a) and b, (Category b)

The simulation results indicated that the guardrail system failed at a splice connection, and increasing the number of bolts to 10 at the connection was not suitable. Figure 4-18 shows that the guardrail system ruptured at a splice connection.





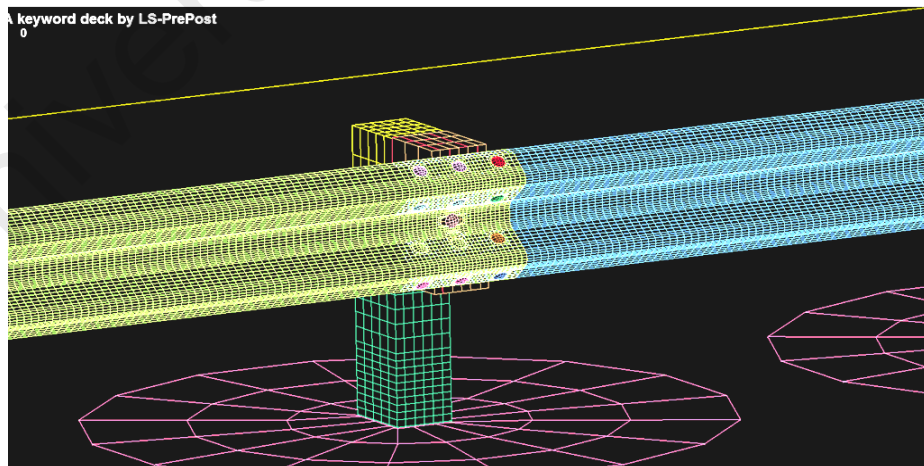
(a)

(b)

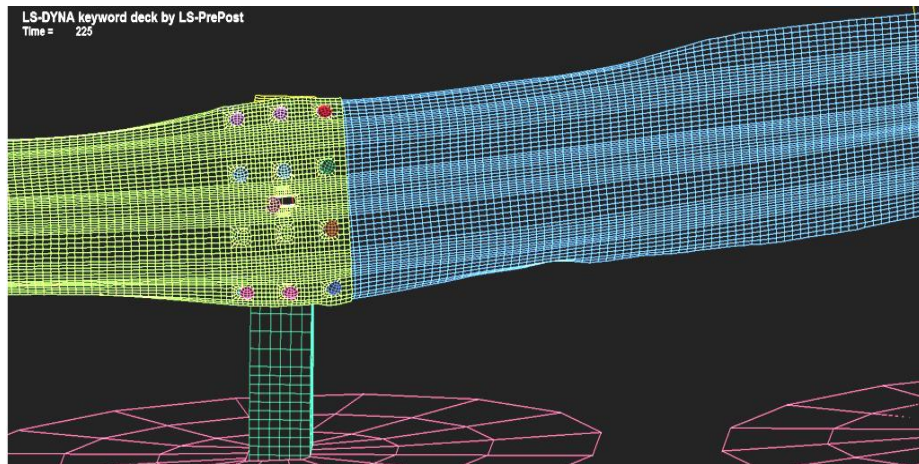
Figure 4-18. Top view of a splice connection in the ruptured rail
a, (Category a) b, (Category b)

- ***Increasing the number of bolts to 12***

Increasing the number of bolts to 12 was also considered in case 10 bolts per splice connection did not satisfy the structural adequacy criteria. The proposed 12 bolt splice connections are presented in Figure 4-19.



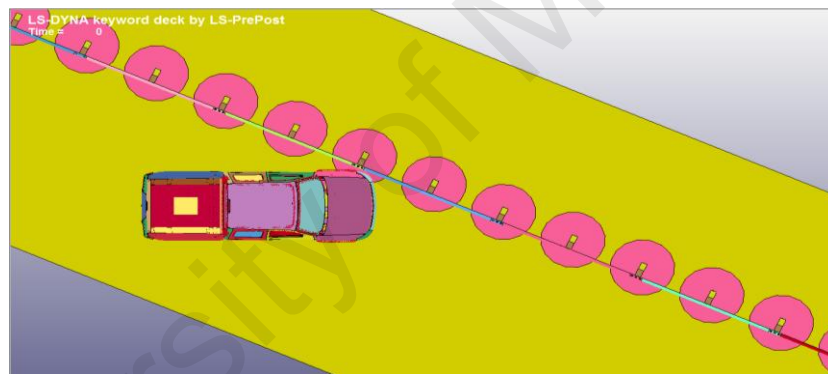
(a)



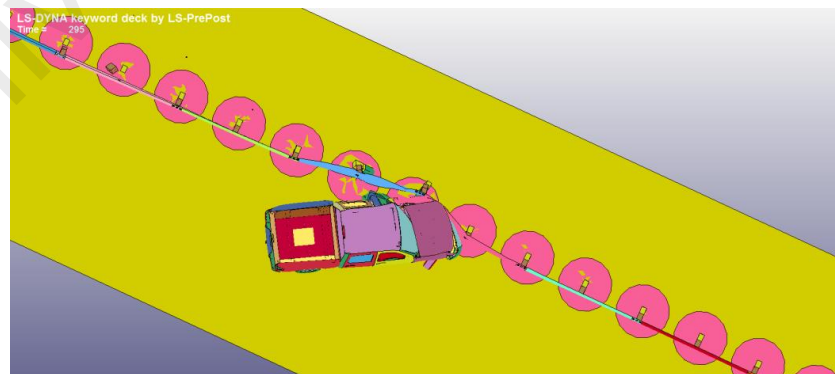
(b)

Figure 4-19. Proposed splice connection locations for 12 bolts

(a), before the crash test (b), after the crash test



(a)



(b)

Figure 4-20. Model of a 12-bolt splice connection in the guardrail system (top view)

(a), before the crash test (b), after the crash test

The results of the model revealed that the guardrail system successfully contained the vehicle and the barrier absorbed the impact energy of pickup truck. However, the barrier failed to redirect the vehicle in a safe manner. In the following sections, different factors are evaluated to improve the G4(2W) guardrail system enough for it to satisfy the vehicle trajectory and occupant risk factor requirements outlined in the MASH's criteria for Length of Need test 3-11 (Figure 4-20).

Once the use of 12-bolt splice connections was confirmed, the parametric study continued with changes to the two main parameters, the post spacing and the guardrail height. Then, the responses, including the structural adequacy, the vehicle trajectory and the occupant risk factors, were evaluated for all the systems. Three different post spacings, 1.5, 2 and 2.5 metres, and three different guardrail heights, 71cm (28 inches), 76cm (30 inches), or 81cm (32 inches), were considered, and a model of each configuration was developed based on the MASH's criteria for Length of Need test 3-11. The results are discussed in following sections.

4.4.1.2 Evaluating the guardrail deflection

The displacement of the rail was measured using the perpendicular distance from the line to the rail or post. When a rail or post was bent or twisted, the measurement was made from the point that was farthest from the line of reference. Only the longitudinal and lateral coordinates were used in the distance calculations.

The deflection was measured from the barrier's original location to its current deformed location, as shown in Figure 4-21.

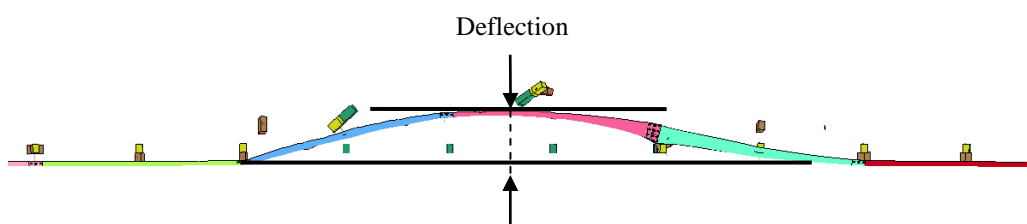


Figure 4-21. Deflection of a W-beam guardrail system

To examine hypothesis 3, the deflection was measured for different system configurations. Three different post spacings were considered, as discussed earlier, and the results of the LS-DYNA simulation of each different guardrail height between 71cm (28 inches) high and 81 cm high (32 inches) were graphed for each post spacing.

When the guardrail height is changed, the relationship between the height of the car's bumper and the barrier also changes. Several LS-DYNA simulations were performed using various guardrail heights to examine the relationships among the guardrail height, the post spacing and the crashworthiness of the G4(2W) guardrail system. After the splice connection was modified as described in the previous section, 9 additional simulations involving various guardrail heights and post spacings between 1.5 metres and 2.5 metres were run. From the standard height of 71cm (28 inches), the guardrail height was increased to 81cm (32 inches). In these simulations, the guardrail height, which was measured from the ground to the top of the W-beam, was 71cm (28 inches), 76cm (30 inches), or 81cm (32 inches). The minimum and maximum heights were selected to determine how the guardrail height affects the safety performance of the barrier in the containment and redirection zone. During the analysis of the results and the evaluation of the barrier's performance, emphasis was placed on the potential of the barrier to contain and redirect the vehicle; the acceptable impact severity and working width were set in accordance with the MASH's criteria.

The results for the lateral deflection are presented in Figures 4-22 through 4-24. In these figures "ps" represents the post spacing, and the following number specifies the post spacing in metres. Another term, "gh", represents the guardrail height, and the following number represents the height of the guardrail in inches. In addition, a sequence of pictures from each simulation is presented in the appendix B.

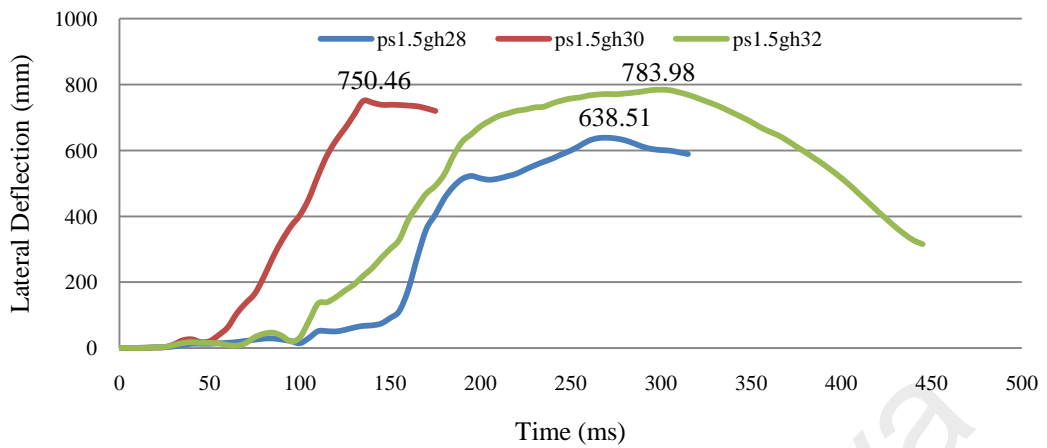


Figure 4-22. Lateral deflection for a post spacing of 1.5 metres and different guardrail heights

The highest deflection was recorded For a post spacing of 1.5 metres for the 81cm high (32 inches) guardrail. The results for the 81 cm (32inches) and 76cm (30inches) high guardrails were similar. However, the 71 cm high (28 inches) guardrail was deflected less, which could be due to lower post height, which also reduced the probability of a post fracturing (Figure 4-22).

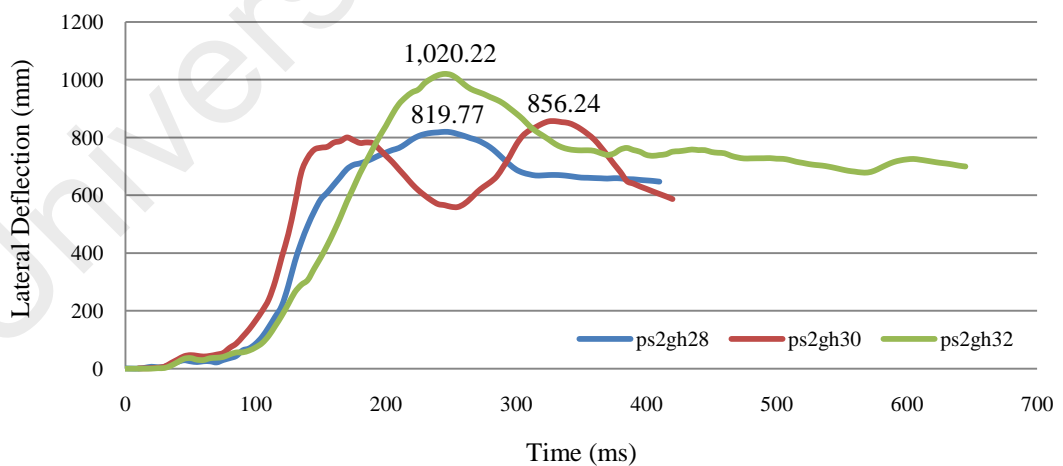


Figure 4-23. Lateral deflection for a post spacing of 2 metres and different guardrail heights

For a post spacing of 2 metres, the 81 cm (32 inches) high guardrail deflected 1020.22 mm, which was the highest value in this category. The results for 71cm (28 inches) and 76 cm (30 inches) high guardrails were similar, but the 76 cm (30 inches) high guardrail deflected slightly more (Figure 4-23).

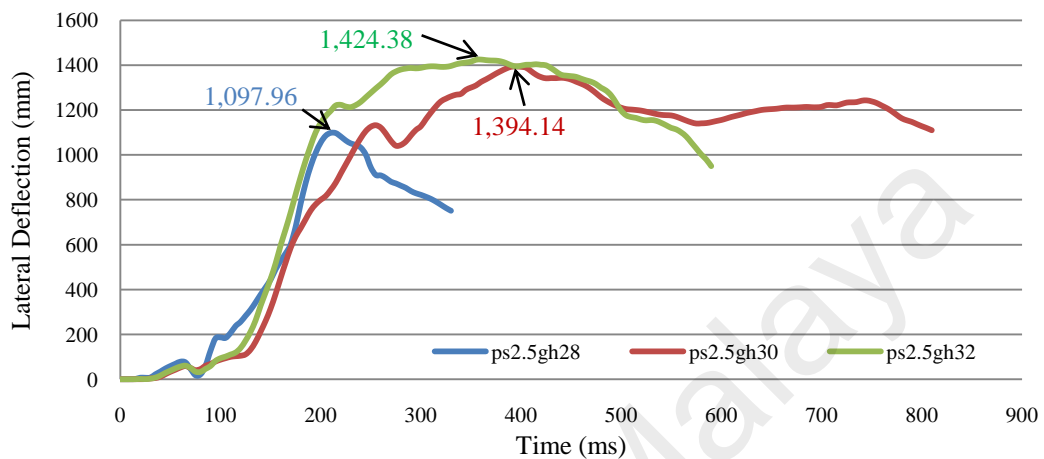


Figure 4-24. Lateral deflection for a post spacing of 2.5 metres post spacing and different guardrail heights

For the greater post spacing shown in Figure 4-24, the wood posts were placed 2.5 metres apart (centre-to-centre). The results show that increasing the guardrail height resulted in more dynamic guardrail deflection. Increasing the nominal mounting height of the W-beam decreases the effective soil yield forces in two ways. Increasing the height of the guardrail system increases the moment arm of the load applied to each post and thus, increases the moment that the soil must resist and perhaps also the deflection of the guardrail system.

In addition, reducing the post spacing resulted in less deformation of the guardrail system. To improve the crashworthiness of the guardrail system, the deflection of the guardrail system in the direction perpendicular to the W-beam is expected to increase. An appropriate reduction in the lateral stiffness of the guardrail could cause the posts to break earlier and help redirect the truck more smoothly and make wheel snagging less likely. This is can be observed for a post spacing of 2.5 metres.

However, special attention should be paid to the splice connections. The proposed guardrail system, which has 12 bolts per splice connection, was able to contain the vehicle with an acceptable range of lateral deflection.

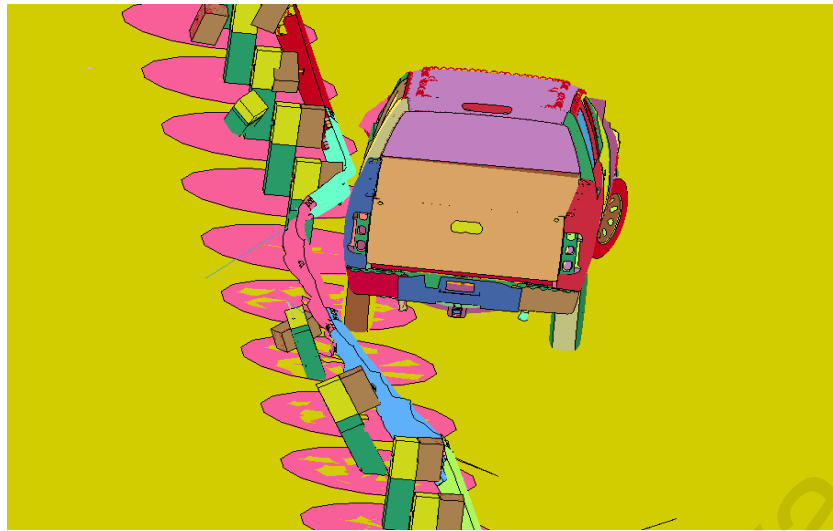
The results for a guardrail height of 81 cm (32 inches) and a post spacing of 2 metres are shown in Figure 4-25 (a, b, and c). As seen, several posts fractured, but the W-beam section was able to contain and redirect vehicle with an acceptable range of deflection.



(a)



(b)



(c)

Figure 4-25. Guardrail deflection and vehicle redirection for a guardrail height of 81 cm (32 inches) and a post spacing of 2 metres (a, b, c).

4.4.2 Vehicle trajectory

Vehicular responses are the most important parameters in evaluating the safety performance of a barrier system in state-of-the-art research and practical applications. Crash testing agencies need to follow the procedures defined in the MASH. Similar procedures were used in the crash test simulations described here. In this part of the study, the vehicle's response was simulated first, and then, a detailed analysis of a standard impact conditions (an impact speed of 100 km/hr and an impact angle of 25°) was performed. This was done to examine hypothesis 4 and to identify a relationship between variations of the post spacing and the guardrail height and the required vehicle trajectory.

The yaw, pitch and roll of the vehicle, which are defined in Figure 4-26, were used to examine the vehicle's orientation and stability during the impact. The yaw angle indicates how much the vehicle was redirected, and the pitch and roll angles were used to assess the stability of the vehicle during the crash. A large pitch or roll angle implies

unstable vehicle behaviour, and the MASH requires the pitch and roll angles to remain below 75° . The resulting vehicle trajectory is presented in several sections, which include descriptions of the vehicle's exit speed and the angles and values of the rotation obtained from the simulation.

A sequence of pictures that shows the vehicle's trajectory in each simulation is provided in the appendix B.

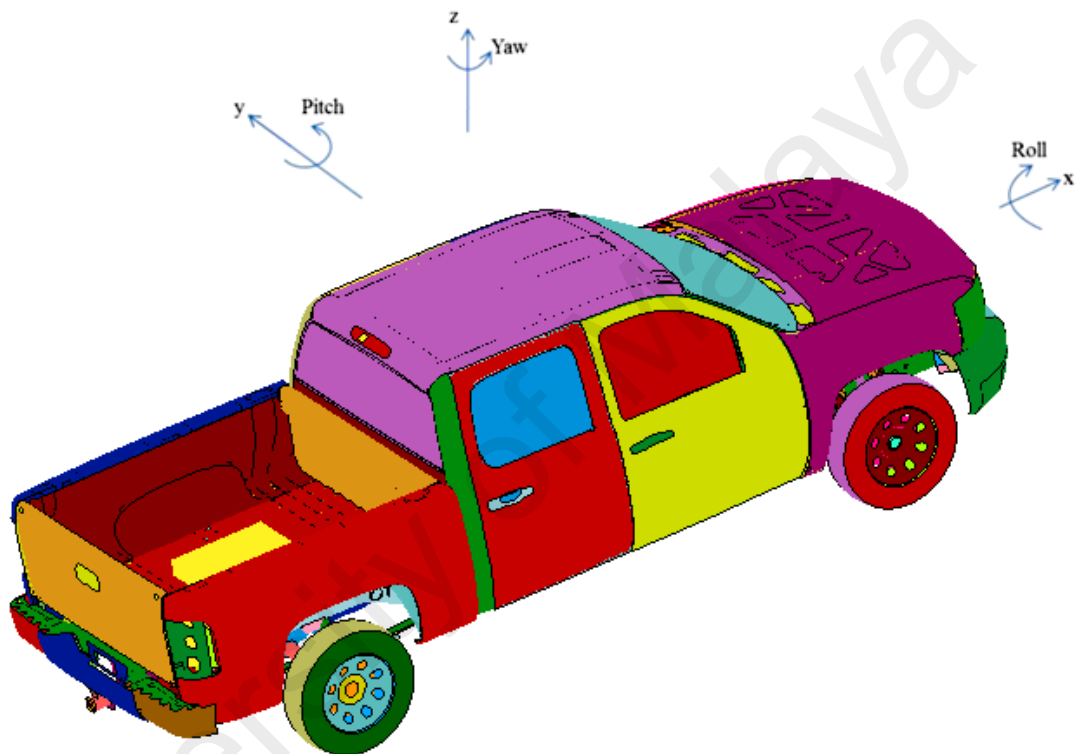


Figure 4-26. Definitions of yaw, pitch and roll

4.4.2.1 Impact configurations

The results of the 9 simulations showed that the total engagement time of the pickup truck with the guardrail system ranged from 345 to 720 ms; the results are summarised in Table 4-2. In general, the total engagement time increased with the post spacing.

Table 4-2: The length of the Silverado pickup truck's engagement with the strong-post guardrail system (in ms)

Post spacing (ps)(m)	Guardrail height (gh) (cm)		
	71cm (28 inches)	76cm (28 inches)	81cm (28 inches)
1.5	345	425	450
2	350	580	625
2.5	720	705	695

4.4.2.2 Evaluation of the vehicle's exit speed

Figures 4-27 to 4-29 show the vehicle's exit speed under all the simulated impact conditions. A higher exit speed means that the barrier acted more flexibly and that the vehicle's impact was less severe. For the period from 100 ms to 125 ms and the 1.5 metres post spacing, the vehicle's exit speed increased with the guardrail height up to 73.66 km/hr, which was recorded for the 81 cm (32 inches) high guardrail (Figure 4-27).

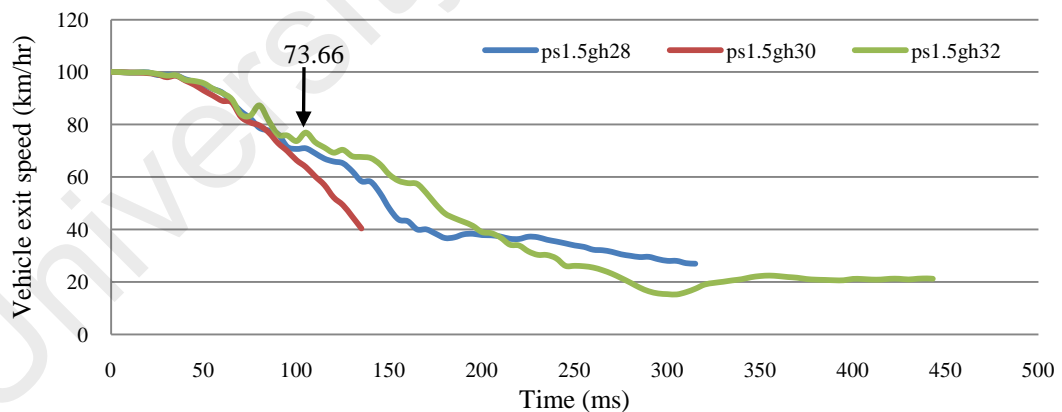


Figure 4-27. Comparison of the vehicle's exit speed for a post spacing of 1.5 metres and different guardrail heights

For the 2 metres post spacing, no significant changes in the vehicle's exit speed were found for guardrail heights of 76 cm (30 inches) and 81 cm (32 inches). The results are very similar from the beginning to 350 ms. After 350 ms, with the 76 cm (30 inches)

high guardrail, the vehicle rotated counterclockwise and eventually, the guardrail failed to redirect the vehicle, which lead to a lower exit speed (Figure 4-28).

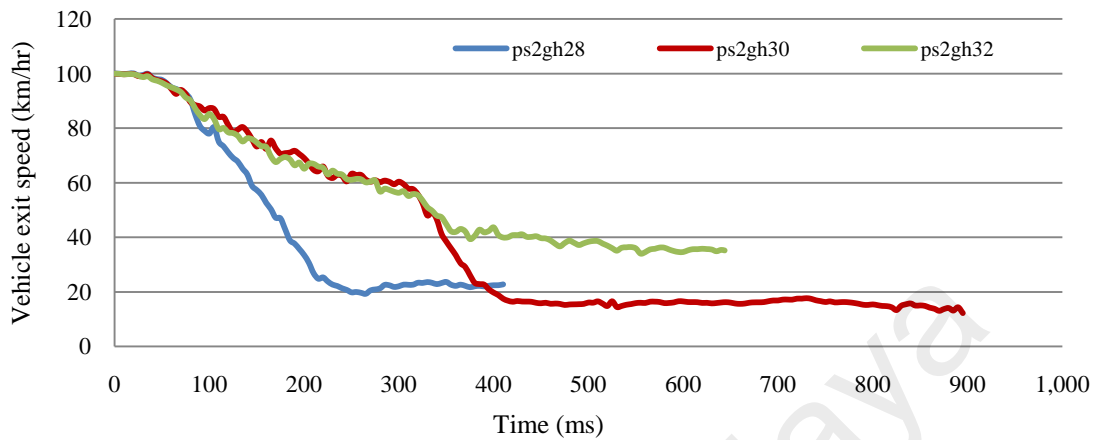


Figure 4-28. Comparison of the vehicle’s exit speed for a post spacing of 2 metres and different guardrail heights

The results for the 2.5 metres post spacing were interesting; higher exit speeds were found for the 76 cm (30 inches) and 81 cm (32 inches) high guardrails. The highest speed exit, 58 km/hr, was found for the 81 cm (32 inches) high guardrail. Figure 4-29 shows that as the guardrail height increases, the impact becomes less severe, and eventually, the vehicle is redirected with a higher exit speed. This relationship is found for the post spacings. In addition, comparing the results for all the post spacings shows that wider post spacings result in higher vehicle exit speeds.

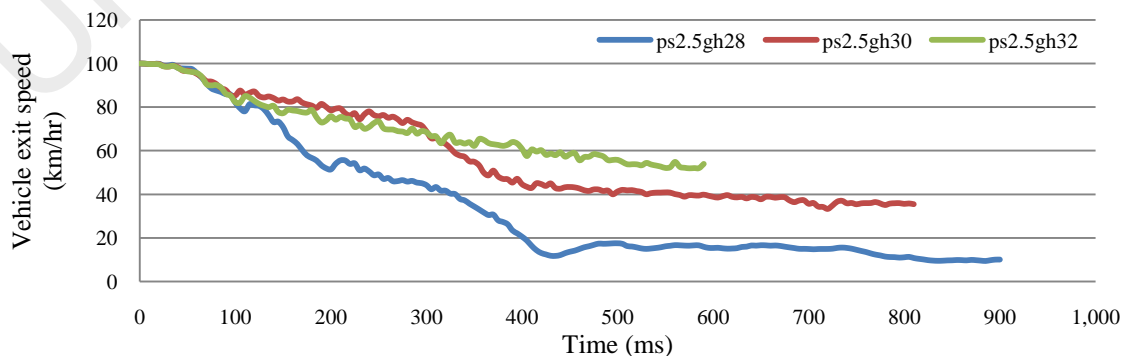


Figure 4-29. Comparison of vehicle exit speed for 2.5 metres post spacing guardrail with different guardrail heights

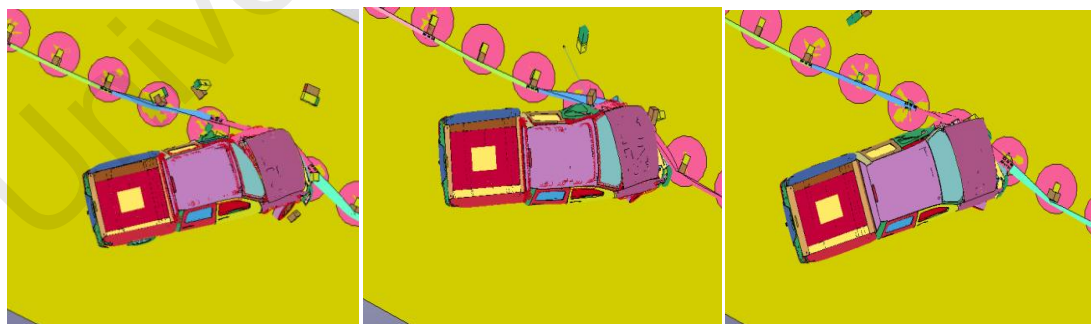
4.4.2.3 Evaluation of the vehicle's exit angle

The vehicle's post-impact response is also important. It is preferred that the vehicle avoids intruding into adjacent traffic lanes after being redirected by the guardrail system. One measure of the vehicle's post-impact response is its exit angle, which is defined as the angle between the barrier's longitudinal direction and the vehicle's direction of travel when it loses contact with the barrier. The preferred exit angle specified in the MASH is less than 60% of the initial impact angle (Table 4-3). A larger exit angle is discouraged because it implies a higher probability of the vehicle rebounding into the traffic lanes and being exposed to secondary impacts.

Table 4-3: Preferred maximum exit angles specified in the MASH

Impact angle	15°	20°	25°	30°
Preferred maximum exit angle	9°	12°	15°	18°

Figure 4-30 shows three impacts with a post spacing of 1.5 metres in which the barrier failed to redirect the vehicle. The vehicle rotated counterclockwise and was not redirected safely for any guardrail height when the post spacing was 1.5 metres.



(a)

(b)

(c)

Figure 4-30. Vehicle trajectory for a guardrail system with a post spacing of 1.5 metres and a guardrail height of

(a) 71 cm (28 inches), (b) 76 cm (30 inches), and (c) 81 cm (32 inches)

For a post spacing of 2 metres, the results show that only the 81 cm (32 inches) high guardrails redirected vehicle safely. The vehicle's exit angle was 11.51 degrees. However, the other guardrails were not successful; they failed to redirect the vehicle safely (Figure 4-31).

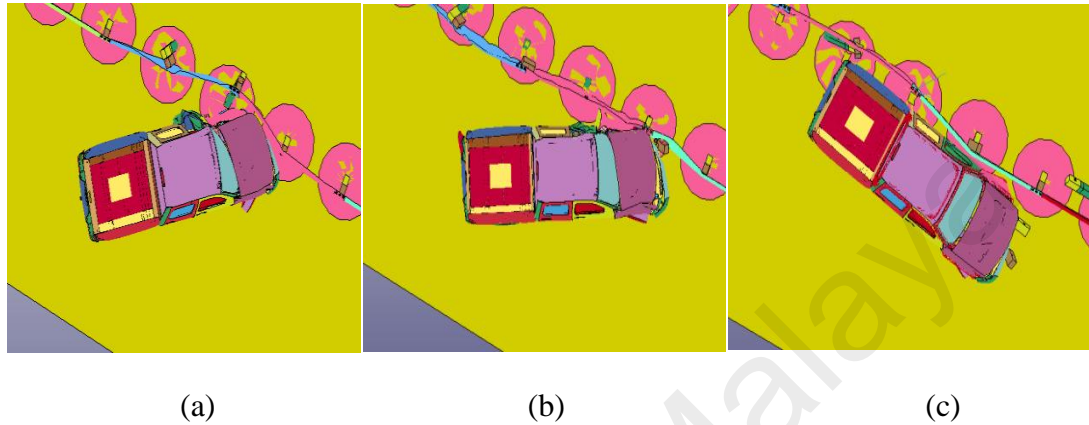


Figure 4-31. Vehicle trajectory for a guardrail system with a post spacing of 2 metres and a guardrail height of

(a) 71 cm (28 inches), (b) 76 cm (30 inches), and (c) 81 cm (32 inches)

When the post spacing was 2.5 metres, the simulation results showed that the vehicle exit angles for 76 cm (30 inches) and 81 cm (32 inches) high guardrails were considered acceptable. An appropriate reduction in the lateral stiffness of the guardrail could cause the truck to swerve earlier and the guardrail to move more, which, combined with a fractured post, might reduce the probability of wheel snagging. In this modification, the increase in the lateral stiffness was achieved by increasing the post spacing (Figure 4-32). Vehicle exit angles of 13.62 and 6.56 degrees were found for a post spacing of 2.5 metres for 76 cm (30 inches) and 81 cm (32 inches) high guardrails, respectively.

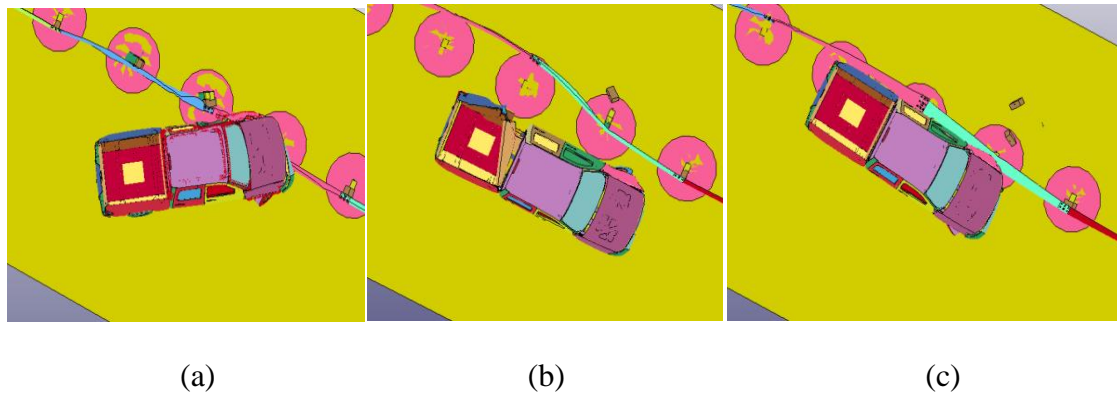


Figure 4-32. Vehicle trajectory for a guardrail system with a post spacing of 2.5 metres and a guardrail height of

(a) 71 cm (28 inches), (b) 76 cm (30 inches), and (c) 81 cm (32 inches)

The results revealed that in the cases involving the standard guardrail height 71 cm (28 inches), the vehicle was not redirected with any of the post spacings. With a guardrail that was 5 centimetres higher, the vehicle was redirected when the post spacing was 2.5 metres, which indicates that the barrier met the MASH's standard for the vehicle trajectory. In addition, with an additional 10 centimetres of height, the guardrails with post spacings of 2 and 2.5 metres were able to redirect the vehicle safely. However, the guardrails with post spacings of 1.5 metres were not successful for any guardrail heights between 71cm (28inches) to 81 cm (32 inches).

4.4.2.4 Comparing the yaw values

The rotation of the vehicle during the impact gives further insight into the behaviour of the vehicle and can be a useful comparison tool. Figure 4-33 to 4-35 show the truck's yaw, quantifies the redirection of the pickup truck by the W-beam guardrail system. A negative yaw angle and an increase in magnitude implies a clockwise yaw. A decrease in the magnitude of the yaw indicates that the vehicle underwent an undesired counterclockwise yaw. This is a direct result of the wheels and guardrail becoming entangled.

When the post spacing was 1.5 metres, comparing the different yaw angles shows that the higher guardrail resulted in a smaller yaw angle. However, the yaw angle was positive for all the guardrail heights when the post spacing was 1.5 metres. This indicates that the guardrails were not able to redirect the vehicle to the road; instead, the vehicle turned counterclockwise (Figure 4-33).

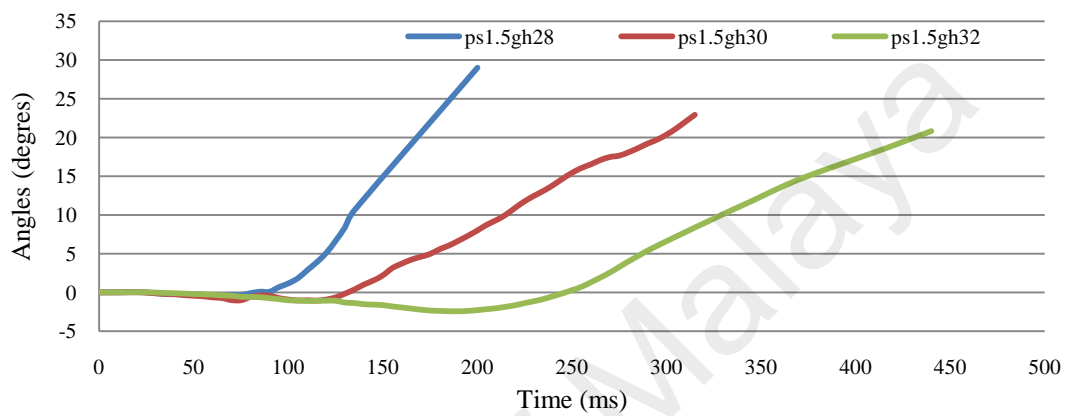


Figure 4-33. Yaw calculation for the guardrail system with a post spacing of 1.5 metres

When the post spacing was 2 metres, the yaw was negative for the 81 cm (32 inches) high guardrail, which indicates that the vehicle rotated clockwise and was safely redirected to the road. The maximum recorded value was -46.3 degrees, which is less than 75 degrees and satisfies the MASH's criteria. However, the other guardrail systems in this category resulted in positive yaws and failed to redirect the vehicle safely (Figure 4-34).

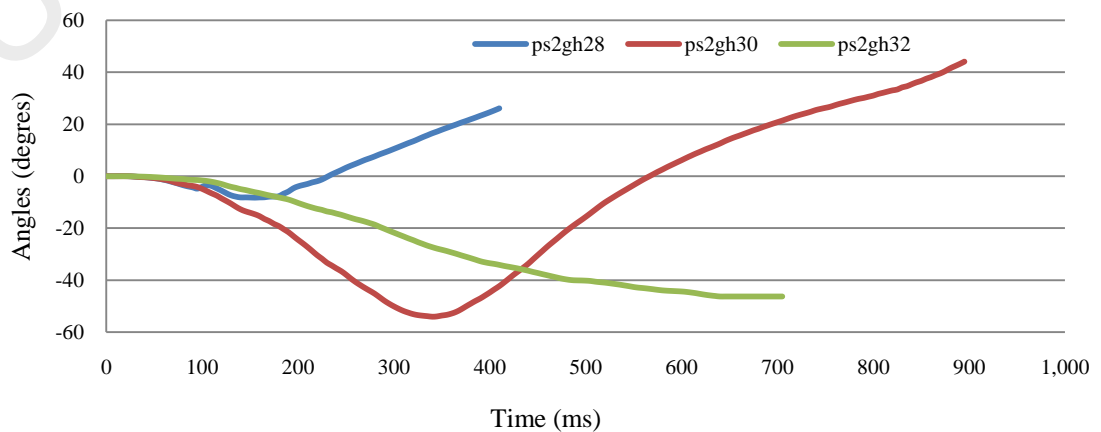


Figure 4-34. Yaw calculation for the guardrail system with a post spacing of 2 metres

When the post spacing was 2.5 metres, the 76 cm (30 inches) and 81 cm (32 inches) high guardrails were able to redirect the vehicle to the road safely, and the yaw was negative. In this modification, the post spacing was extended to the entire guardrail system. Increasing the post spacing could increase the time required for the vehicle to travel from one post to the next. It was expected that the left front wheel of the vehicle might yaw enough to avoid contacting the next post as the vehicle travelled. The 71 cm (28 inches) high guardrail failed to redirect the vehicle safely with any of the post spacings, which indicates that 71 cm (28 inches) high guardrail are not able to satisfy the MASH's criteria (Figure 4-35).

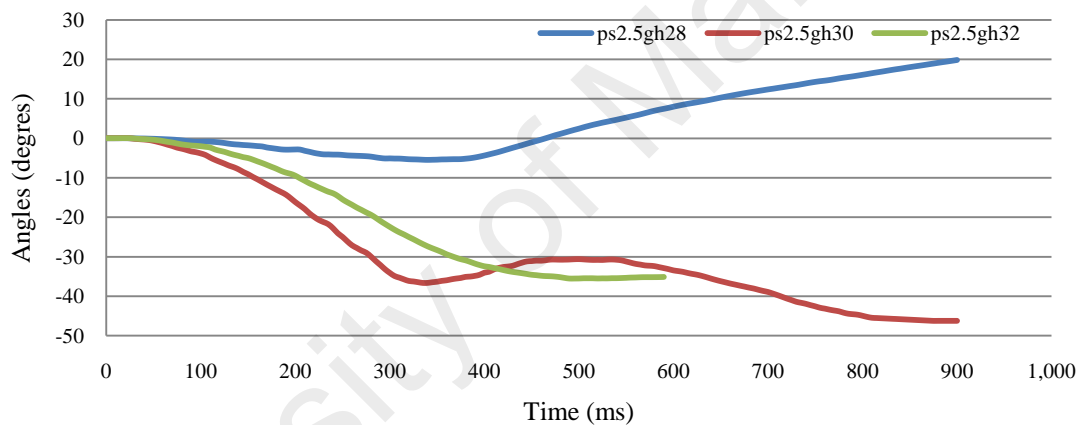


Figure 4-35. Yaw calculation for the guardrail system with a post spacing of 2 metres

4.4.2.5 Comparing the roll values

Two of the important factors for assessing a vehicle's stability during an impact with guardrail system are its pitch and roll. In systems with higher guardrails, the guardrail was able to redirect the vehicle smoothly and deflect more. The results of this study indicate that when it impacted a system with a higher guardrail, the pickup truck was essentially more stable than it was during an impact with a system with a lower guardrail. When it exited, the pickup truck rolled back to normal when the guardrail height was 81cm (32 inches) and the post spacing was 2 or 2.5 metres. The pitch and

roll angles were both small, which suggests that the vehicle was in a stable upright position.

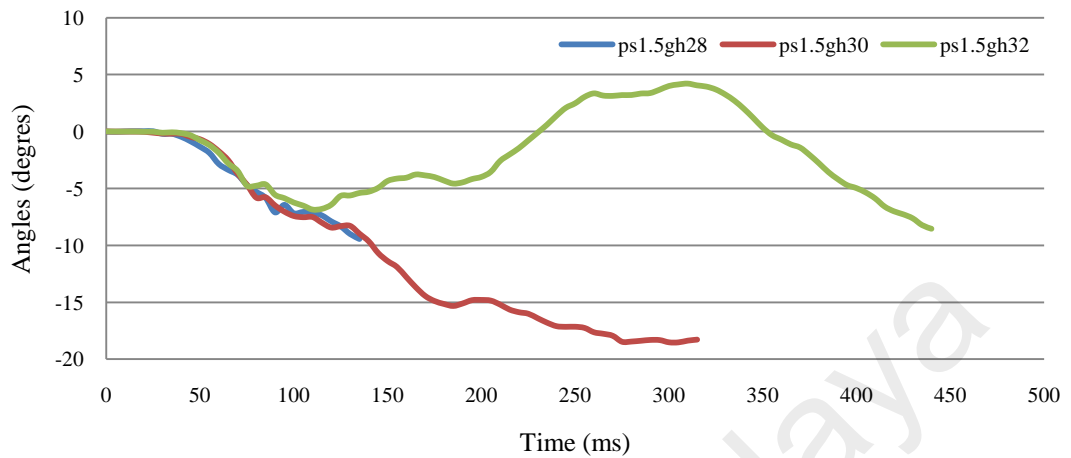


Figure 4-36. Roll calculation for the guardrail system with a post spacing of 1.5 metres

For a post spacing of 1.5 metres, the roll for all guardrail heights is graphed. As shown in Figure 4-36, a lower guardrail height resulted in a higher roll angle; these results indicate that the probability of the vehicle rolling over was higher when the guardrail was lower.

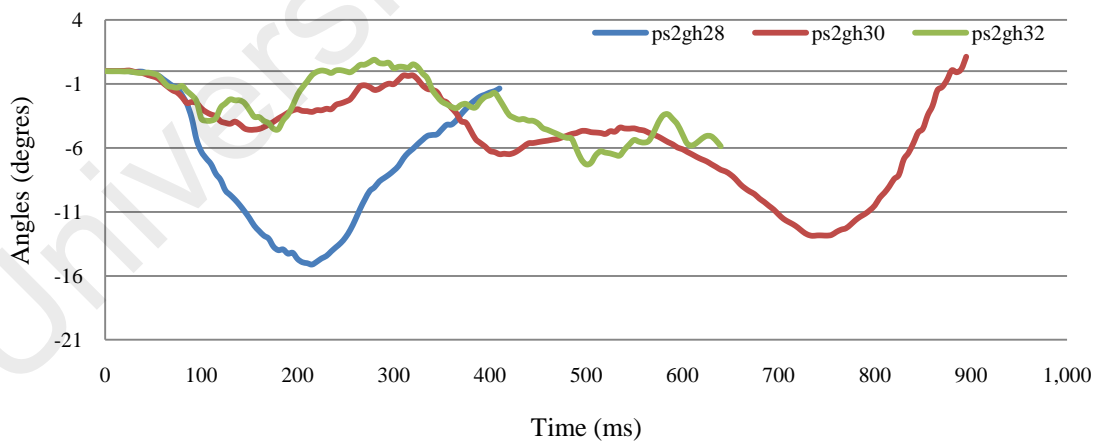


Figure 4-37. Roll calculation for a guardrail system with a post spacing of 2 metres

The same relationship was found for a post spacing of 2 metres; as the guardrail height increased, the probability of the vehicle rolling over decreased significantly (Figure 4-37).

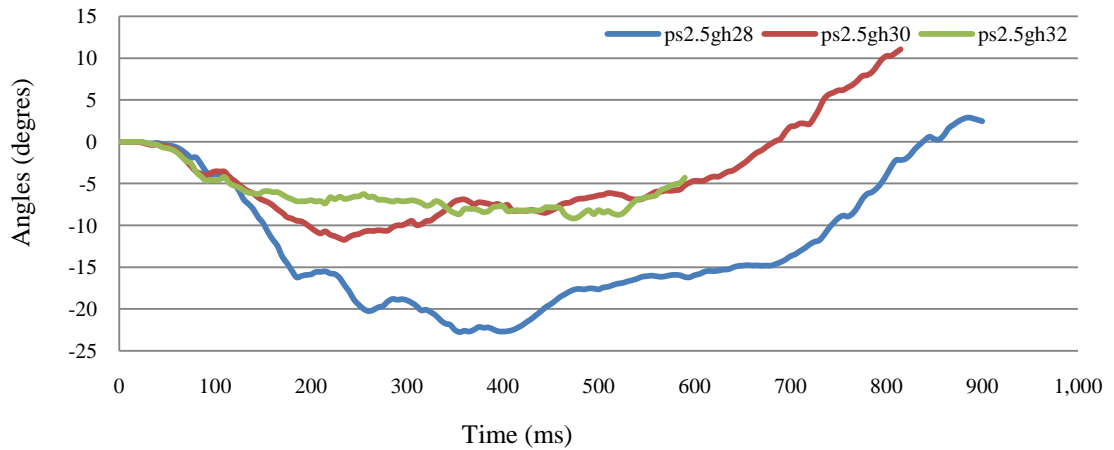


Figure 4-38. Roll calculation for a guardrail system with a post spacing of 2.5 metres. The effect of the guardrail height was very clear when the post spacing was 2.5 metres; the 71 cm (28 inches) high guardrail resulted in the greatest roll, which indicates that the vehicle had a higher probability of rolling over than it did after impacting the other guardrail systems in this category (Figure 4-38).

4.4.2.6 Comparing the pitch values

Decreases in the roll and pitch show that the redirection of the car may depend on the deformation characteristics of the guardrail system.

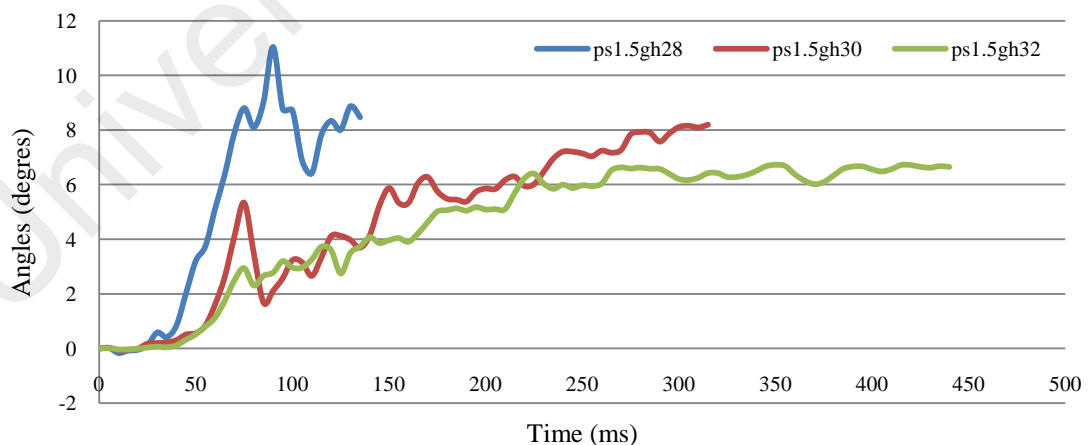


Figure 4-39. Pitch calculation for a guardrail system with a post spacing of 1.5 metres

When the post spacing was 1.5 metres, the 71 cm (28 inches) high guardrail resulted in a higher pitch than the other guardrail systems. The results for the 76 cm (30 inches)

and 81 cm (32 inches) high guardrails were similar; however, the 81 cm (32 inches) high guardrail provided the lowest values. The results are shown in Figure 4-39.

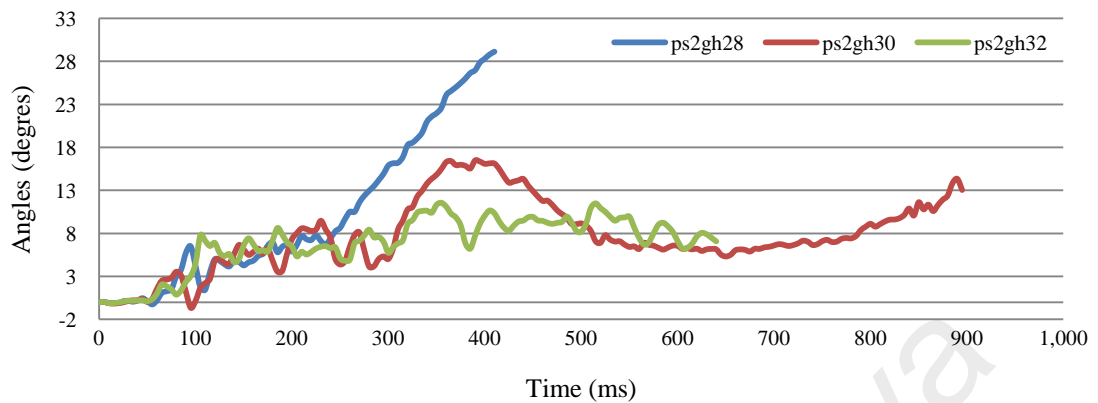


Figure 4-40. Pitch calculation for a guardrail system with a post spacing of 2 metres

The same relationship was found for a post spacing of 2 metres. The results are shown in Figure 4-40.

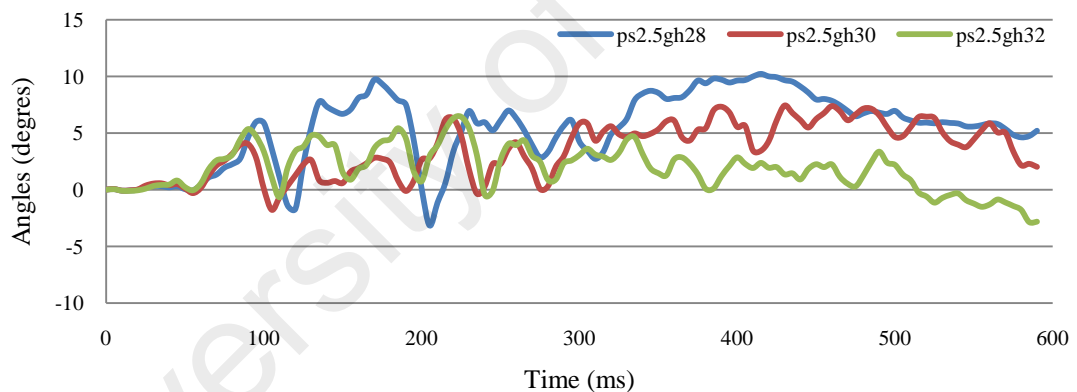


Figure 4-41. Pitch calculation for a guardrail system with a post spacing of 2.5 metres

The results for a post spacing of 2.5 metres indicate that all the guardrail heights resulted in low pitches, and it was concluded that as post spacing increased, the pitch decreased for all guardrail heights (Figure 4-41).

4.4.3 Evaluating the occupant risk factors

Assessing the impact acceleration of the vehicle's centre of gravity is required for evaluating and measuring the acceleration in different directions to assess the occupant

risk factors. A comparison between different systems is made to examine hypothesis 5. The results are discussed in the following section.

4.4.3.1 Comparison of the acceleration data

The acceleration results were compared for three different guardrail heights and post spacings to explore their effects on the vehicle's occupants. The accelerations in two directions were recorded, and the results are presented in Figures 4-42 to 4-47.

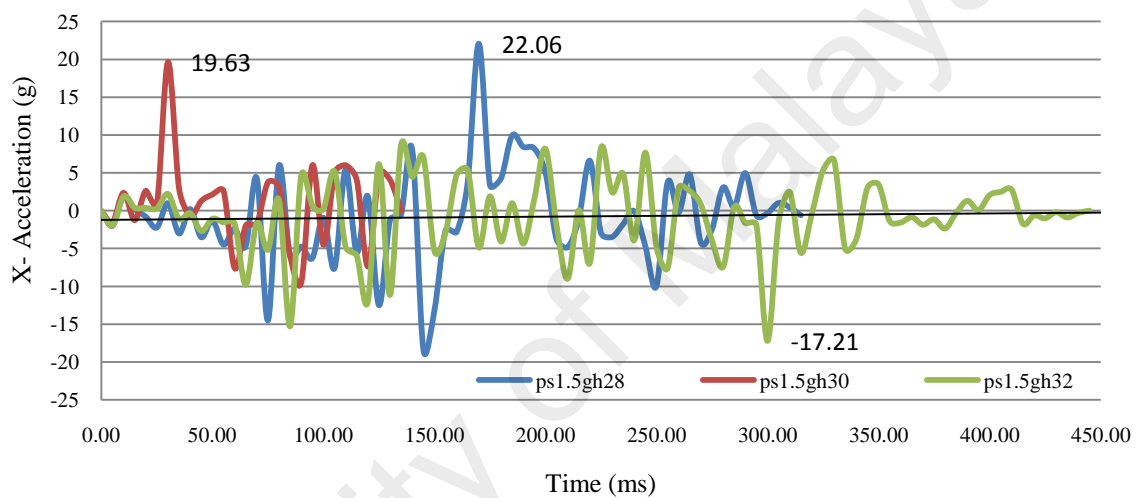


Figure 4-42. Longitudinal acceleration for a post spacing of 1.5 metres

As seen in Figure 4-42, the 71 cm (28 inches) high guardrail resulted in the highest acceleration (22.06 g), and the 81 cm (32 inches) high guardrail resulted in the lowest value (-17.21 g) in the longitudinal direction when the post spacing was 1.5 metres.

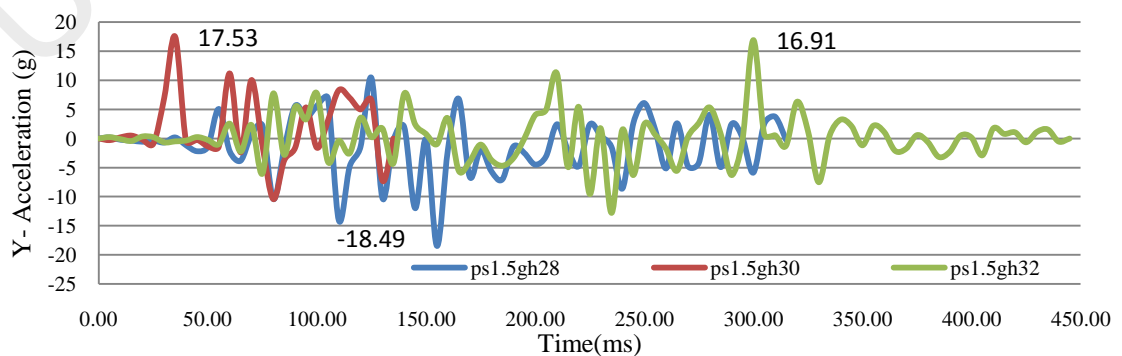


Figure 4-43. Lateral acceleration for a post spacing of 1.5 metres

The same relationship was found for the lateral acceleration when the post spacing was 1.5 metres. The 81 cm (32 inches) high guardrail resulted in the lowest acceleration. All the values exceeded the preferred value (15 g); however, they are in the range considered acceptable by the MASH's criteria (Figure 4-43).

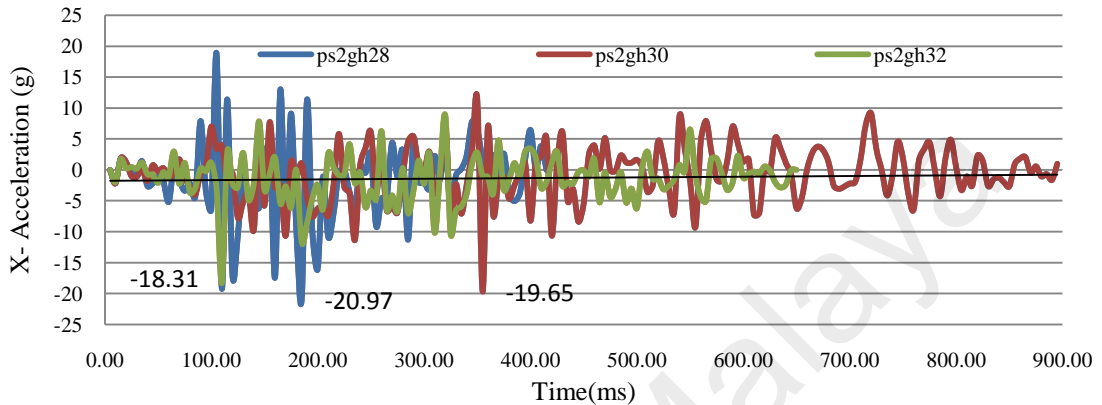


Figure 4-44. Longitudinal acceleration for a post spacing of 2 metres

The longitudinal acceleration for a post spacing of 2 metres and different guardrail heights were similar. However, the highest value was recorded for the lowest guardrail. The 76 cm (30 inches) and 81 cm (32 inches) high guardrails were in the acceptable range, according to the MASH's criteria (Figure 4-44).

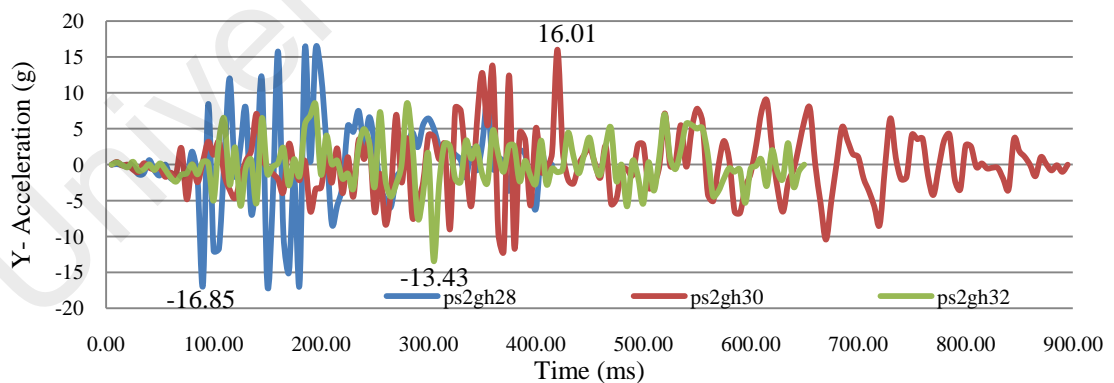


Figure 4-45. Lateral acceleration for a post spacing of 2 metres

The lateral acceleration resulting from the 81 cm (32 inches) high guardrail with a post spacing of 2 metres was in the preferred range specified by the MASH. As previously discussed, this barrier successfully redirected the vehicle; all the factors, including the

structural adequacy, the vehicle trajectory and the occupant risk factors, were in the acceptable range (Figure 4-45).

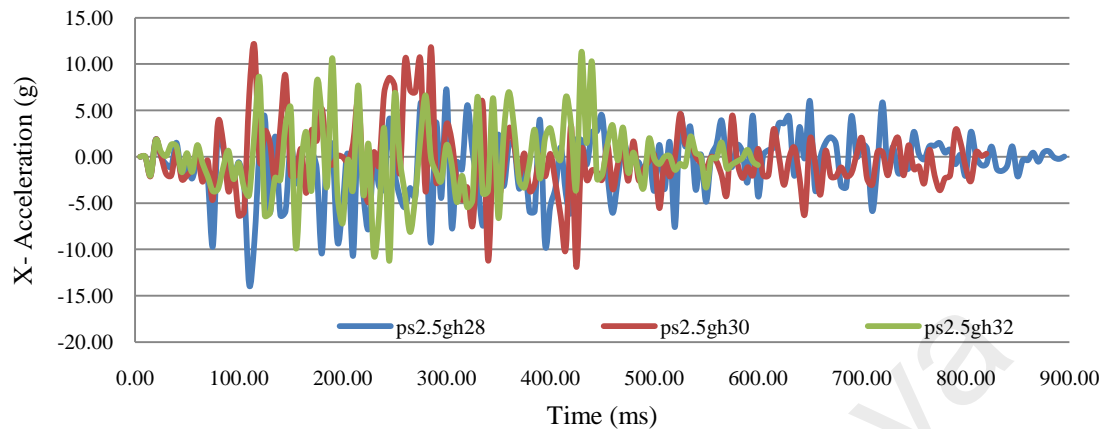


Figure 4-46. Longitudinal acceleration for a post spacing of 2.5 metres

Comparing the acceleration when the post spacing was 2.5 metres those when the post spacing was 1.5 and 2 metres reveals that the acceleration decreased significantly and, as shown in Figure 4-46, the values are in the ranges preferred by the MASH (<15 g) for all guardrail heights.

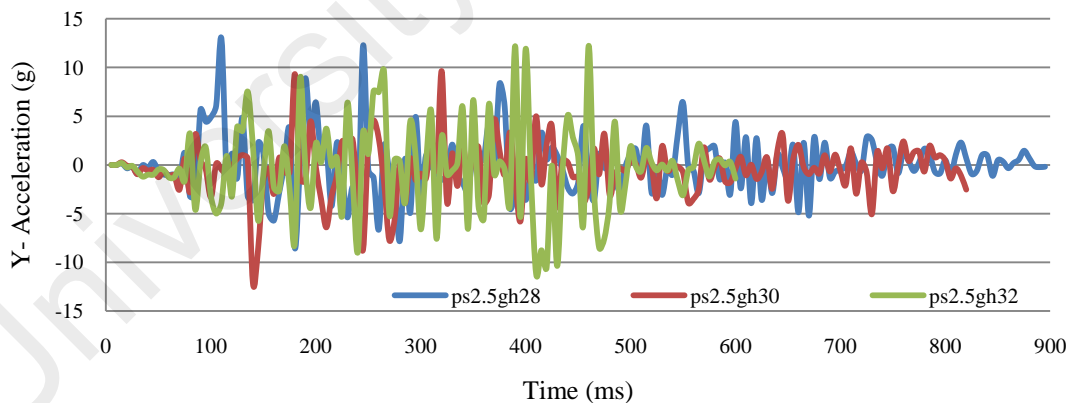


Figure 4-47. Lateral acceleration for a post spacing of 2.5 metres

The lateral accelerations were recorded and were all less than 15 g. The results were within the preferred range specified in the MASH's criteria. The results revealed that the 81 cm (32 inches) high guardrail provided the pickup truck with the smallest lateral acceleration (Figure 4-47).

4.5 Statistical analysis

The effect of each variable, including the post spacing and guardrail height, on the two main responses, the lateral deflection and the occupant risk factors, was analysed using the RSM to achieve objective 5. This was completed to approve the results of the parametric study and further evaluate hypotheses 3 and 5. The most important factors in the vehicle trajectory criteria are the vehicle's exit angle and exit speed. Because some of the barriers failed to redirect the vehicle to the road, it was not possible to perform a statistical analysis and compare the results. Therefore, a statistical analysis is used to test the deflection and occupant risk factors that are the subject of hypotheses 3 and 5. Table 4-4 shows a CCD in the form of a 2^3 full factorial design. The independent variables are presented in their original units. The coded values for the post spacing (A) and guardrail height (B) were set to one of three values: -1 (minimum), -0.5, 0 (central), +0.5, and +1 (maximum).

Table 4-4: Finite element results

Run.No	Factor 1 A: post spacing (m)	Factor 2 B: Guardrail heights (inch)	Response 1: X-acceleration (g)	Response 2: Y- acceleration (g)	Response 3: lateral deflection (mm)
1	1.5	28	22.07	18.49	638.5
2	1.5	30	19.63	17.53	750.46
3	1.5	32	17.21	16.91	783.97
4	2	28	20.97	16.85	819.76
5	2	30	19.65	14.11	856.24
6	2	32	18.31	13.43	1020.21
7	2.5	28	13.82	12.97	1097.95
8	2.5	30	12.01	12.6	1393.43
9	2.5	32	11.29	12.21	1424.37

When a multiple regression analysis of the design matrix and the responses, a fitted quadratic equation was generated. Equation. 3.7 was used to optimise the amination conditions. For all the responses, a quadratic model was suggested by the software based on the highest order polynomial. The general response models expressed in terms of the coded factors included all the numerical parameters. The CCD shown in Tables 4-5 to 4-7 allowed the development of mathematical equations that assess the results were predicted as functions of the post spacing (A) and the guardrail height (B) that

were calculated as the sum of a constant, two first-order effects (terms in A and B), one interaction effect (AB) and two second-order effects (A^2 and B^2), as shown in Equation. 3.7. An ANOVA was performed to assess the goodness of fit. In addition, the tables illustrate the reduced quadratic models (in terms of the coded factors) and other statistical parameters. The data demonstrate that all the models were significant at the 1% confidence level. The P values (PLOF) (>0.05) presented in each table show that the F-statistic was insignificant. The AP values, which were greater than 4 for all the responses, confirm that all the predictive models can be used to navigate the design space defined by the CCD.

Table 4-5: ANOVA and the final equation for the lateral deflection

	Sum of Squares	df	Mean Square	F Value	P-value Prob > F	Model Performance
Model	6.193E+005	5	1.239E+005	28.07	0.0101	Significant
A-Post spacing	5.062E+005	1	5.062E+005	114.72	0.0017	Significant
B-Guardrail heights	75340.18	1	75340.18	17.07	0.0257	Significant
AB	8185.73	1	8185.73	1.86	0.2665	Insignificant
A^2	26932.11	1	26932.11	6.10	0.0900	Insignificant
B^2	2580.01	1	2580.01	0.58	0.5001	Insignificant
Residual	13238.20	3	4412.73			
Cor Total	6.325E+005	8				
R-Squared				0.9791		
Adj R-Squared				0.9442		
AP				14.843		

$$\text{Lateral deflection} = 922.68 + 290.47A + 112.06B + 45.24AB + 116.04A^2 - 35.92B^2$$

For the lateral deflection, the F-value of the model, 28.07, implies that the model is significant. There is only a 1.01% chance that an F-value this large could be the result of noise. Values of "Prob > F" that are less than 0.0500 indicate model terms that are significant. In this case, factors A and B are significant model terms. This shows that the post spacing and the guardrail height affect the lateral deflection significantly. The results shown in Table 4-5 reveal that the post spacing has the lowest P-value for lateral deflection. The coded equation for the lateral deflection is also provided in Table 4-5.

Table 4-6: ANOVA and final equation for the longitudinal acceleration (X)

	Sum of Squares	df	Mean Square	F Value	P-value Prob > F	Model performance
Model	123.87	5	24.77	151.91	0.0008	significant
A-Post spacing	79.13	1	79.13	485.27	0.0002	significant
B-Guardrail heights	16.83	1	16.83	103.23	0.0020	significant
AB	1.36	1	1.36	8.32	0.0633	Insignificant
A ²	26.47	1	26.47	162.35	0.0010	significant
B ²	0.066	1	0.066	0.40	0.5699	Insignificant
Residual	0.49	3	0.16			
Cor Total	124.36	8				
R-Squared				0.9961		
Adj R-Squared				0.9895		
AP				32.189		

$$\text{Acceleration (X)} = 19.52 - 3.63A - 1.68B + 0.58AB - 3.64A^2 + 0.18B^2$$

In case of the longitudinal acceleration, the F-value of the model, 151.91, implies that the model is significant. There is only a 0.08 % chance that an F-value this large is due to noise. In this case, the factors A, B and A² are significant terms in the model. This shows that the post spacing and the guardrail height affect the longitudinal acceleration significantly. However, the post spacing (A), which has a P-value of 0.0002, indicates higher correlation with longitudinal acceleration than guardrail heights (B). The coded equation based on the post spacing and guardrail height is also provided in Table 4-6.

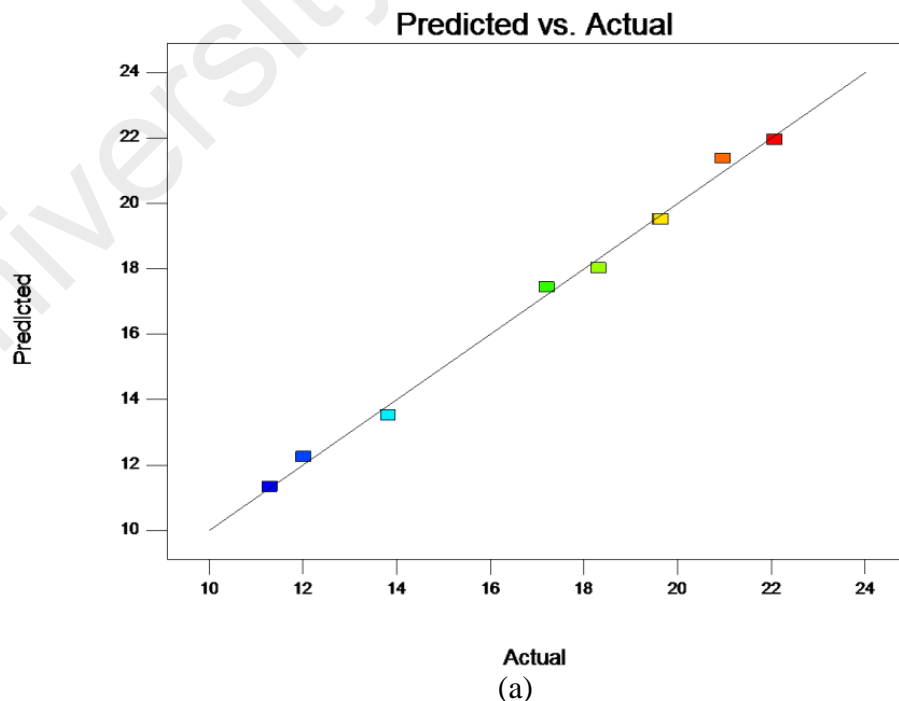
Table 4-7: ANOVA and the final equation for the lateral acceleration (Y)

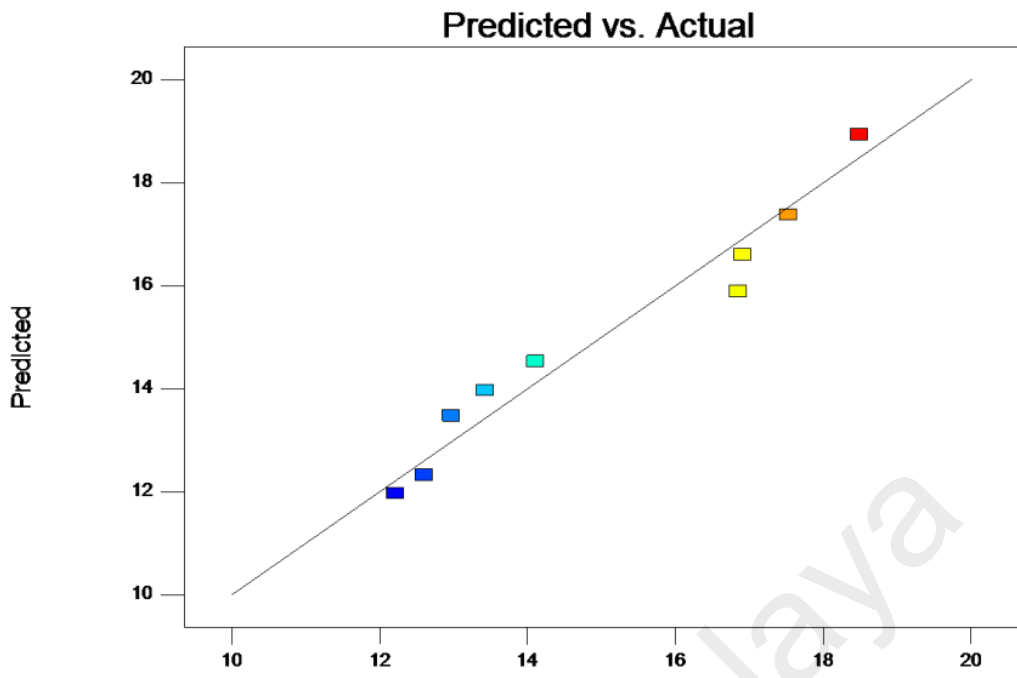
	Sum of Squares	df	Mean Square	F Value	P-value Prob > F	Model performance
Model	44.47	5	8.89	12.71	0.0312	Significant
A-Post spacing	38.25	1	38.25	54.66	0.0051	Significant
B-Guardrail heights	5.53	1	5.53	7.90	0.0672	Insignificant
AB	0.17	1	0.17	0.24	0.6577	Insignificant
A ²	0.21	1	0.21	0.30	0.6244	Insignificant
B ²	0.31	1	0.31	0.45	0.5505	Insignificant
Residual	2.10	3	0.70			
Cor Total	46.57	8				
R-Squared				0.9549		
Adj R-Squared				0.8798		
AP				10.204		

$$\text{Acceleration (Y)} = 14.53 - 2.52A - 0.96B + 0.20AB + 0.32A^2 + 0.40B^2$$

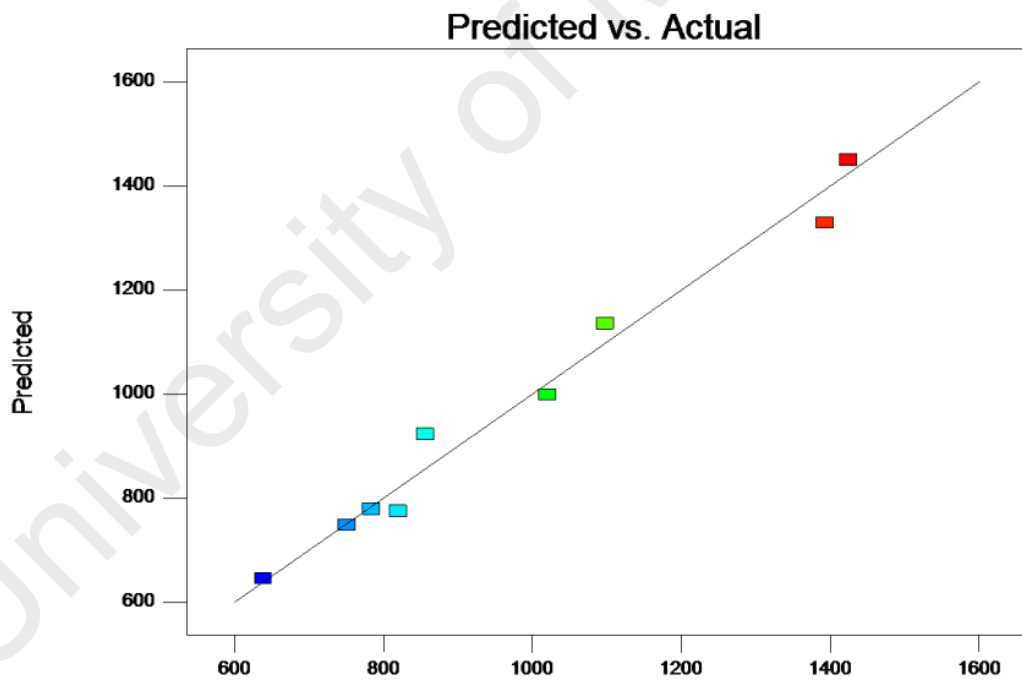
In case of the lateral acceleration, the F-value of the model, 12.71, implies the model is significant. There is only a 3.12 % chance that an F-value this large could result from to noise. In this case, only the post spacing (A) is a significant term in the model. This shows that only the post spacing affects the lateral acceleration significantly. The coded equation for the lateral acceleration based on the post spacing and guardrail height is also provided in Table 4-7. Finally, the coded equation for the lateral acceleration based on the post spacing and guardrail height is provided in Table 4-7.

To obtain a better understating of model's adequacy, diagnostic graphs such as those comparing the predicted and actual values are worthwhile. Figure 4-48 a, b, and c show the actual and predicted values of the removed parameters for all responses. As shown in these figures, there is adequate agreement between the actual and predicted values. The same result can be found using the AP values ($AP > 4$) for all the responses (refer to Tables 4-5 through 4-7). This verifies that the predictive models can be used to navigate the design space defined by the CCD.





Actual
(b)



Actual
(c)

Figure 4-48. Actual and predicted values of the

X -acceleration (a), Y -acceleration (b), and lateral deflection (c)

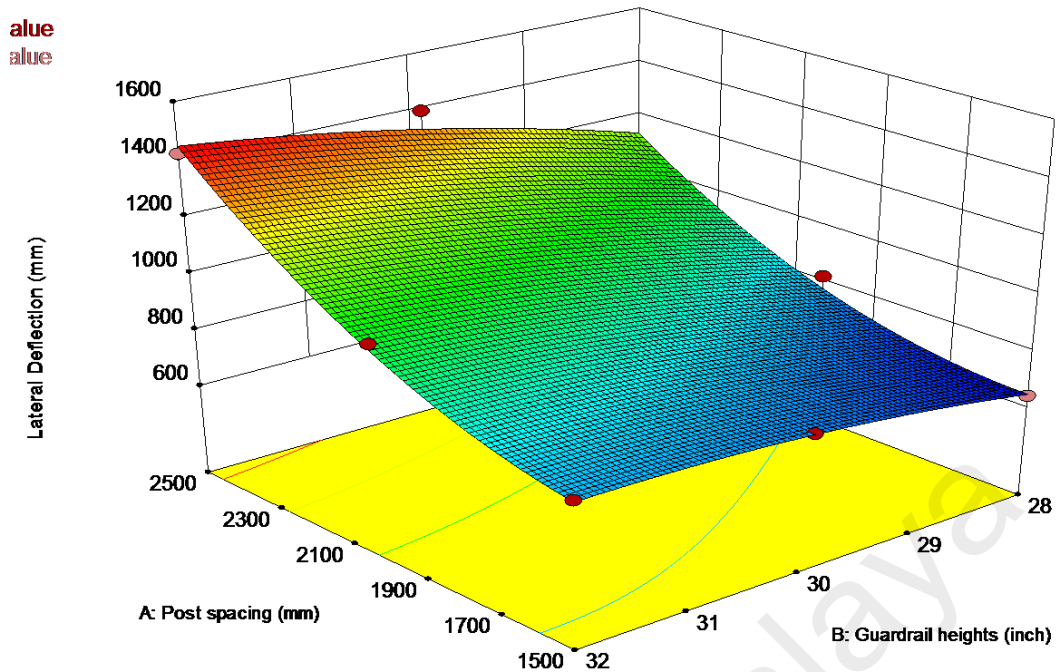


Figure 4-49. Effects of the post spacing and the guardrail height on the lateral deflection

One of the most important factors affecting the barrier's performance is the amount of deflection during a crash. This information can be used by designers as they select a guardrail design that is appropriate for the desired maximum deflection. To test hypothesis 3, the lateral deflection is evaluated for the different post spacings and guardrail heights. As shown in Figure 4-49, the amount of lateral deflection decreases sharply with the reduction of post spacing. This shows that reducing the post spacing with each guardrail height can effectively reduce the amount of deflection. However, changes in the guardrail height seem to be more significant for the highest post spacing; when the post spacing is 2.5 metres, the lateral deflection decreases from 1424.37 to 1097.95 mm.

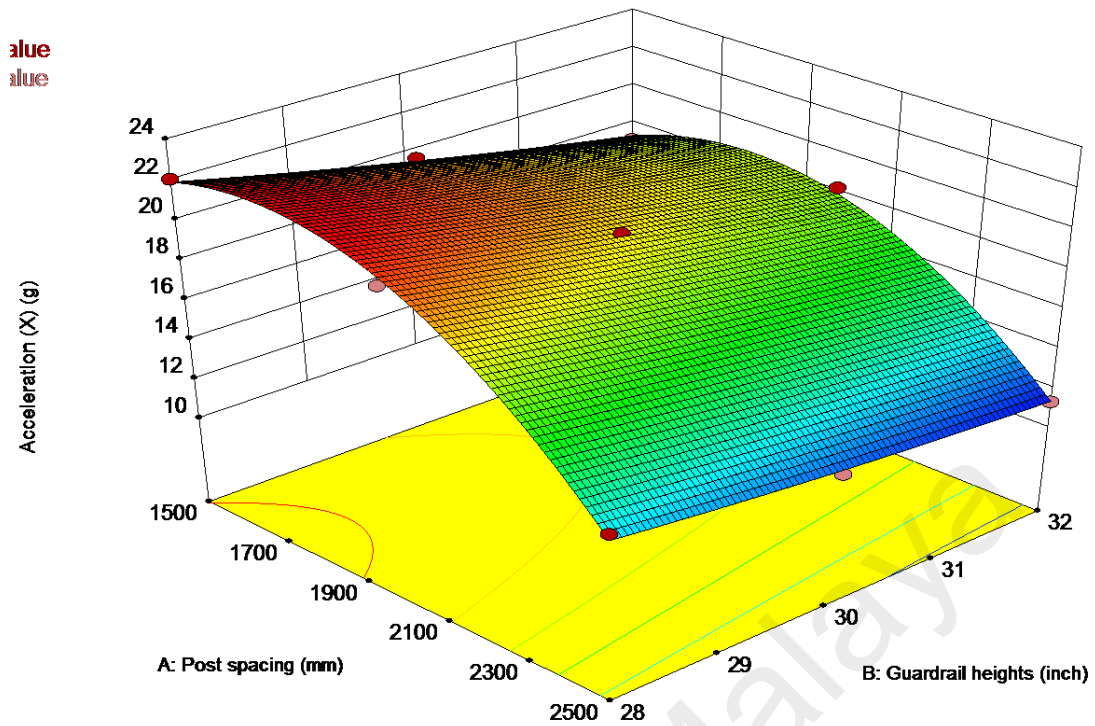


Figure 4-50. Effects of the post spacing and the guardrail height on the longitudinal acceleration

The distribution of the acceleration in longitudinal direction for the post spacing and the guardrail height is shown in Figure 4-50. This is to examine hypothesis 5. It can be seen that varying the guardrail height has a greater influence on the longitudinal acceleration when the post spacing is 1.5 metres, as shown in Figure 4-50, and that increasing the guardrail height from 71cm (28 inches) to 81 cm (32 inches) causes the longitudinal acceleration to decrease from 22.07 to 17.21 g. Additionally, it is shown that the acceleration decreases slightly when the post spacing is changed from 1.5 metres to 2 metres and then, suddenly drops significantly when the post spacing is changed from 2 metres to 2.5 metres.

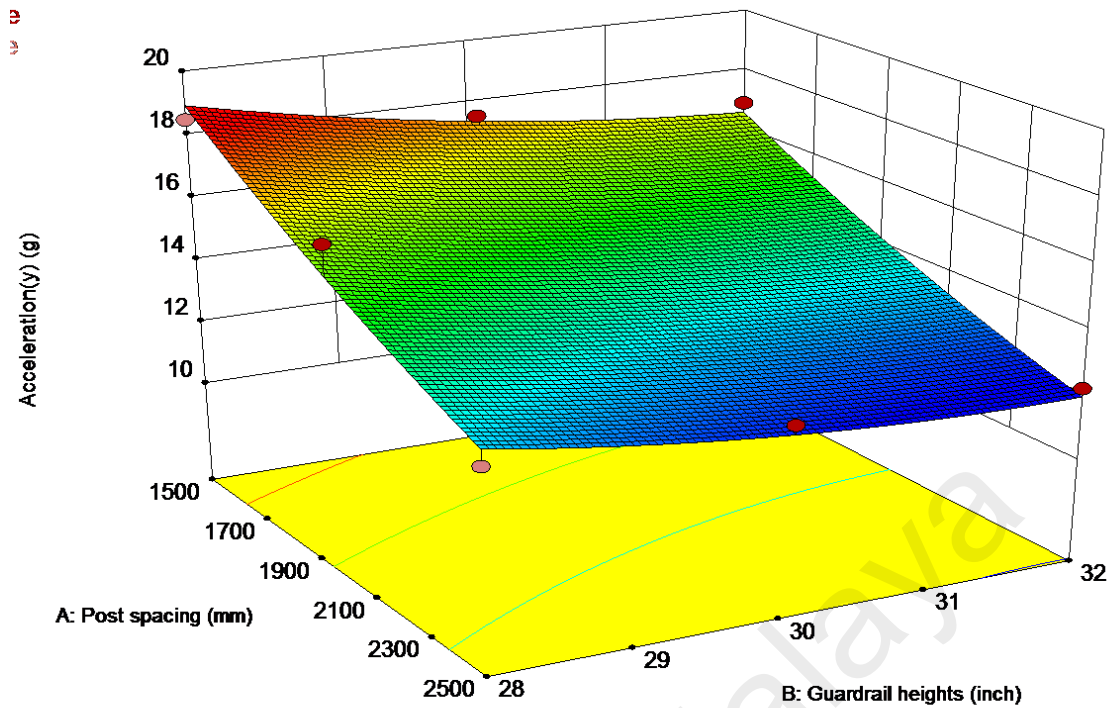


Figure 4-51. Effects of the post spacing and the guardrail height on the lateral acceleration

Figure 4-51 shows that the lateral acceleration is strongly affected by the post spacing. A reduction is observed for all the guardrail heights. The highest accelerations were achieved by the guardrail system with the smallest post spacing.

In addition, a decrease in the acceleration was found as the guardrail height increased. However, when the post spacing is 2.5 metres, this reduction seems insignificant.

4.6 Chapter summary

The static experimental and simulated static tests demonstrated the basic mechanical behaviour and the different stages of deformation mechanism of the W-beams guardrail systems. Based on the results of these static tests, the optimum mesh size of for the W-beam guardrail model was found; it was used in the full-scale model of the guardrail system.

The G4(2W) guardrail system was modelled using LS-DYNA, and the model was validated with a full-scale crash test that had previously been conducted by the TTI. The model was qualitatively and quantitatively validated with data from the full-scale crash test.

The results of the full-scale crash into the G4(2W) guardrail system and the finite element analysis indicated that the basic model of the guardrail system failed because it was structurally inadequate. Therefore, using the validated model, a parametric study of selected factors was conducted to improve the guardrail system's performance. First, improving the splice connections to increase the stiffness was considered. After a suitable splice configuration was identified, the parametric study of important parameters, including the post spacing and the guardrail height, was continued. The results for different outputs (the structural adequacy, the vehicle trajectory and occupant risk factors) of the parametric study were discussed. Suitable guardrail systems were identified based on the requirements for structural adequacy, vehicle trajectory and occupant risk factors. Finally, a statistical analysis was performed to evaluate the effect of each factor on each particular output. This was completed to examine the significance of each factor.

CHAPTER 5: CONCLUSION

5.1 Introduction

The purpose of this chapter is to summarise the results described in the previous chapter. These results are subsequently used to explain how the research objectives were achieved and to clarify suggestions for future studies. This are followed by a discussion of the contributions of this study and suggestions for future research, which is followed by the conclusion.

5.1.1 Overview of the study

This study started with a review of the performance of different types of guardrail system that focused on the following aspects: the structural capacity, the vehicle trajectory and occupant risk factors. After evaluating the previously conducted studies, it was observed that when the MASH's criteria were implemented, most guardrail systems had difficulty satisfying the structural adequacy requirement. Therefore, one of the guardrail systems that failed, the G4(2W) guardrail system, was chosen for analysis and model development to improve its performance. Finally, the results of the experiment and the finite element model are analysed using a parametric study and statistical analysis.

The data used in the study were obtained from the literature, experiments, a crash test conducted at the TTI and the results of the LS-DYNA finite element model. Furthermore, the results of the proposed models were discussed as part of the parametric and statistical analyses. Finally, the results and suggestions for future research were presented.

5.2 Conclusion for objective 1 (analysis of previous guardrail systems' performance)

The results of the analysis of previously designed guardrail systems are presented in this section. Understanding each guardrail system's performance helps with improving and enhancing the development of guardrail systems. According to the discussion presented in chapter 2, this objective led to the following conclusions:

1. In a strong-post system, the value of the longitudinal ride-down acceleration was higher when the guardrail height was 686 mm than when it was 788 mm. In contrast, a lower lateral ride-down acceleration was observed for the 686-mm-high barrier than for the other designs. However, the results obtained in this section need to be confirmed by an extensive parametric study using the finite element method.
2. The probability of sharp vehicle redirection parallels the stiffness of the barrier. For instance, larger vehicle exit angles were reported for the Thrie-beam system. Guardrails with kerbs caused vehicles to exit at larger angles, which could be due to the instability of the vehicles after striking the kerb.
3. In two strong-post systems, the W-beam guardrails ruptured during the crash tests, and the guardrail systems failed to contain the pickup trucks. This raised a concern about the ability of a strong-post system to contain a pickup truck.
4. Guardrail strengthening techniques were evaluated by conducting crash tests on W-beam guardrails that had been strengthened by nesting the W-beams and reducing the post spacing by half. The test results showed that nesting the W-beams provided little benefit, whereas reducing the post spacing increased the guardrail's performance considerably.

5. Comparing the occupant risk factors of the strong-post guardrail systems showed that the results were very different for the different designs and configurations. A small change into a design factor can change the performance of a strong-post system.
6. The guardrails that deflected the most were attached to posts with the smallest embedment depths. Factors other than the embedment depth, such as the post spacing and the guardrail height, may also be effective at controlling the guardrail's deflection. However, because there is a smaller body of literature containing crash test data, the comparison cannot be made and therefore, the effects of these parameters cannot be evaluated.

5.3 Conclusion for objective 2: Verification of rail system

To improve the model of a W-beam section, further consideration was performed in this section. Three different mesh sizes were considered; they were 40 mm, 20 mm and 10 mm. The 40 mm mesh was used in for the basic model of a strong-post guardrail system that was provided by the NCAC. The following conclusions were drawn:

1. The results when the 40 mm mesh was used (i.e., in the NCAC's basic model of a W-beam guardrail) were not accurate; the W-beam section flattened unrealistically under simulated static tests.
2. Comparing the results showed that the results for the 40 mm mesh were not comparable to the experimental results. The results for the 40 mm mesh were more unrealistic when the loading was placed near the supports.
3. The results obtained with 20 and 10 mm meshes were very comparable to the experimental results. To reduce the computation time, the 20 mm mesh was

chosen for the simulations of the W-beam guardrail in the G4(2W) guardrail system. Based on the achieved results the first hypothesis has been confirmed.

4. When the static load was applied near a support (at 0.16 of the length of the beam), the highest forces were reported.

5.4 Conclusion for objective 3: Validation of the G4(2W) guardrail system

A finite element model of the G4(2W) guardrail system was developed following the procedure described in chapter 3. To validate this model of a G4(2W) strong-post guardrail system, and to assess the accuracy of the simulation of a truck impacting the guardrail system a full-scale crash test (Bullard et al., 2010a) was used. The following results were obtained during the validation process:

- When the sequences of pictures are compared, the finite element simulation was in good agreement with the full-scale crash test in terms of the vehicle's position and interaction with the guardrail system.
- A comparison of the accelerations in all three of the cases considered performed using the RSVVP showed that the numerical data are correlated well with the experimental results.

5.5 Conclusion for objective 4. Conducting the parametric study

The parametric study on of the finite element results obtained from the LS-DYNA model of the G4(2W) guardrail system subjected to Length of Need test 3-11 described in the MASH is summarised in the following sections. The results are categorised by the three main factors: the structural adequacy, the vehicle trajectory and the occupant risk factors.

5.5.1 Results for the structural adequacy

Improving the splice connections was considered. The parametric study was then continued by changing the two main design parameters, the post spacing and the guardrail height. The results relating to the system's structural adequacy are presented in the following subsections.

Results for improving the stiffness of the splice connections

The results of full-scale crash test conducted by the TTI showed that the guardrail ruptured at the splice connections. Increasing the number of bolts in each splice connection was considered to increase the stiffness of the connection. The results obtained from the simulations are as follows:

- The analysis was performed with the number of bolts increasing from 8 to 10 and 12 bolts. The results of the modelled crash test indicated that the guardrail system failed at its splice connections, and increasing the number of bolts in each splice connection to 10 was not sufficient.
- The results showed that increasing the number of bolts in each splice connection to 12 based on the LS-DYNA simulation resulted in the guardrail successfully containing the vehicle and the barrier absorbed the impact energy of the pickup truck. Consequently, the second hypothesis has been confirmed. However, the barrier failed to redirect the vehicle to the road in a safe manner.

Results for guardrail deflection

Splice connections with 12 bolts were used in the G4(2W) guardrail system. Subsequently, further evaluation was performed to determine the effects of post spacings ranging from 1.5 to 2.5 metres and of guardrail heights ranging from 71 cm

(28 inches) to 81 cm (32 inches). The following results were obtained when the lateral deflection was calculated by LS-DYNA.

- When the post spacing was 1.5 metres, the greatest deflection was recorded when the guardrail was 81 cm (32 inches) high. The results for 76 cm (30 inches) and 81 cm (32 inches) high guardrails were similar. However, the 71 cm (28 inches) high guardrails deflected the least.
- When the post spacing was 2 metres, the 81 cm (32 inches) high guardrails deflected 1020.22 mm, which was more than the other guardrails. The results for the 71 cm (28 inches) and 76cm (30inches) high guardrails were similar; however, the result for the 76 cm (30 inches) high guardrail was slightly higher.
- The results show that increasing the guardrail height resulted in greater dynamic rail deflections and it confirms the third hypothesis of this study.

5.5.2 Vehicle trajectory

In following subsections, the results of the finite element model that relate to the vehicle's response to the G4(2W) guardrail system are summarised under the standard impact conditions for Length of Need test 3-11 described in the MASH for several post spacings and guardrail heights.

5.5.2.1 Evaluation of the vehicle's exit speed

- During the period from 100 ms to 125 ms, when the post spacing was 1.5 metres and the guardrail height was increased, the vehicle's exit speed increased, and 73.66 km/hr was recorded for the 81 cm (32 inches) high guardrail.
- When the post spacing was 2 metres, no significant difference in the vehicle's exit speed for the 76 cm (30 inches) and 81 cm (32 inches) high guardrails between the beginning of the crash and 350 ms into the model of the crash. After

350 ms, when the guardrail was 76 cm (30 inches) high, the vehicle rotated counterclockwise, and the guardrail eventually failed to redirect the vehicle, which resulted in its lower exit speed.

- When the post spacing was 2.5 metres, the results were interesting. Higher vehicle exit speeds were found for the 76 cm (30 inches) and 81 cm (32 inches) high guardrails. The highest exit speed, 58 km/hr, was found for the 81 cm (32 inches) high guardrails system.
- The results showed that as the guardrail height increased, the impact became less severe.
- The guardrails with greater post spacings provided higher vehicle exit speeds.

5.5.2.2 Evaluation of vehicle Exit angle

The preferred vehicle exit angle is less than 60° of the initial impact angle according to the MASH. A greater exit angle is not encouraged because it makes the vehicle more likely to rebound back into the traffic lanes and exposes it to secondary impacts.

- Under three impact conditions, the guardrail with a post spacing of 1.5 metres failed to redirect the vehicle. The vehicle rotated counterclockwise and was not redirected safely by a guardrail with any of the heights evaluated when the post spacing was 1.5 metres.
- When the post spacing was 2 metres, the results showed that only the 81 cm (32 inches) high guardrails redirected the vehicle safely. However, the other guardrails with same post spacing were not successful; these guardrails failed to redirect the vehicle safely.
- The results of the model with a post spacing of 2.5 metres indicated that the vehicle's exit angle was acceptable when the guardrail was 76cm (30inches) or 81cm (32 inches) inches high.

5.5.2.3 Comparing the yaw values

The rotation of the vehicle during the impact provides further insight into the behaviour of the vehicle and can be a useful comparison tool.

- When the post spacing was 1.5 metres, comparing the yaw angles showed that the higher guardrails resulted in smaller yaw angles. In addition, guardrail systems post spaced 1.5 metres apart were not able to redirect the vehicle to the road and instead, twisted the vehicle counterclockwise.
- When the guardrail's height was 81 cm (32 inches) and its post spacing was 2 metres, the yaw was negative, indicating that the vehicle rotated clockwise and was safely redirected. The maximum value recorded was -46.3 degrees. However, the other guardrail systems in this category exhibited positive values for the yaw and failed to redirect the vehicle safely.
- When the post spacing was 2.5 metres, the 76 cm (30 inches) and 81 cm (32 inches) high guardrails were able to redirect the vehicle to the road safely and exhibited negative values for the yaw.
- The 71 cm (28 inches) high guardrail failed for all the post spacings, which indicates that 71 cm (28 inches) high guardrail systems are unable to satisfy the MASH's criteria.

5.5.2.4 Comparing the roll values

One of the important factors for assessing the vehicle's stability during an impact with a guardrail system its roll behaviour. The results of the finite element analysis for the vehicle's roll were as follows:

- When the post spacing was 1.5 metres, the results for the all guardrails showed that lower guardrail heights led to higher roll angles, which indicates that the probability of the vehicle rolling over is high when the guardrail system is low.

- The same relationship was found when the post spacing was 2 metres; as the guardrail height increased, the probability of the vehicle rolling over decreased significantly.
- The effect of the guardrail height was very clear when the post spacing was 2.5 metres; the guardrail that was 71 cm (28 inches) high provided the greatest roll angle, which indicates that the probability of the vehicle rolling was the highest of the guardrail systems in this category.

5.5.2.5 Comparing the pitch values

The following conclusions were obtained by analysing the pitch values:

- When the post spacing was 1.5, 2 or 2.5 metres, the 71 cm (28 inches) high guardrail provided the highest pitch value of the guardrail systems. The results for the 76 cm (30 inches) and 81 cm (32 inches) high guardrails were similar; however, the 81 cm (32 inches) high guardrails provided the lowest value.
- The results when the post spacing was 2.5 metres indicated that all the guardrail heights provided low pitch values, and it was concluded that as the post spacing increased, the pitch was reduced for all guardrails with heights between 71cm (28 inches) and 81cm (32 inches).
- based on the achieved results the fourth hypothesis has been confirmed.

5.5.3 Evaluating the occupant risk factors

Assessing the impact of the acceleration of the vehicle's centre of gravity is required for evaluating the occupant risk factors. A comparison of systems different post spacings and guardrail heights is made and the acceleration in different directions is calculated and discussed in following section.

- When the post spacing was 1.5 metres, the 71 cm (28 inches) high guardrail showed the greatest acceleration (22.06 g), and the 81 cm (32 inches) high guardrail provided the lowest value (-17.21 g) in the longitudinal direction, which indicates that a higher guardrail system may effectively reduce the occupant risk factors for pickup trucks.
- The same relationship was found for the lateral acceleration when the post spacing was 1.5 metres. The 81 cm (32 inches) high guardrail provided the lowest acceleration.
- The longitudinal acceleration when the post spacing was 2 metres showed that guardrails with lower heights resulted in greater accelerations. The 76 cm (30 inches) and 81 cm (32 inches) high guardrails were in acceptable range, according to the MASH's criteria.
- When the post spacing was 2 metres and the guardrail height was 81 cm (32 inches), the lateral acceleration was in the range of preferred values, according to the MASH's criteria. This barrier successfully redirected the vehicle and all the factors, including the structural adequacy, the vehicle trajectory and the occupant risk factors, were in the acceptable ranges.
- Comparing the accelerations for post spacings of 2.5 metres revealed that the acceleration decreased significantly; all the values were in the preferred range (< 15 g), according to the MASH's criteria, for all the guardrail heights.
- The values of the lateral acceleration recorded were all less than 15 g. The results were within the preferred range, according to the MASH's criteria. The results revealed that the 81 cm (32 inches) high guardrail provided the lowest lateral acceleration in the simulated pickup truck crash.
- the achieved results for evaluating the occupant risk factors approved the fifth hypothesis of this study.

5.6 Conclusion for objective 5: Statistical analysis

- Adequate agreement between the actual values and the model's predictions was found, which shows that the model's predictions can be used to navigate the design space defined by the CCD.
- One of the most important factors of the barrier's performance is the amount of deflection it experiences during a crash. The amount of lateral deflection sharply decreases when the post spacing is decreased. In other words, decreasing the post spacing for any guardrail height can effectively reduce the amount of deflection. However, varying the guardrail height seems to be more significant when the post spacing is greater; when the post spacing was 2.5 metres, the lateral deflection decreased from 1424.37 to 1097.95 mm.
- Varying the guardrail's height had a stronger influence on the longitudinal acceleration when its post spacing was 1.5 metres. Increasing the guardrail's height from 71 (28 inches) to 81 (32 inches) resulted in the longitudinal acceleration decreasing from 22.07 to 17.21 g.
- The results show that the lateral acceleration was strongly affected the post spacing. This reduction was observed for all guardrail heights.
- This decrease in acceleration was found as the guardrail's height increased. However, when the post spacing was 2.5 metres, the decrease seemed insignificant.

5.7 Contributions

This study has enhanced the ability of researchers to design guardrail systems that satisfy the new standards in the MASH for protecting errant vehicles travelling at high speeds. As a result, this study may help identify suitable guardrail systems that

decrease the occupant risk factors. This study can enhance the understanding of barrier performance. This will help engineers and designers optimise the performance of roadside safety barriers using mathematical modelling.

In addition, the results of this study will provide safety engineers and designers with a crashworthy system that reduces the probability of injuries after a vehicle crashes into a barrier.

5.8 Limitations

The analyses of vehicles impacting a G4(2W) wood post guardrail system G4(2W) conducted in this study were limited to one vehicle type, a 2270-kg pickup truck, and one test, the Length of Need test 3-11 in the MASH. Therefore, a model based solely on the results of these analyses is only applicable to one type of vehicle and one test. To develop a more general analysis, additional information about the responses of a broader range of vehicle types and tests is needed.

The modified G4(2W) guardrail model and the Silverado pickup truck model were used to determine the impact responses of guardrails configured in various ways. The number of analyses that can be conducted is limited due to the situation's complexity and time constraints; however, very useful information can be obtained from the results of selected cases.

This study showed that finite element analysis provides savings in terms of both time and resources over full-scale crash testing to an extent. Although finite element analysis attempts to replicate the actual dynamic interactions and mechanics of an impact, there are always approximations that may introduce a small amount of error into the model. For example, the boundary conditions and the post-to-W-beam connections were simplified outside the area of contact.

5.9 Recommendation and future work

To compare the performances of different barriers, it is worthwhile to develop a comprehensive database of models of safety components such as bridge rails, crash cushions, cable barriers and concrete barriers that could be used in an optimisation process that considers a variety of design factors. The same method can be used to improve the performance of other roadside safety components.

Different strengthening techniques to increase the stiffness of the splice connections using bolts of different sizes with different material properties in different configurations could be studied. As the splice connection's stiffness increases, the W-beam guardrail becomes able to carry greater tensile and bending forces. Subsequently, a wider post spacing can be considered as part of the design of a barrier system that has the benefits of lower costs and reduced occupant risk factors.

Not only should research into improving the crashworthiness of guardrail systems continue, but research into improving passenger cars and pickup trucks should also be considered. The research programme presented in this thesis will continue both in the direction of improving other guardrail systems in accordance with the MASH criteria for different vehicle types.

REFERENCES

- AASHTO. (1990). Aggregate and soil-aggregate subbase, base, and surface courses: M147-70. Standard Specifications for Transportation Materials and Methods of Sampling and Testing, Washington, D. C.
- AASHTO. (2000). AASHTO Guide to Standardized Highway Barrier Hardware. Task Force 13. AASHTO-AGC-ARTBA Joint Committee, Washington, DC.
- AASHTO-AGC-ARTBA. (1995). Task Force 13, A Guide to Standardized Highway Barrier Hardware. American Association of State Highway and Transportation Officials.
- Abu-Odeh, A.Y., K.M. Kim, & R.P. Bligh. (2011). Guardrail deflection analysis. Phase I. Texas Transportation Institute, Texas A & M University System.
- Atahan, A. O. (2002). Finite element simulation of a strong-post W-beam guardrail system. *Simulation*, 78(10), 587-599.
- Atahan, A. O., Bonin, G., Cicinnati, L., & Yasarer, H. I. (2008). Development of European end-treatment twiny using simulation and crash testing. *Journal of Transportation Engineering*, 134(11), 467-476.
- Ayati, E., Pirayesh Neghab, M.A., asghar Sadeghi, A., & Moghaddam, A. M. (2012). Introducing roadside hazard severity indicator based on evidential reasoning approach. *Safety science*, 50(7), 1618-1626.
- Azargohar, R., & Dalai, A. K. (2005). Production of activated carbon from Luscar char: experimental and modeling studies. *Microporous and mesoporous materials*, 85(3), 219-225.
- Basu, S., & Haghghi, A. (1988). Numerical analysis of roadside design (NARD) vol. III: validation procedure manual. Report No. FHWA-RD-88-213. FHWA, US Department of Transportation.
- Ben-Bassat, T., & Shinar, D. (2011). Effect of shoulder width, guardrail and roadway geometry on driver perception and behavior. *Accident Analysis & Prevention*, 43(6), 2142-2152.
- Bielenberg, R., Faller, R., Sicking, D., Rohde, J., & Reid, J. (2007). Midwest Guardrail System for Long-Span Culvert Applications. *Transportation Research Record: Journal of the Transportation Research Board*, (2025), 3-17.
- Bielenberg, R., Reid, J., Faller, R., Rosenbaugh, S., & Lechtenberg, K. (2014). Performance of the Midwest Guardrail System with Rectangular Wood Posts. *Transportation Research Record: Journal of the Transportation Research Board*, (2437), 27-40.
- Bligh, R.P., & W. Menges. (1997). Testing and Evaluation of a Modified Steel Post W-Beam Guardrail System with Recycled Polyethylene Blockouts. Texas Transportation Institute, Texas A & M University, Texas.

- Bligh, R. P., Menges, W. L., & Butler, B. G. (1997). Evaluation of a Modified Steel Post W-Beam Guardrail System (No. TX-98/3963-S.). Texas Transportation Institute, Texas A & M University System.
- Bligh, R. P., & Mak, K. (1999). Crashworthiness of roadside features across vehicle platforms. *Transportation Research Record: Journal of the Transportation Research Board*, (1690), 68-77.
- Bligh, R. P., & Mak, K. (2002). Critical impact points for transitions and terminals. *Transportation Research Record: Journal of the Transportation Research Board*, (1797), 105-112.
- Bligh, R.P, Seckinger, N R, Abu-Odeh, A Y, Roschke, P N, Menges, W L, Haug, R R. (2004). Dynamic response of guardrail systems encased in pavement mow strips, Texas Transportation Institute, Texas A&M University System.
- Bligh, R. P., Abu-Odeh, A. Y., & Menges, W. L. (2011). MASH Test 3-10 on 31-inch W-beam Guardrail with Standard Offset blocks, Texas Department of Transportation, FHWA/TX-11/9-1002-4, Austin, Texas.
- Borovinšek, M., Vesenjāk, M., Ulbin, M., & Ren, Z. (2007). Simulation of crash tests for high containment levels of road safety barriers. *Engineering failure analysis*, 14(8), 1711-1718.
- Borovinšek, M., Vesenjāk, M., & Ren, Z. (2013). Improving the crashworthiness of reinforced wooden road safety barrier using simulations of pre-stressed bolt connections with failure. *Engineering Failure Analysis*, 35, 625-635.
- Bullard Jr, D. L., Menges, W. L., & Alberson, D. C. (1996). NCHRP report 350 compliance test 3-11 of the modified G4 (1S) guardrail with timber blockouts. FHWA Contract DTFH61-95-C-00090, Research Project, 405421-1.
- Bullard Jr, D. L., Bligh, R. P., & Menges, W. L. (2010a). Appendix D: MASH TL-3 Testing and Evaluation of the G4 (2W) W-Beam Guardrail. Report 476460-1-5. Texas A&M Transportation Institute, Texas A&M University System, College Station.
- Bullard Jr, D. L., Bligh, R. P., Menges, W. L., & Haug, R. R. (2010b). Volume I: Evaluation of Existing Roadside Safety Hardware Using Updated Criteria- Technical Report. Transportation Research Board, Washington, DC.
- Burnett, W. C., Gibson, J. L., & Freer, R. H. (1967). *New Highway Barriers: The Practical Application of Theoretical Design*. Research Report 67-1. Bureau of Physical Research, New York State Department of Public Works, Albany.
- Buth, C. E., & Menges, W. L. (1999). NCHRP Report 350 Test 3-11 of the Strong Wood Post Thrie Beam Guardrail. Texas Transportation Institute, Texas A & M University System. Texas.
- Buth, C. E., Zimmer, R. A., & Menges, W. L. (1999). Testing and Evaluation of a Modified G4 (1S) Guardrail with W150x17. 9 Steel Blockouts. TTI Report, (405421-2).

- Buth, C. E., Menges, W. L., Williams, W. F., & Schoeneman, S. K. (2000a). NCHRP Report 350 Test 3-11 on the Modified PennDOT Type 2 Guide Rail-Test 3 (No. Project No. RF473750-3.). Texas Transportation Institute, Texas A & M University System, Texas.
- Buth, C. E., Menges, W. L., & Schoeneman, S. K. (2000b). NCHRP Report 350 assessment of existing roadside safety hardware. Texas Transportation Institute, Texas A & M University System.
- Chang, L. Y., & Mannering, F. (1999). Analysis of injury severity and vehicle occupancy in truck-and non-truck-involved accidents. *Accident Analysis & Prevention*, 31(5), 579-592.
- Chen, D. H. (2012). The collapse mechanism of corrugated cross section beams subjected to three-point bending. *Thin-Walled Structures*, 51, 82-86.
- Cichowski, W. G., Skeels, P. C., & Hawkins, W. R. (1961). Appraisal of Guardrail Installations by Car Impact and Laboratory Tests. In *Highway Research Board Proceedings* (Vol. 40). Transportation Research Board, Highway Research Board.
- Coon, B. A., & Reid, J. D. (2005). Crash reconstruction technique for longitudinal barriers. *Journal of transportation engineering*, 131(1), 54-62.
- Coon, B. A., & Reid, J. D. (2006). Reconstruction techniques for energy-absorbing guardrail end terminals. *Accident Analysis & Prevention*, 38(1), 1-13.
- Corben, B. F., Logan, D. B., Fanciulli, L., Farley, R., & Cameron, I. (2010). Strengthening road safety strategy development 'Towards Zero' 2008–2020–Western Australia's experience scientific research on road safety management SWOV workshop 16 and 17 November 2009. *Safety Science*, 48(9), 1085-1097.
- Council, F.M., Stewart, J.R. (1993). Attempt to define relationship between forces to crash-test vehicles and occupant injury in similar real-world crashes. *Journal of Transport Research Record*, 78-78.
- Drucker, D. C., & Prager, W., "Soil mechanics and plastic analysis or limit design," *Quarterly of Applied Mathematics*, Vol. X, No. 2, 157-165, 1952.
- Eggers, D. W., & Hirsch, T. J. (1986). The effects of embedment depth, soil properties, and post type on the performance of highway guardrail posts. Report No. FHWA/TX-86/64+405-1, Texas Transportation Institute, Texas A&M University, College Station, Texas, 1986.
- EN 1317-2. (1998). Road restraint systems – Part 2: Performance classes, impact test acceptance criteria and test methods for safety barriers, CEN – European Committee for Standardisation, Central Secretariat, Brussels, Belgium.
- Faller, R., Reid, J., & Rohde, J. (1998). Approach guardrail transition for concrete safety shape barriers. *Transportation Research Record: Journal of the Transportation Research Board*, (1647), 111-121.

- Faller, R., Sicking, D., Polivka, K., Rohde, J., & Bielenberg, B. (2000). Long-span guardrail system for culvert applications. *Transportation Research Record: Journal of the Transportation Research Board*, (1720), 19-29.
- Faller, R., Polivka, K., Kuipers, B., Bielenberg, R., Reid, J., Rohde, J., & Sicking, D. (2004). Midwest guardrail system for standard and special applications. *Transportation Research Record: Journal of the Transportation Research Board*, (1890), 19-33.
- Faller, R., Sicking, D., Bielenberg, R., Rohde, J., Polivka, K., & Reid, J. (2007). Performance of steel-post, W-beam guardrail systems. *Transportation Research Record: Journal of the Transportation Research Board*, (2025), 18-33.
- Faller, R. (2008). In Reply Refer To: HSSD/B-175. U.S. Department of Transportation, Federal Highway Administration, Washington DC.
- Faller, R., Reid, J., Kretschmann, D., Hascall, J., & Sicking, D. (2009). Midwest Guardrail System with round timber posts. *Transportation Research Record: Journal of the Transportation Research Board*, (2120), 47-59.
- Fang, H., Gutowski, M., Li, N., & DiSogra, M. (2013). Performance Evaluation of NCDOT W-beam Guardrails under MASH TL-2 Conditions (No. FHWA/NC/2012-11).
- Ferdous, M. R., Abu-Odeh, A., Bligh, R. P., Jones, H. L., & Sheikh, N. M. (2011). Performance limit analysis for common roadside and median barriers using LS-DYNA. *International Journal of Crashworthiness*, 16(6), 691-706.
- Ferdous, M. R., Abu-Odeh, A., Bligh, R. P., & Jones, H. L. (2013). Placement of traffic barriers on roadside and median slopes—guidelines based on numerical simulations. *International Journal of Crashworthiness*, 18(2), 110-125.
- G.H. Products. (2006). In Reply Refer To: HSA-10/B-150. U.S. Department of Transportation Federal Highway Administration, Washington.
- G.H. Products. (2008). In Reply Refer To: HSSD/B-150A. U.S. Department of Transportation Federal Highway Administration, Washington.
- Gabauer, D. J. & Gabler, H. (2004). Methodology to evaluate the flail space model by using event data recorder technology. *Transportation Research Record: Journal of the Transportation Research Board*, (1890), 49-57.
- Gabauer, D. J. & Gabler, H. C. (2008). Comparison of roadside crash injury metrics using event data recorders. *Accident Analysis & Prevention*, 548-558.
- Gabauer, D. J., Kusano, K.D., Marzougui, D., Opiela, K., Hargrave, M., Gabler, H.C. (2010). Pendulum testing as a means of assessing the crash performance of longitudinal barrier with minor damage. *International Journal of Impact Engineering*, 1121-1137.

- Geers, T.L. (1984). An objective error measure for the comparison of calculated and measured transient response histories. *The Shock and vibration bulletin*, 54, 99–107.
- Guide. R.D. (2002). American Association of State Highway and Transportation Officials (AASHTO), Washington DC.
- Hascall, J. A., Reid, J. D., Faller, R. K., Sicking, D. L., & Kretschmann, D. E. (2007). Investigating the use of small-diameter softwood as guardrail posts (dynamic test results). Midwest Roadside Safety Facility, University of Nebraska–Lincoln.
- Hendricks, B.F., & Wekezer, J. (1996). Finite-element modeling of G2 guardrail. *Transportation Research Record: Journal of the Transportation Research Board*, (1528), 130-137.
- Hendricks, B.F., Martin, O.S., & Wekezer, J.W. (1996). Impact Simulation of the 820C Vehicle with the G2 Guardrail. Federal Highway Administration Vehicle Crash Analysis, FHWA, Washington DC.
- Holloway, J. C., Bierman, M. G., Pfeifer, B. G., Rosson, B. T., & Sicking, D. L. (1996). Performance Evaluation of KDOT W-Beam Systems Volume II: Component Testing and Computer Simulation. Transportation Research Report TRP-03-39-96, Project SPR-3 (17). Midwest Roadside Safety Facility, University of Nebraska–Lincoln.
- Hui, J. T. Y., Yu, T. X., & Huang, X. Q. (2002). Experiment and analysis of a scaled-down guardrail system under static and impact loading. In *Advances in Steel Structures. Proceedings of the Third International Conference on Advanced in Steel Structures*.
- Ivey, D. L., Robertson, R., & Buth, C. E. (1986). Test and evaluation of W beam and thrie beam guardrails. U.S. Department of Transportation, Federal Highway Administration, Research, Development, and Technology.
- Jiang, X., Yan, X., Huang, B., & Richards, S. H. (2011). Influence of curbs on traffic crash frequency on high-speed roadways. *Traffic injury prevention*, 12(4), 412-421.
- Johnson, E. A., Lechtenberg, K. A., Reid, J. D., Sicking, D. L., Faller, R. K., Bielenberg, R. W., & Rohde, J. R. (2008). Approach slope for Midwest guardrail system (No. TRP-03-188-08). Midwest Roadside Safety Facility, University of Nebraska–Lincoln.
- Jones, N. (1989). *Structural impact*. Cambridge University Press.
- Kammel, C. (2007). Safety barrier performance predicted by multi-body dynamics simulation. *International Journal of Crashworthiness*, 12(2), 115-125.
- Karlsson, J. E. (2000). Design of a non-snagging guardrail post (Doctoral dissertation, Worcester Polytechnic Institute).

- Keall, M. D., & Frith, W. J. (2004). Adjusting for car occupant injury liability in relation to age, speed limit, and gender-specific driver crash involvement risk. *Traffic Injury Prevention*, 5(4), 336-342.
- Kennedy Jr, J., Plaxico, C., & Miele, C. (2006). Design, development, and qualification of new guardrail post. *Transportation Research Record: Journal of the Transportation Research Board*, (1984), 69-81.
- Kockelman, K. M., & Kweon, Y. J. (2002). Driver injury severity: an application of ordered probit models. *Accident Analysis & Prevention*, 34(3), 313-321.
- Körbahti, B. K., & Rauf, M. A. (2008). Response surface methodology (RSM) analysis of photoinduced decoloration of toludine blue. *Chemical Engineering Journal*, 136(1), 25-30.
- Körbahti, B. K., & Rauf, M. A. (2009). Determination of optimum operating conditions of carmine decoloration by UV/H₂O₂ using response surface methodology. *Journal of Hazardous Materials*, 161, 281–6.
- Kullgren, A., Ydenius, A., & Tingvall, C. (1998). Frontal impacts with small partial overlap: real life data from crash recorders. *International Journal of Crashworthiness*, 3(4), 335-346.
- LS-DYNA, Livermore Software Technology Corporation (LSTC), LS-DYNA Keyword User's Manual Volume I, Version R7.0, Livermore, California, February 2013.
- M.I. Molding. (2008). Safety Acceptance Letter B-174. US department of transportation, Federal highway administration Washington DC.
- M.P. Technologies. (2002). HSA-10/B39A. U.S. Department of Transportation Federal Highway Administration, Washington DC.
- M.R.S. Facility. (2005). In Reply Refer To: HSA-10/B-133. U.S. Department of Transportation Federal Highway Administration, Washington.
- Mak, K. K., Bligh, R. P., & Menges, W. L. (1990). Testing of state roadside safety systems. Volume xi: appendix j-crash testing and evaluation of existing guardrail systems (No. FHWA-RD-98-046, Research). Texas Transportation Institute, Texas A & M University System.
- Mak, K. K., Bligh, R. P., & Menges, W. L. (1995). Crash testing and evaluation of existing guardrail systems. TTI Project, 471470, 13. Texas Transportation Institute, Texas A & M University System.
- Mak, K. K., Bligh, R. P., & Menges, W. L. (1996). Testing of State Roadside Safety Systems. Volume I: Technical Report (No. Research Foundation). Texas Transportation Institute. Texas A & M University System.
- Mak, K. K., & Bligh, R. P. (2002a). Assessment of NCHRP Report 350 test conditions. *Hydrology, Hydraulics, and Water Quality; Roadside Safety Features*. 1797, 38-43.

- Mak, K. K., & Bligh, R.P. (2002b). Assessment of NCHRP report 350 test vehicles. *Transportation Research Record: Journal of the Transportation Research Board*, (1797), 33-37.
- Marzougui, D., Buyuk, M., & Kan, S. (2007). Performance Evaluation of the Portable Concrete Barriers. Contract No. DTFH61-02-X-00076. NCAC Report, 4.
- Marzougui, D., Mahadevaiah, U., & Opiela, K. S. (2010). Development of a Modified MGS Design for Test Level 2 Impact Conditions Using Crash Simulation. The National Crash Analysis Center, The George Washington University.
- Marzougui, D., Mohan, P., Kan, C. D., & Opiela, K. S. (2012). Assessing options for improving barrier crashworthiness using finite element models and crash simulations (Vol. 8). Final Report NCAC-2012-W.
- MASH. (2009). Manual for assessing safety hardware (MASH). American Association of State Highway and Transportation, Washington, DC.
- Michie, J.D. (1981). Collision risk assessment based on occupant flail-space model. *Journal of Transportation Research Record*, Washington, D.C.
- Mongiardini, M., & M.H. Ray. Roadside Safety Verification and Validation Program User's Manual. Worcester Polytechnic Institute, Worcester, MA, 2009.
- Montgomery, DC. (2005) "Design and analysis of experiment." John Wiley & Sons Inc, sixth edition, 2005.
- Myer RH, Montgomery DC. (2002). Response surface methodology. Process and product optimization using designed experiment, John Wiley and Sons, New York.
- N.S.M. Inc. (2007). In Reply Refer To: HSSD/B-162. U.S. Department of Transportation Federal Highway Administration, Washington.
- N.S.M. Inc. (2009). In Reply Refer To: HSSD/B-186, U.S. Department of Transportation Federal Highway Administration, Washington.
- NCHRP Report 230. (1981). Recommended Procedures for the Safety Performance Evaluation of Highway Appurtenances, Transportation Research Board, Washington, DC.
- NCHRP Report 350. (1993). Recommended procedures for the safety performance evaluation of highway features, National Cooperative Highway Research Program (NCHRP).
- Ochoa, C., & Ochoa, T. (2011). Guardrail optimization for rural roads. *Transportation Research Record: Journal of the Transportation Research Board*, (2203), 71-78.
- Otte, D., Pape, C., & Krettek, C. (2005). Kinematics and injury pattern in rollover accidents of cars in German road traffic—an in-depth-analysis by GIDAS. *International Journal of Crashworthiness*, 10(1), 75-86.

- Partheeban, P., Arunbabu, E., Hemamalini, R.R. (2008). Road accident cost prediction model using systems dynamics approach. *Transport*, 59-66.
- Patzner, G. S., Plaxico, C. A. and Ray, M. H. (1998). Effect of post and soil strength on the performance of a guardrail terminal. *Engineering mechanics: A Force for the 21st Century, Proceedings of 12th Engineering Mechanics Conference, ASCE, New York, New York.*
- Pfeifer, B., & Sicking, D. (1998). NCHRP Report 350 compliance testing of the beam-eating steel terminal system. *Transportation Research Record: Journal of the Transportation Research Board*, (1647), 130-138.
- Plaxico, C. A., Patzner, G. S. & Ray, M. H. (1998) "Finite-element modeling of guardrail timber posts and soil-post interaction." *Transportation Research Record No. 1647, Transportation Research Board, Washington, D.C.*
- Plaxico, C. A., Ray, M., & Hiranmayee, K. (2000). Impact performance of the G4 (1W) and G4 (2W) guardrail systems: comparison under NCHRP Report 350 Test 3-11 conditions. *Transportation Research Record: Journal of the Transportation Research Board*, (1720), 7-18.
- Plaxico, C. A., Mozzarelli, F., & Ray, M. H. (2003). Tests and simulation of a w-beam rail-to-post connection. *International Journal of Crashworthiness*, 8(6), 543-551.
- Polivka, K. A., Faller, R. K., Sicking, D. L., Rohde, J. R., Reid, J. D., & Holloway, J. C. (2000). *Guardrail and Guardrail Terminals Installed Over Curbs* (No. TRP-03-83-99,).
- Polivka, K.A., John, R.R., Bob, W.B., Ronald K. Faller., James, C.H., Sicking, D.L. (2003). Development and evaluation of a tie-down system for the redesigned f-shape concrete temporary barrier. *Midwest Roadside Safety Facility (MwRSF), Lincoln, Nebraska.*
- Polivka, K. A., Faller, R. K., Sicking, D. L., Reid, J. D., Rohde, J. R., Holloway, J. C., ... & Kuipers, B. D. (2004). Development of the Midwest guardrail system (MGS) for standard and reduced post spacing and in combination with curbs (No. TRP-03-139-04,). *Midwest Roadside Safety Facility, University of Nebraska–Lincoln.*
- Polivka, K. A., Sicking, D.L. Bielenberg, B.W. Faller, R.K. John, R.R., Reid, J. D. (2006a). Performance Evaluation of the Midwest Guardrail System-Update to NCHRP 350 Test No. 3-11 with 28" CG Height (2214MG-2). *Midwest Roadside Safety Facility, University of Lincoln-Nebraska.*
- Polivka, K. A., Faller, R. K., Sicking, D., Rohde, J. R., Bielenberg, B. W., Reid, J. D. (2006b). Performance Evaluation of the Modified G4 (1S) Guardrail-Update to NCHRP 350 Test No. 3-11 (2214WB-1). *Midwest Roadside Safety Facility, University of Nebraska–Lincoln.*
- Prentkovskis, O., Beljatynskij, A., Prentkovskiene, R., Dyakov, I., & Dabulevičiene, L. (2009). A study of the deflections of metal road guardrail elements. *Transport*, 24(3), 225-233.

- Ray, M. H., Michie, J. D., & Hargrave, M. (1986). Events that produce occupant injury in longitudinal barrier accidents. *Transportation Research Record*, 1065, 19-30.
- Ray, M.H. (1996). Repeatability of full-scale crash tests and criteria for validating simulation results. *Transportation Research Record: Journal of the Transportation Research Board*. 1528, 155-160.
- Ray, M.H. (1997). The use of finite element analysis in roadside hardware design. *International Journal of Crashworthiness*, 2(4), 333-348.
- Ray, M. H., & McGinnis, R. G. (1997). NCHRP Synthesis 244: Guardrail and Median Barrier Crashworthiness-A Synthesis of Highway Practice. *Transportation Research Board/National Research Council, National Academy Press, Washington, DC*.
- Ray, M. H., Hargrave, M., Carney III, J., & Hiranmayee, K. (1998). Side-impact crash test and evaluation criteria for roadside safety hardware. *Transportation Research Record: Journal of the Transportation Research Board*, (1647), 97-103.
- Ray, M. H., & Weir, J. (2001). Unreported collisions with post-and-beam guardrails in Connecticut, Iowa, and North Carolina. *Transportation Research Record: Journal of the Transportation Research Board*, (1743), 111-119.
- Ray, M. H., Engstrand, K. Plaxico, C. A. & McGinnis, R. G. (2001a). Improvements to the weak-post W-beam guardrail, *Hydrology, Hydraulics, and Water Quality. Roadside Safety Features 1743*, 88-96.
- Ray, M. H., Plaxico, C. & Engstrand, K. (2001b). "Performance of W-Beam Splices." *Transportation Research Record: Journal of the Transportation Research Board 1743(1)*: 120-125.
- Ray, M. H., Mongiardini, M., Atahan, A. O., Plaxico, C. A., & Anghileri, M. (2007). Recommended procedures for verification and validation of computer simulations used for roadside safety applications. *National Cooperative Highways Research Program (NCHRP), Washington, DC*.
- Ray, M. H., Carrigan, C. E., Plaxico, C. A., Sicking, D. L., & Bligh, R. (2014). Recommended Guidelines for the Selection of Test Levels 2 through 5 Bridge Railings. *NCHRP Project, 22-12*.
- Reid, J. D., Sicking, D., Faller, R., & Pfeifer, B. (1997). Development of a new guardrail system. *Transportation Research Record: Journal of the Transportation Research Board*, (1599), 72-80.
- Reid, J. D. (1999). Dynamic impact testing of guardrail posts embedded in soil. *Federal Highway Administration (FHWA), United States Department of Transportation*.
- Reid, J.D. (2000). Designing for the critical impact point on a new bullnose guardrail system, *International Journal of Crashworthiness*, 2, 141-152.
- Reid, J. D., Rohde, J. R., & Sicking, D. L. (2002). Box-beam bursting energy absorbing terminal. *Journal of transportation engineering*, 128(3), 287-294.

- Reid, J.D., Hascall, J., Sicking, D., & Faller, R. (2009). Inertial effects during impact testing. *Transportation Research Record: Journal of the Transportation Research Board*, (2120), 39-46.
- Ren, Z., & Vesenjajk, M. (2005). Computational and experimental crash analysis of the road safety barrier. *Engineering failure analysis*, 12(6), 963-973.
- Ross, H. E., Bligh, R. P., & Mak, K. K. (2002). Evaluation of Roadside Features to Accomodate Vans, Minivans, Pickup Trucks, and 4-wheel Drive Vehicles (No. 471). Transportation Research Board.
- Rosson, B., Bierman, M., & Rohde, J. (1996). Assessment of guardrail-strengthening techniques. *Transportation Research Record: Journal of the Transportation Research Board*, (1528), 69-77.
- Roy, K. R. (2001) "Design of Experiments using Taguchi approach 16 steps to product and process improvement." John Wiley & Sons, Inc.
- Sassi, A. (2011). Analysis of W-beam guardrail systems subjected to lateral impact (Doctoral dissertation). University of Windsor.
- Schwer, L. E. (2007). Validation metrics for response histories: perspectives and case studies. *Engineering with Computers*, 23(4), 295-309.
- Seckinger, N. R., & Roschke, P. N. (2002). Numerical simulation of dynamic soil structure interaction using an explicit finite element code," *Proceedings of The Ninth International Conference on Computing in Civil and Building Engineering*, Taipei, Taiwan.
- Seckinger, N. R., Abu-Odeh, A. Y., Bligh, R. P., & Roschke, P. N. (2004, January). Evaluation of guardrail systems performance when encased in pavement mow strips. In *Transportation Research Board, 83rd Annual Meeting*.
- Seckinger, N. R., Roschke, P. N., Abu-Odeh, A., & Bligh, R. P. (2005). Numerical simulation of mow strip subcomponents used with strong post guardrail systems. *International Journal of Crashworthiness*, 10(4), 419-427.
- Seo, T., Ando, K., Fukuya, T., & Kaji, S. (1995). Development of guardrails for high-speed collisions. *Transportation research record*, (1500), 52-58.
- Sicking, D., Reid, J., & Rohde, J. (1999). Development of a flared energy-absorbing terminal for W-beam guardrails. *Transportation Research Record: Journal of the Transportation Research Board*, (1690), 8-16.
- Sicking, D., Reid, J., & Rohde, J. (2002). Development of the midwest guardrail system. *Transportation Research Record: Journal of the Transportation Research Board*, (1797), 44-52.
- Simpson. D. (2000). A new tool in accident reduction, *Traffic engineering & control*, 41, 264–265.

- Tabiei, A., & Wu, J. (2000a). Validated crash simulation of the most common guardrail system in the USA. *International Journal of Crashworthiness*, 5(2), 153-168.
- Tabiei, A., & Wu, J. (2000b). Roadmap for crashworthiness finite element simulation of roadside safety structures. *Finite Elements in Analysis and Design*, 34(2), 145-157.
- Taylor, H.W. (2005). Preventing roadway departures, Public roads 2005/06. Federal Highway Administration, Washington, DC, USA.
- Trap, (1998). Test risk assessment program. Version 1.01: User's manual. Texas Transportation Institute, Texas A&M University, Texas.
- Trinity. L Highway Products. (2007). In Reply Refer To: HSSD/B-85E. U.S. Department of Transportation Federal Highway Administration, Washington DC.
- Van Zweden, J., & Bryden, J. E. (1977). In-service performance of highway barriers (No. NYSDOT-ERD-77-RR 51,).
- Wang, Y.G., Chena, K.M., Ci, Y.S., Hu, L.W. (2011). Safety performance audit for roadside and median barriers using freeway crash records: Case study in jiangxi, china. *Scientia Iranica A*, 1222–1230.
- Wolford, D., & Sicking, D. (1996). Guardrail runout lengths revisited. *Transportation Research Record: Journal of the Transportation Research Board*, (1528), 78-86.
- Wood, D. P. (1997). Safety and the car size effect: a fundamental explanation. *Accident Analysis & Prevention*, 29(2), 139-151.
- Wright, A.E., & Ray, M.H. (1996). Characterizing guardrail steel for ls-dyna 3d simulations. *Transportation Research Record: Journal of the Transportation Research Board*, 1528, 138-145.
- Wu, W., & Thomson, R. (2004). Compatibility between passenger vehicles and road barriers during oblique collisions. *International journal of crashworthiness*, 9(3), 245-253.
- Wu, W., & Thomson, R. (2007). A study of the interaction between a guardrail post and soil during quasi-static and dynamic loading. *International Journal of Impact Engineering*, 34(5), 883-898.
- Wu, J., & Tabiei, A (2002) Parametric Study on Improvement of G4 (1S) Strong Post Guardrail System. In 7th International LS-DYNA Users Conference.
- Ydenius, A. (2009). Frontal crash severity in different road environments measured in real-world crashes. *International Journal of Crashworthiness*, 14(6), 525-532.
- Zeidler, F., Schreier, H. H., & Stadelmann, R. (1985). Accident research and accident reconstruction by the EES-accident reconstruction method. *SAE transactions*, 94, 2399-2413.

Zhu, X., & Srinivasan, S. (2011). Modeling occupant-level injury severity: An application to large-truck crashes. *Accident Analysis & Prevention*, 43(4), 1427-1437.

University of Malaya